R. & M. No. 3272

MINISTRY OF AVIATION

AERONAUTICAL RESEARCH COUNCIL
REPORTS AND MEMORANDA

A Theoretical Investigation of the Longitudinal Stability, Control and Response Characteristics of Jet-Flap Aircraft

Parts I and II

By A. S. TAYLOR, M.Sc., A.F.R.Ae.S.

LONDON: HER MAJESTY'S STATIONERY OFFICE
1962
PRICE £1 15s. 0d. NET

A Theoretical Investigation of the Longitudinal Stability, Control and Response Characteristics of Jet-Flap Aircraft

Parts I and II

By A. S. TAYLOR, M.Sc., A.F.R.Ae.S.

*Reports and Memoranda No. 3272**

February, 1960

Foreword (1961). Parts I and II of this R. & M. were written as separate Reports in 1958 and 1960. They deal with two stages of an exploratory investigation into the stability, control and response characteristics of jet-flap aircraft, undertaken at a time when the basic aerodynamic theory of the jet-flapped aerofoil was still being developed by such people as Spence, Maskell, Küchemann and Ross. The aerodynamic assumptions on which the investigation were based were thus necessarily of a tentative and approximate nature. In particular, the incompleteness of the three-dimensional theory, combined with its relative complexity, virtually dictated the use of two-dimensional theoretical lift and moment data as the basis of a tractable stability and control analysis of the generalized nature which was envisaged. Inevitably, therefore, the field of application of the results of these investigations is somewhat restricted, and in any fresh approach to the problem one would certainly hope to proceed from alternative assumptions, based on three-dimensional theory.

In Part I, where attention was restricted to considerations of trim, static stability and quasi-steady manoeuvrability, some further simplifying assumptions were made, in particular by neglecting the contributions of thrust and drag forces to the pitching moment of the aircraft about its c.g. However, to ensure self-consistency of the dynamic analysis undertaken in Part II, it was found necessary to revise the trim and stability analysis of Part I so as to include the effects of thrust and drag forces. This was done only for the case where the aircraft is trimmed by variation of the jet deflection, although in Part I, trimming by variation of tailplane setting or thrust/weight ratio (throttle setting) had also been considered. Thus although some sections of Part I have effectively been superseded in Part II, much of the earlier Report remains valid as a first approximation which has not, so far, been improved upon. Accordingly it has been thought worth while to publish both Reports in what is substantially their original form, with a few minor amendments and the addition of one or two footnotes, explaining where the analysis or conclusions of Part I need to be modified in the light of Part II.

The overall scope of the work is indicated by the summaries for the respective Parts.

* Previously issued as R.A.E. Report No. Aero. 2600, and Tech. Note No. Aero. 2670—A.R.C. 19,925 and 21,867.

Part I

An Examination of some Longitudinal Stability and Control Problems of Jet-Flap Aircraft with Particular Reference to the Use of Jet Thrust and Jet-Flap Deflection Controls

Summary. This Part of the Report extends and largely supersedes the work of Ref. 1 by considering the jet-flap controls (throttle, flap deflection) as alternatives to conventional (tail) controls, for the longitudinal control of jet-flapped aircraft. The investigation has been based on Spence's theoretical two-dimensional lift and moment data (Ref. 2) so that its results should not be applied to low-aspect-ratio layouts.

Attention has been restricted to considerations of trim, static stability and quasi-steady manoeuvrability, on the basis of which jet controls appear to compare somewhat unfavourably with tail controls.

In order to effect this comparison it has been necessary to postulate a particular 'basic design condition' (Section 3) but the proposed method of analysis may be applied quite generally, whatever design condition is adopted.

An aircraft with high-aspect-ratio jet-flapped wing, employing jet thrust and jet-flap deflection controls respectively for the high lift and cruising conditions, would require a tail volume ratio of about 0·86, coupled with a c.g. position of 0·46c. If tail controls were used, a reduction in tail volume to about 0·71 might be possible.

---

1. *Introduction.* In Ref. 1, the author made a preliminary examination of some of the stability and control problems associated with the design of a jet-flapped aircraft. The investigation was restricted to a consideration of static longitudinal stability and of the manoeuvrability criterion related to the quasi-steady condition of flight at constant speed in a vertical circle. It was assumed that the aircraft would be stabilized and controlled longitudinally by a conventional tailplane and elevator (or all-moving tailplane). At the same time it was recognised that since, at a given airspeed, the lift of a jet-flapped aerofoil is a function not only of aerofoil incidence α, but also of jet deflection angle ϑ and thrust/weight ratio λ, some other method of control might ultimately be examined and prove to be superior. I. M. Davidson of the National Gas Turbine Establishment had, for instance, maintained that, under cruising conditions, a jet-flapped aircraft should be controlled longitudinally by variations in ϑ with λ held constant, while for take-off and landing approach, he argued that ϑ should be fixed and the throttle (varying λ) alone used for control.

It is the purpose of the present Report (Parts I and II) to examine these alternative methods of control. In Part I the investigation is again restricted to considerations of trim, static longitudinal stability and quasi-steady manoeuvrability criteria. Dynamic stability and response characteristics are investigated in Part II.

It was originally intended to base the work on the same empirical two-dimensional data as were used in Ref. 1, since at the time, the theoretical results of Spence[2] (two-dimensional) and Maskell and Spence[3] (three-dimensional) had not been published. In fact, a good deal of work was accomplished using the old data, but with the appearance of Spence's results, which permit of some simplification in the stability and control analysis, it was decided to make a fresh start, using the theoretical two-dimensional data as a basis. The possible use of Maskell's three-dimensional results was rejected on the grounds that the mathematical analysis would thereby be rendered too

complicated for the present generalized investigation, whose aim is a qualitative, rather than a precise quantitative, assessment of the effects under consideration. In these circumstances, while the results of the investigation are probably applicable qualitatively to aircraft with jet-flapped aerofoils of fairly large aspect ratio, it would be unwise to apply them in cases where the wing aspect ratio is small.

The work of Ref. 1 is largely superseded by that of the present Report, inasmuch as the characteristics of the jet-flap aircraft with conventional tail control have been re-assessed, on the basis of Spence's results, and are presented here for comparison with the corresponding characteristics appertaining to the use of the jet controls for trimming and manoeuvring of the aircraft.

Stability and control analysis is inevitably more complicated for jet-flapped aircraft than for conventional aircraft because more parameters are involved. This increased complication also makes it more difficult to decide on the best basis of design (from the stability and control point of view) for a jet-flapped aircraft. The fundamental parameters at the disposal of the designer in this connection are the position of the c.g. and tail volume, which may be determined so as to satisfy a specified set of conditions; once these parameters have been fixed, the trim and stability characteristics of the aircraft are determined throughout the flight range. The choice of a set of conditions to be satisfied, such that the resulting design will be an optimum, not only from trim and stability considerations, but also from the performance point of view, is a problem of some complexity, the formal solution of which has not been attempted here. Instead, in Section 3, semi-intuitive reasoning has been used in arriving at the definition of a 'basic design condition' which, while it may not lead to the optimum design, should at least produce one which provides a sufficiently realistic basis for the comparison of the respective merits of different types of longitudinal control, which is the main object of this investigation.

The analysis is not fundamentally affected by this particular choice of a basic design condition and the designer of a jet-flap aircraft who chooses some other basis of design may still follow the general method described herein, to determine the stability and control characteristics of his design.

Since the completion of the work described in the main text of this Report, an alternative method of formulating the trim and manoeuvrability analysis has been suggested to the author by S. B. Gates. This is set out in the Appendix, which includes the results of some sample calculations which have been made to illustrate how the method would be applied in practice.

2. *General Theory.* If the results of Spence's two-dimensional theory[2] are accepted, it can be inferred that the total lift acting on a wing at incidence α, with jet emerging at angle ϑ to the wing chord, may be written

$$L = C_L \tfrac{1}{2}\rho U^2 S = L(\alpha) + L(\vartheta) = \{C_{L(\alpha)} + C_{L(\vartheta)}\} \tfrac{1}{2}\rho U^2 S \tag{1a}$$

with

$$C_{L(\alpha)} = A\alpha,\ C_{L(\vartheta)} = B\vartheta, \tag{1b}$$

where A and B are functions of C_J only (C_J being the jet coefficient defined by $C_J = J/\frac{1}{2}\rho U^2 c$), and that the two components of lift act respectively at distances $\xi_\alpha c$, $\xi_\vartheta c$ behind the leading edge, where ξ_α, ξ_ϑ are also functions of C_J only.

Thus the system of forces acting normally to the flight path of a jet-flapped aircraft with tail is as illustrated in Fig. 1, where G is the centre of gravity, at distance hc from the wing leading edge, C_{LT} is the lift coefficient of the tail, whose volume ratio is $\bar{V}$ and γ is the inclination of the flight path to the horizontal. To simplify the analysis it is assumed, when considering the balance of

normal forces, that the lift provided by the tailplane is negligible in comparison with the wing lift (1a), which may accordingly be taken as the total lift on the aircraft. The wing zero-lift pitching moment will be assumed zero and in addition, the body pitching moment and any moments due to thrust or drag will be neglected.*

Then the pitching-moment coefficient about the c.g. is

$$C_m = C_{L(\alpha)}(h-\xi_\alpha) + C_{L(\vartheta)}(h-\xi_\vartheta) - \bar{V}C_{LT} \tag{2}$$

with

$$C_{LT} = a_1(\alpha-\epsilon+\eta_T), \tag{3}$$

where η_T is the setting of the (all-moving) tailplane relative to the wing, and ϵ is the downwash angle at the tailplane, where we may write

$$\epsilon = \epsilon(C_{L(\alpha)}, C_{L(\vartheta)}) = \epsilon(C_J, \alpha, \vartheta). \tag{4}$$

From (2) and (3)

$$C_m = C_{L(\alpha)}(h-\xi_\alpha) + C_{L(\vartheta)}(h-\xi_\vartheta) - a_1\bar{V}(\alpha-\epsilon+\eta_T). \tag{5}$$

It will be useful to consider the partial derivatives of C_m with respect to $C_{L(\alpha)}$ and $C_{L(\vartheta)}$ respectively, when speed and thrust (and hence C_J) are held constant. We have

$$K_{r\alpha} = -\frac{\partial C_m}{\partial C_{L(\alpha)}} = \xi_\alpha - h + \frac{\bar{V}a_1}{A}\left(1-\frac{\partial\epsilon}{\partial\alpha}\right) \tag{6}$$

and

$$K_{r\vartheta} = -\frac{\partial C_m}{\partial C_{L(\vartheta)}} = \xi_\vartheta - h - \frac{\bar{V}a_1}{B}\frac{\partial\epsilon}{\partial\vartheta}, \tag{7}$$

where $K_{r\alpha}$, $K_{r\vartheta}$ may be referred to as the aircraft restoring margins with respect to changes of incidence and jet deflection respectively.

$K_{r\alpha}$ is directly analogous to the restoring margin $K_m = -\partial C_m/\partial C_L$ for a conventional aircraft and provides a measure of the (initial) tendency of the aircraft to return to its trimmed condition following an inadvertent change of incidence.

In considering the significance of $K_{r\vartheta}$ it should be remembered that whereas changes of incidence (and hence of $C_{L(\alpha)}$) may occur accidentally, changes of jet deflection (and hence of $C_{L(\vartheta)}$) should normally occur only at the pilot's behest, when he requires an increment of lift for control purposes. For the purposes of argument it will be assumed that the pilot's immediate objective in applying ϑ-control is to provide an increment of lift $\Delta L(\vartheta)$ which will produce a linear acceleration of the aircraft c.g. normal to the flight path, without producing any angular acceleration about the c.g. The complete response of the aircraft to a given control action can be determined theoretically, only by a full mathematical analysis, but in order that the initial response should be in accordance with the pilot's (assumed) requirement, it is evident that the lift increment $\Delta L(\vartheta)$ corresponding to the increment $\Delta\vartheta$ of jet-flap deflection should act through the aircraft c.g. If it does not, then a moment will be produced which tends to increase or decrease the incidence (and hence $C_{L(\alpha)}$) according as $\Delta L(\vartheta)$ acts ahead of or behind the c.g. The quantity $K_{r\vartheta}$ is clearly a measure of the tendency for the lift increment $\Delta L(\vartheta)$ to be cancelled out as a result of the change in incidence

---

* *Footnote* (1961). The inclusion of moments due to thrust and drag is shown in Part II to exert an appreciable effect on the tail volume and c.g. position required to satisfy specified design conditions.

(*i.e.*, it is a measure of the tendency for the total lift coefficient to be restored to its initial value). Thus the direct lift increment resulting from an increment in jet-flap deflection is diminished or augmented according as $K_{r\vartheta}$ is positive or negative.

The values of h for which $K_{r\alpha}$, $K_{r\vartheta}$ are respectively zero, namely

$$h = h_{r\alpha} = \xi_\alpha + \frac{\overline{V}a_1}{A}\left(1 - \frac{\partial\epsilon}{\partial\alpha}\right) \tag{8}$$

and

$$h = h_{r\vartheta} = \xi_\vartheta - \frac{\overline{V}a_1}{B}\frac{\partial\epsilon}{\partial\vartheta} \tag{9}$$

correspond to points N_α, N_ϑ on the aerofoil chord (*see* Fig. 2), which may be referred to as the aerodynamic centres with respect to incidence and jet deflection respectively, for the complete aircraft. Through N_α will act the resultant of the forces produced on the wing and tailplane by a change of incidence at constant speed and angular velocity with the thrust fixed (C_J constant). Similarly, through N_ϑ will act the resultant of the forces produced on the wing and tailplane by a change of jet deflection under the same conditions. Since ξ_α, A and $\partial\epsilon/\partial\alpha$ in (8) and ξ_ϑ, B and $\partial\epsilon/\partial\vartheta$ in (9) are functions of C_J, it follows that the positions of N_α and N_ϑ vary with the jet coefficient, which itself varies with both aircraft speed and jet thrust.

It will be noted that $K_{r\alpha}$, $K_{r\vartheta}$ are the distances (expressed as fractions of the wing chord) of the points N_α, N_ϑ respectively, aft of the centre of gravity.

From the foregoing analysis it follows that the system of three aerodynamic forces shown in Fig. 1 may be replaced by an equivalent set of two forces and a moment, as illustrated in Fig. 2. $L(\alpha)$, $L(\vartheta)$ representing the resultant normal forces on the complete aircraft, due respectively to wing incidence and jet-flap deflection, act at N_α, N_ϑ respectively. The moment $M(\eta_T)$ about the centre of gravity is due to that part of the tail lift which arises from the tail-setting η_T.

2.1. *Trimmed Rectilinear Flight.* [*Note.* An alternative formulation of the trim and manoeuvrability analysis of Sections 2.1 and 2.2, suggested by S. B. Gates, is outlined in the Appendix.]

For steady rectilinear flight at a small angle γ to the horizontal, the aerodynamic force and moment system of Fig. 2 must balance the component of the weight normal to the flight path, *viz.*, $W\cos\gamma$, acting through G. In the following analysis it will be assumed that $\cos\gamma \approx 1$. Then if for the present, symbols appropriate to steady (trimmed) rectilinear flight are distinguished by the suffix 's', and if the thrust/weight ratio J/W is denoted by λ, the condition of equilibrium of the normal forces, in conjunction with Equations (1a) leads directly to the relationship

$$C_{Js} = \lambda C_{Ls}, \tag{10}$$

where

$$C_{Ls} = A_s\alpha_s + B_s\vartheta, \tag{11}$$

giving

$$\alpha_s = \frac{C_{Ls} - B_s\vartheta}{A_s}, \tag{12}$$

from which equation it is possible to construct C_{Ls} vs. α_s curves with ϑ, λ as parameters. In the process, C_{Js} having been calculated from (10), A_s, B_s will also have been determined as functions

of α_s and subsequently, $(\xi_\alpha)_s$ and $(\xi_\vartheta)_s$ may similarly be determined. Thus C_{Ls}, A_s, B_s, $(\xi_\alpha)_s$ and $(\xi_\vartheta)_s$ may all be plotted against α_s, with ϑ and λ as parameters.*

The trim condition $C_m = 0$, using (5) with (1), gives

$$A_s\left\{h - (\xi_\alpha)_s - \frac{a_1\bar{V}}{A_s}\right\}\alpha_s + B_s\left\{h - (\xi_\vartheta)_s\right\}\vartheta + a_1\bar{V}\epsilon_s - a_1\bar{V}(\eta_T)_s = 0\,. \tag{13}$$

For a given aircraft, whose tail volume ($\bar{V}$) and c.g. position (h) have been fixed (remembering that A_s, B_s, etc. are expressible as functions of α_s for given λ and ϑ), Equation (13) may be regarded as an equation for determining the trimmed incidence α_s, corresponding to a prescribed combination of control settings λ, ϑ, η_T, while Equations (6) and (7) give the values of the two restoring margins.

2.1.1. *Tail volume and c.g. position required to satisfy a prescribed design condition.* If Equations (6) and (13)† are rearranged thus:

$$h - \frac{\bar{V}a_1}{A}\left(1 - \frac{\partial\epsilon}{\partial\alpha}\right) = \xi_\alpha - K_{r\alpha}\,, \tag{6a}$$

$$(A\alpha + B\vartheta)h - \bar{V}a_1(\alpha - \epsilon + \eta_T) = A\alpha\xi_\alpha + B\vartheta\xi_\vartheta\,, \tag{13a}$$

we may regard them as equations to determine the tail volume and c.g. position required to satisfy a prescribed design condition. Examining the equations we see that before they can be solved explicitly for $\bar{V}$ and h, values must be known for the following somewhat formidable list of parameters: a_1, A, B, ξ_α, ξ_ϑ, ϑ, α, η_T, ϵ, $\partial\epsilon/\partial\alpha$, $K_{r\alpha}$.

As we are employing two-dimensional data, the tailplane lift slope a_1 may be considered fixed. Of the other parameters, A, B, ξ_α and ξ_ϑ have been shown to be functions of the jet parameters λ, ϑ and trimmed incidence α. Further, it may be assumed (*see* Section 2.1.2) that ϵ and $\partial\epsilon/\partial\alpha$ are also known if λ, ϑ and α are known. Thus values of only five parameters—λ, ϑ, η_T, α, $K_{r\alpha}$—need, in fact, be assigned in order that all the coefficients in Equations (6a) and (13a) should be calculable and the equations themselves soluble for $\bar{V}$ and h. Hence, one way of determining the tail volume and c.g. position for a projected aircraft is to specify that it should trim at a given incidence ($\bar{\alpha}$) and with a given α-restoring margin ($\bar{K}_{r\alpha}$) for a particular combination of jet and tail control settings ($\bar{\lambda}$, $\bar{\vartheta}$, $\bar{\eta}_T$).

The difficulty of choosing $\bar{\alpha}$, $\bar{K}_{r\alpha}$, $\bar{\lambda}$, $\bar{\vartheta}$ and $\bar{\eta}_T$ so that the resulting design should be an optimum, not only from trim and stability considerations but also from the point of view of performance, has already been alluded to in the Introduction and, in Section 3, we shall discuss in some detail the

---

* Numerical work, results of which are presented in Figs. 4 to 6, indicates that over most of the practical incidence range, C_{Ls} can be well approximated by a linear relationship $C_{Ls} = P\alpha_s + Q$ where P and Q are functions of λ and ϑ only, for which numerical values may be derived from the plotted curves. Similarly, A_s, B_s, $(\xi_\alpha)_s$ and $(\xi_\vartheta)_s$ may be expressed as $p_r\,\alpha_s + q_r$, $r = 1, \ldots 4$, respectively, where p_r, q_r are functions of λ and ϑ only.

† The suffix 's' is now dropped to simplify the writing although the following analysis refers to trimmed conditions.

selection of a 'basic design condition'. Meanwhile, on the assumption that values have been assigned to these parameters, the solution of equations (6a) and (13a) may be written as

$$\left.\begin{aligned} \overline{V} &= \frac{\overline{A}}{a_1}\frac{F}{G}, \\ h &= \frac{F}{G}\left(1-\overline{\frac{\partial\epsilon}{\partial\alpha}}\right)+\overline{\xi}_\alpha-\overline{K}_{r\alpha}, \end{aligned}\right\} \tag{14a}$$

where

and

$$\left.\begin{aligned} F &= \overline{A}\bar{\alpha}\,\overline{K}_{r\alpha}+\overline{B}\overline{\vartheta}(\overline{\xi}_\vartheta-\overline{\xi}_\alpha+\overline{K}_{r\alpha}) \\ G &= \overline{B}\overline{\vartheta}\left(1-\overline{\frac{\partial\epsilon}{\partial\alpha}}\right)-\overline{A}\bar{\alpha}\,\overline{\frac{\partial\epsilon}{\partial\alpha}}+\overline{A}(\bar{\epsilon}-\bar{\eta}_T). \end{aligned}\right\} \tag{14b}$$

$\overline{A}$, $\overline{B}$, $\overline{\xi}_\vartheta$, $\overline{\xi}_\alpha$, $\bar{\epsilon}$, $\overline{\partial\epsilon/\partial\alpha}$ are values of A, B, ξ_ϑ, ξ_α, ϵ, $\partial\epsilon/\partial\alpha$ corresponding to trimmed incidence $\bar{\alpha}$, for which the trimmed lift coefficient is $\overline{C}_L \approx \overline{P}\bar{\alpha}+\overline{Q}$; (*see* footnote Section 2.1) and the jet coefficient is $\overline{C}_J = \overline{\lambda}\overline{C}_L$.

The value of the 'ϑ-restoring margin' in the design condition ($\overline{K}_{r\vartheta}$) cannot be independently assigned for, with $\overline{V}$ and h fixed by (14a), its value follows from (7) as

$$\overline{K}_{r\vartheta} = \overline{\xi}_\vartheta-\overline{\xi}_\alpha+\overline{K}_{r\alpha}-\frac{F}{G}\left(1-\overline{\frac{\partial\epsilon}{\partial\alpha}}+\frac{\overline{A}}{\overline{B}}\overline{\frac{\partial\epsilon}{\partial\vartheta}}\right). \tag{15}$$

In general, when $\overline{V}$ and h have been fixed to satisfy the specified design condition (trim at incidence $\bar{\alpha}$ with control settings $\overline{\lambda}$, $\overline{\vartheta}$, $\bar{\eta}_T$), any change in the control settings, singly or in combination, will produce changes in the trimmed incidence and trimmed lift coefficient which may be determined from Equations (13) and (11). At the same time, the values of the restoring margins $K_{r\alpha}$, $K_{r\vartheta}$, given by (6) and (7) will change.

2.1.2. *The effect of downwash on the required tail volume and c.g. position.* For a given wing geometry and tailplane location, the downwash at the tail (ϵ) will depend on the values of C_J, α and ϑ. Since G (Equation (14b)) involves $\bar{\epsilon}$ and $\overline{\partial\epsilon/\partial\alpha}$ and since it appears in the equations for $\overline{V}$ and h (14a), the second of which also contains a factor $\overline{(1-\partial\epsilon/\partial\alpha)}$, it may be expected that, in general, the required tail volume and c.g. position will both depend on the value of the downwash at the tail.

The simplest assumption (based on the behaviour of a conventional wing) which could be made regarding the downwash would be that it is proportional to total C_L, in which case we could write

$$\epsilon = EC_L = E(C_{L(\alpha)}+C_{L(\vartheta)}) = E(A\alpha+B\vartheta), \tag{16}$$

where E is a constant.

Then the function G reduces to

$$G = G_1 = \overline{B}\overline{\vartheta}-\overline{A}\bar{\eta}_T, \tag{17}$$

which is independent of E. Hence the tail volume, given by

$$\overline{V} = \frac{\overline{A}}{a_1}\frac{F}{G_1} \tag{18}$$

is independent of the downwash when the latter varies in accordance with (16). The c.g. position, given by

$$h = \frac{F}{G_1}(1-E\bar{A}) + \bar{\xi}_\alpha - \bar{K}_{r\alpha} \tag{19}$$

depends on the value of E, however. The equation for the 'ϑ-restoring margin' (15) reduces to

$$\bar{K}_{r\vartheta} = \bar{\xi}_\vartheta - \bar{\xi}_\alpha + \bar{K}_{r\alpha} - \frac{F}{G_1}, \tag{20}$$

so that $\bar{K}_{r\vartheta}$, like $\bar{V}$ is independent of E.

In the special case under consideration, the pitching-moment equation (5) may be written in the form

$$-C_m = K_{r\alpha}\, C_{L(\alpha)} + K_{r\vartheta}\, C_{L(\vartheta)} + \bar{V}a_1\eta_T, \tag{21a}$$

where the restoring margins are given by

$$\left.\begin{aligned} K_{r\alpha} &= \xi_\alpha - h + \frac{\bar{V}a_1}{A}(1-EA), \\ K_{r\vartheta} &= \xi_\vartheta - h - E\bar{V}a_1. \end{aligned}\right\} \tag{21b}$$

The results of a theoretical downwash investigation by Miss Ross[4] suggest that the assumption (16) may not be far removed from the truth for a two-dimensional jet-flapped wing, although it might be more accurate to write

$$\epsilon = E_1 C_{L(\alpha)} + E_2 C_{L(\vartheta)} = E_1 A\alpha + E_2 B\vartheta, \tag{22}$$

where E_1 is somewhat greater than E_2. In that case

$$G = G_1 - \bar{A}\bar{B}\bar{\vartheta}(E_1 - E_2) < G_1$$

and the tail volume required is greater than in the case where $E_1 = E_2 = E$. It can also be seen that if E_1 and E_2 are both increased in the same ratio, the required tail volume is also increased. The foregoing conclusions would be reversed if E_2 were greater than E_1.

From Miss Ross's results for a three-dimensional jet-flapped wing it is clear that the downwash is not related to the total lift coefficient by a simple equation of type (16) for the manner in which ϵ varies with C_L depends very much on whether C_L is varied by changing α or by changing the jet parameters C_J or ϑ. In fact, it does not appear possible at the moment, to express ϵ as a function of C_J, α, and ϑ in a form sufficiently simple for use in developing the trim and stability equations for the three-dimensional case, beyond the stage corresponding to Equations (13) and (6) for the two-dimensional case. In a particular three-dimensional design problem, it would be necessary to calculate ϵ and $\partial\epsilon/\partial\alpha$ for a range of parameters and then for each flight condition under consideration, to substitute appropriate values directly into the equations.

For the present investigation, whose object is to study broad trends, it has been considered satisfactory to employ two-dimensional data throughout and in the following section, dealing with constant speed manoeuvres, it will therefore be assumed that the downwash is given by (16) so that Equations (21a) and (21b) are applicable.

2.2. *Constant Speed Manoeuvres.* We consider motion in a steady circle following application of tail and jet controls (separately or in combination), when the aircraft is in trimmed (rectilinear) flight at incidence α_s and lift coefficient C_{Ls}, corresponding to initial control settings η_{Ts}, λ_s, ϑ_s.

Let $\Delta\eta_T$, $\Delta\lambda$, $\Delta\vartheta$ denote the increments of control settings; $\Delta\alpha$, ΔC_L and Δn the incremental incidence, lift coefficient and load factor respectively and q the angular velocity.

In accordance with Equations (1), the lift coefficient C_L in the circle is given by

$$\left.\begin{aligned} C_L &= C_{Ls} + \Delta C_L = A\alpha + B\vartheta, \\ \alpha &= \alpha_s + \Delta\alpha, \\ \vartheta &= \vartheta_s + \Delta\vartheta \end{aligned}\right\} \quad (23)$$

where

and A and B are functions of the jet coefficient C_J appertaining to circling flight. Since the speed remains constant in the manoeuvre,

$$\left.\begin{aligned} C_J &= \frac{\lambda}{\lambda_s} C_{Js} = \lambda C_{Ls}, \\ \lambda &= \lambda_s + \Delta\lambda. \end{aligned}\right\} \quad (24)$$

where

Thus A, B (and also ξ_α, ξ_ϑ, $K_{r\alpha}$, $K_{r\vartheta}$) are functions of λ only and the incremental lift coefficient may be written as

$$\Delta C_L = \Delta C_{L(\alpha)} + \Delta C_{L(\vartheta)},$$

where

$$\left.\begin{aligned} \Delta C_{L(\alpha)} &= A_s\Delta\alpha + \alpha_s\left(\frac{\partial A}{\partial\lambda}\right)_s \Delta\lambda \\ \Delta C_{L(\vartheta)} &= B_s\Delta\vartheta + \vartheta_s\left(\frac{\partial B}{\partial\lambda}\right)_s \Delta\lambda, \end{aligned}\right\} \quad (25)$$

and

so that

$$\Delta C_L = A_s\Delta\alpha + \left\{\alpha_s\left(\frac{\partial A}{\partial\lambda}\right)_s + \vartheta_s\left(\frac{\partial B}{\partial\lambda}\right)_s\right\}\Delta\lambda + B_s\Delta\vartheta. \quad (26)$$

The incremental load factor is given by

$$\Delta n = \frac{\Delta C_L}{C_{Ls}}. \quad (27)$$

The radial force equation is

$$mqV = \Delta C_L\, S\, \tfrac{1}{2}\rho V^2.$$

or

$$\left.\begin{aligned} \frac{ql_T}{V} &= \frac{\Delta C_L}{2\mu_1}, \\ \mu_1 &= \frac{m}{\rho S l_T}. \end{aligned}\right\} \quad (28)$$

where

From (21a), the incremental pitching-moment coefficient is

$$\begin{aligned} -\Delta C_m &= K_{r\alpha}\Delta C_{L(\alpha)} + C_{L(\alpha)}\Delta K_{r\alpha} + K_{r\vartheta}\Delta C_{L(\vartheta)} + C_{L(\vartheta)}\Delta K_{r\vartheta} + \bar{V}a_1\Delta\eta_T - \frac{2l_T}{c} m_q \frac{ql_T}{V} \\ &= K_{r\alpha}\Delta C_{L(\alpha)} + C_{L(\alpha)}\Delta K_{r\alpha} + K_{r\vartheta}\Delta C_{L(\vartheta)} + C_{L(\vartheta)}\Delta K_{r\vartheta} + \bar{V}a_1\Delta\eta_T - \frac{l_T}{c} m_q \frac{\Delta C_L}{\mu_1} \end{aligned} \quad (29)$$

(using (28)), where the last term on the right-hand side is due to rotary damping. For steady conditions, $\Delta C_m = 0$; then if we use (25), and drop the suffix 's' from now on to simplify the writing, Equation (29) gives

$$K_{r\alpha}A\Delta\alpha = -\left(K_{r\alpha}\alpha\frac{\partial A}{\partial\lambda} + A\alpha\frac{\partial K_{r\alpha}}{\partial\lambda} + K_{r\vartheta}\vartheta\frac{\partial B}{\partial\lambda} + B\vartheta\frac{\partial K_{r\vartheta}}{\partial\lambda}\right)\Delta\lambda - \\ - K_{r\vartheta}B\Delta\vartheta - \bar{V}a_1\Delta\eta_T + \frac{l_T}{c}m_q\frac{\Delta C_L}{\mu_1}. \tag{30}$$

Eliminating $\Delta\alpha$ between (26) and (30) and solving for ΔC_L, we have

$$\left(K_{r\alpha} - \frac{l_T}{c}\frac{m_q}{\mu_1}\right)\Delta C_L = -\Delta\lambda\left\{A\alpha\frac{\partial K_{r\alpha}}{\partial\lambda} + B\vartheta\frac{\partial K_{r\vartheta}}{\partial\lambda} + \vartheta\frac{\partial B}{\partial\lambda}(K_{r\vartheta} - K_{r\alpha})\right\} - \\ - \Delta\vartheta\{B(K_{r\vartheta} - K_{r\alpha})\} - \\ - \Delta\eta_T\,\bar{V}a_1. \tag{31}$$

From (21)

$$\left.\begin{aligned} K_{r\vartheta} - K_{r\alpha} &= \xi_\vartheta - \xi_\alpha - \frac{\bar{V}a_1}{A}, \\ \frac{\partial K_{r\alpha}}{\partial\lambda} &= \frac{\partial\xi_\alpha}{\partial\lambda} - \frac{\bar{V}a_1}{A^2}\frac{\partial A}{\partial\lambda}, \\ \frac{\partial K_{r\vartheta}}{\partial\lambda} &= \frac{\partial\xi_\vartheta}{\partial\lambda}. \end{aligned}\right\} \tag{32}$$

Writing

$$H_{m\alpha} = K_{r\alpha} - \frac{l_T}{c}\frac{m_q}{\mu_1} \tag{33}$$

in Equation (31), substituting from (32) therein and using (27), we obtain the following expressions for $\partial n/\partial\lambda$, $\partial n/\partial\vartheta$ and $\partial n/\partial\eta_T$:

$$\left.\begin{aligned} \frac{\partial n}{\partial\lambda} &= \frac{1}{C_L}\frac{\partial C_L}{\partial\lambda} \\ &= \frac{-1}{C_L H_{m\alpha}}\left[\left(A\frac{\partial\xi_\alpha}{\partial\lambda} - \frac{\bar{V}a_1}{A}\frac{\partial A}{\partial\lambda}\right)\alpha + \left\{B\frac{\partial\xi_\vartheta}{\partial\lambda} + \left(\xi_\vartheta - \xi_\alpha - \frac{\bar{V}a_1}{A}\right)\frac{\partial B}{\partial\lambda}\right\}\vartheta\right], \\ \frac{\partial n}{\partial\vartheta} &= \frac{1}{C_L}\frac{\partial C_L}{\partial\vartheta} = \frac{-B}{C_L H_{m\alpha}}\left(\xi_\vartheta - \xi_\alpha - \frac{\bar{V}a_1}{A}\right), \\ \frac{\partial n}{\partial\eta_T} &= \frac{1}{C_L}\frac{\partial C_L}{\partial\eta_T} = -\frac{\bar{V}a_1}{C_L H_{m\alpha}}. \end{aligned}\right\} \tag{34}$$

In evaluating the above quantities it must be remembered that all coefficients, derivatives etc. are to be assigned values appropriate to the initial trimmed condition. It may be noted that, using the first of Equations (32), the formula for $\partial n/\partial\vartheta$, (34, (ii)) may be written as

$$\frac{\partial n}{\partial\vartheta} = \frac{B(K_{r\alpha} - K_{r\vartheta})}{C_L H_{m\alpha}}.$$

It may be assumed that $K_{r\alpha}$ and $H_{m\alpha}$ will be positive for all conditions of flight. Thus for effective ϑ-control, $K_{r\vartheta}$ must be negative or, if positive, small in comparison with $K_{r\alpha}$. If $K_{r\vartheta}$ were equal

to $K_{r\alpha}$ (*i.e.*, if the aero-dynamic centres with respect to incidence and jet deflection, N_ϑ, N_α respectively, coincided) ϑ-control would be completely ineffective while for $K_{r\vartheta} > K_{r\alpha}$ there would be a reversal of effectiveness.

3. *The Selection of a Basic Design Condition.* 3.1. *General Design Considerations.* Suppose that we are considering the design of a jet-flapped aircraft. At the outset, a general consideration of operational requirements will determine (approximately) the weight of the aircraft under various conditions and will lead to the choice of a particular engine (or engines) of known performance. Hence the maximum value of the thrust/weight ratio (λ_{max}) may be assumed to be effectively specified. Similar considerations, taken in conjunction with the known or predicted aerodynamic characteristics of the proposed jet-flap installation, will determine the maximum jet-flap deflection (ϑ_{max}) that may usefully be employed.

The aircraft's trim and static stability characteristics will be largely determined by the tail volume ($\bar{V}$) and the c.g. location (h) so that suitable values must be assigned to these parameters at the outset.

3.2. *Design Condition to Determine Tail Volume and c.g. Position.* It has been seen in Section 2.1.1 that $\bar{V}$ and h may be chosen to satisfy one prescribed design condition, namely that the aircraft should trim at a particular incidence $\bar{\alpha}$ and with a given 'α-restoring margin' $\bar{K}_{r\alpha}$, for a particular combination of control settings $\bar{\lambda}$, $\bar{\vartheta}$ and $\bar{\eta}_T$. When $\bar{V}$ and h have been thus chosen, it remains to be established that trim and stability characteristics will remain satisfactory over the full ranges of the control parameters that must be used to enable the aircraft to perform its tasks. Clearly the basic design condition should be selected with some care, although at present the choice is, for various reasons, a difficult one. On the one hand, ideas of how best to operate a jet-flap aircraft, so as to realize its full potentialities, do not seem to have crystallized, while on the other hand, unresolved doubts as to the stalling characteristics of jet-flapped aerofoils and the extent to which such characteristics can be controlled by aerofoil design, make it uncertain what range of incidence may be usefully employed.

It was suggested, some time ago, by I. M. Davidson of N.G.T.E., that a jet-flapped aircraft should be flown continuously at zero effective incidence and that under cruising conditions, control should be exercised by variations in ϑ with λ held constant, while for take-off and landing approach, ϑ should be fixed and the throttle alone used for control. Mathematical analysis indicates that it is not possible to maintain trim at zero incidence for all settings of the controls; moreover there appears to be no good reason why the incidence should be restricted except insofar as this is necessary to avoid flow separations.* Nevertheless, on the assumption that the basic design condition should be associated with a condition of high lift (*i.e.*, $\bar{\lambda}/\lambda_{max}$ and $\bar{\vartheta}/\vartheta_{max}$ to have values not less than 0·75 say) it is not unreasonable to assign $\bar{\alpha}$ and $\bar{\eta}_T$ the value zero, for then any usable range of positive incidence is available for manoeuvres using tailplane control and is, in addition, an insurance against stalling if gusts are encountered.

Accordingly, it is suggested that the basic design condition be taken as:

---

* In the early two-dimensional experimental work at N.G.T.E. flow separation from the leading edge was found to occur at approximately zero incidence for the larger values of C_J and ϑ. It is now considered, however, that unseparated flow could be maintained up to quite large incidences by suitable section design.

Aircraft to trim at zero incidence ($\bar{\alpha} = 0$) with 'α-restoring margin' $\overline{K}_{r\alpha}$ when $\lambda = \bar{\lambda}$, $\vartheta = \bar{\vartheta}$ and $\bar{\eta}_T = 0$.

As a 'datum' condition this has the merit of simplicity, for with the downwash assumption (16), the equations for the required tail volume and c.g. position ((18) and (19)) reduce to

$$\left.\begin{aligned} \overline{V} &= \frac{\overline{A}}{a_1}(\bar{\xi}_\vartheta - \bar{\xi}_\alpha + \overline{K}_{r\alpha}) \\ \text{and} \qquad h &= \bar{\xi}_\vartheta - E\overline{A}(\bar{\xi}_\vartheta - \bar{\xi}_\alpha + \overline{K}_{r\alpha}) = \bar{\xi}_\vartheta - Ea_1\overline{V}, \\ \text{while} \qquad \overline{K}_{r\vartheta} &= 0. \end{aligned}\right\} \tag{35}$$

It is at once seen that the required tail volume is independent of the downwash* but increases linearly with the required 'α-restoring margin', $\overline{K}_{r\alpha}$. For a given value of the downwash, the required c.g. position moves forward as $\overline{K}_{r\alpha}$ is increased, the variation again being linear. If the downwash coefficient E is increased, the rate of forward movement of the c.g. with increasing $\overline{K}_{r\alpha}$ is increased.

3.3. *Manoeuvres Initiated from the Basic Design Condition.* When the aircraft is trimmed in the basic design condition ($\lambda = \bar{\lambda}$, $\vartheta = \bar{\vartheta}$, $\bar{\alpha} = \bar{\eta}_T = 0$, $K_{r\alpha} = \overline{K}_{r\alpha}$) with $\overline{V}$ and h given by (35), Equations (34) reduce to

$$\left.\begin{aligned} \frac{\partial n}{\partial \lambda} &= \frac{\overline{\partial n}}{\partial \lambda} = \frac{-1}{\overline{C}_L \overline{H}_{m\alpha}}\left[\overline{B}\,\frac{\overline{\partial \xi_\vartheta}}{\partial \lambda} - \overline{K}_{r\alpha}\,\frac{\overline{\partial B}}{\partial \lambda}\right]\bar{\vartheta} = \frac{-1}{\overline{H}_{m\alpha}}\,\frac{\overline{\partial \xi_\vartheta}}{\partial \lambda} + \frac{\overline{K}_{r\alpha}}{\overline{H}_{m\alpha}}\,\frac{1}{B}\,\frac{\overline{\partial B}}{\partial \lambda}, \\ \frac{\partial n}{\partial \vartheta} &= \frac{\overline{\partial n}}{\partial \vartheta} = \frac{\overline{B}\overline{K}_{r\alpha}}{\overline{C}_L \overline{H}_{m\alpha}} = \frac{\overline{K}_{r\alpha}}{\overline{H}_{m\alpha}}\,\frac{1}{\bar{\vartheta}}, \\ \frac{\partial n}{\partial \eta_T} &= \frac{\overline{\partial n}}{\partial \eta_T} = -\frac{\overline{V}a_1}{\overline{C}_L \overline{H}_{m\alpha}}, \\ \text{where} \qquad \overline{H}_{m\alpha} &= \overline{K}_{r\alpha} - \frac{l_T}{c}\,\frac{m_q}{\mu_1}. \end{aligned}\right\} \tag{36}$$

3.4. *Manoeuvres Initiated from Other Trimmed Conditions.* For manoeuvres initiated from trimmed conditions other than the basic design condition, $\partial n/\partial\lambda$, $\partial n/\partial\vartheta$ and $\partial n/\partial\eta_T$ must be evaluated from Equations (34) with $\overline{V} = (\overline{A}/a_1)(\bar{\xi}_\vartheta - \bar{\xi}_\alpha + \overline{K}_{r\alpha})$.

4. *Numerical Examples.* In Ref. 2, Spence gives the following formulae for the coefficients A and B appearing in the formula for lift coefficient (Equation (1)):

$$\left.\begin{aligned} A &= 2\pi + 1{\cdot}152C_J^{1/2} + 1{\cdot}106C_J + 0{\cdot}051C_J^{3/2}, \\ B &= \qquad 3{\cdot}545C_J^{1/2} + 0{\cdot}325C_J + 0{\cdot}156C_J^{3/2}. \end{aligned}\right\} \tag{37}$$

These functions of C_J are plotted over the range $0 \leqslant C_J \leqslant 5$ in Fig. 3. The coefficients ξ_α, ξ_ϑ which determine the distances behind the wing leading edge at which the two lift contributions $C_{L(\alpha)}$, $C_{L(\vartheta)}$

* It should be stressed that this is only true on the assumption that the downwash is given by $\epsilon = EC_L$. For an actual (three-dimensional) design, where the downwash relationship is certainly less simple, the required tail volume will depend on the actual values of ϵ and $\partial\epsilon/\partial\alpha$.

respectively act, are also functions of C_J, and values have been calculated from the information given in Table 3 of Spence's report and plotted here in Fig. 3. These curves can be fairly well approximated by the formulae

$$\left.\begin{aligned} \xi_\alpha &= 0{\cdot}25 - 0{\cdot}01 C_J, \\ \xi_\vartheta &= 0{\cdot}50 + 0{\cdot}077 C_J^{1/2}, \end{aligned}\right\} \tag{38}$$

and together with the formulae (37) these have been used as the basis for the numerical work of this Report. Some consideration was given to the possibility of approximating to (37) by series with fewer terms and also to the possibility of taking ξ_α and ξ_ϑ to be constant. Since, however, the computational effort involved in the use of (37) and (38) was not prohibitively large, the author has preferred to work with these formulae, knowing that it could then truly be claimed that the results of the investigation are based on Spence's theoretical results.

In the ensuing sub-sections of Section 4, the derivation of the numerical results presented in Figs. 4 to 18 is described without comment on the results themselves which are, however, discussed at length in Section 5.

4.1. *Trimmed Rectilinear Flight.* Equations (10) to (12) were used with (37) and (38), to compute curves of C_{Ls}, A_s, B_s, $(\xi_\alpha)_s$ and $(\xi_\vartheta)_s$ against α_s for three values of the thrust/weight ratio $\lambda : 0{\cdot}2$, $0{\cdot}3$ and $0{\cdot}4$, and for four values of the jet deflection $\vartheta : 0{\cdot}2$, $0{\cdot}5$, $0{\cdot}75$ and $1{\cdot}0$ radian, in each case. These curves are shown in Figs. 4 to 6. It was found that the various curves could be reasonably well approximated by straight lines over most of the incidence range so that the five coefficients could be expressed as

$$\left.\begin{aligned} C_{Ls} &= Q + P\alpha_s, \quad (\xi_\alpha)_s = q_3 + p_3\alpha_s, \\ A_s &= q_1 + p_1\alpha_s, \quad (\xi_\vartheta)_s = q_4 + p_4\alpha_s, \\ B_s &= q_2 + p_2\alpha_s. \end{aligned}\right\} \tag{39}$$

Values of P, Q, p_1, q_1, etc. were determined by inspection and have been indicated on the appropriate curves.

4.1.1. *Tail volume and c.g. position as determined by basic design conditions.* The basic design condition was taken as: $\bar{\lambda} = 0{\cdot}3$, $\bar{\vartheta} = 1$ radian, $\bar{\alpha} = \bar{\eta}_T = 0$, with α-restoring margin $\bar{K}_{r\alpha}$ as a disposable parameter. Tailplane lift slope a_1 and downwash coefficient E (Equation (16)) were taken as $a_1 = 2\pi$, $E = 0{\cdot}025$.*

From Figs. 5a, b, c the following values were obtained:

$\bar{C}_L = 5{\cdot}3$, $\bar{A} = 9{\cdot}6$, $\bar{B} = 5{\cdot}3$, $\bar{\xi}_\vartheta = 0{\cdot}596$, $\bar{\xi}_\alpha = 0{\cdot}234$.

Equations (35) give

$$\left.\begin{aligned} \bar{V} &= 0{\cdot}553 + 1{\cdot}53\bar{K}_{r\alpha}, \\ h &= 0{\cdot}509 - 0{\cdot}24\bar{K}_{r\alpha}, \\ \bar{K}_{r\vartheta} &= 0. \end{aligned}\right\} \tag{40}$$

$\bar{V}$, h and $\bar{K}_{r\vartheta}$ are plotted against $\bar{K}_{r\alpha}$ in Fig. 7 which also shows corresponding curves for alternative design cases in which trim at zero incidence is achieved with $\bar{\eta}_T = 0{\cdot}1$ and $\bar{\eta}_T = -0{\cdot}1$ respectively, instead of $\bar{\eta}_T = 0$.

* This value of E was selected before the results of Miss Ross's downwash investigation became available. These would suggest a value of about $0{\cdot}016$ for a typical two-dimensional configuration but the higher value assumed here is probably more realistic if the results are to be applied (qualitatively) to actual (three-dimensional) configurations.

When $\bar{\eta}_T \neq 0$, $\bar{V}$, h, $\bar{K}_{r\vartheta}$ must be calculated from (18), (19) and (20) respectively which, in the present example, become

$$\bar{V} = 1{\cdot}53\,\frac{F}{G_1},$$

$$h = 0{\cdot}76\,\frac{F}{G_1} + 0{\cdot}234 - \bar{K}_{r\alpha},$$

$$\bar{K}_{r\vartheta} = 0{\cdot}362 - \frac{F}{G_1} + \bar{K}_{r\alpha},$$

with

$$\frac{F}{G_1} = \frac{\bar{B}\bar{\vartheta}(\bar{x}_\vartheta - \bar{x}_\alpha + \bar{K}_{r\alpha})}{\bar{B}\bar{\vartheta} - \bar{A}\bar{\eta}_T}, \text{ from (14b) and (17)},$$

reducing to

$$\frac{F}{G_1} = (0{\cdot}362 + \bar{K}_{r\alpha})/(1 - 1{\cdot}812\bar{\eta}_T).$$

For the two values of $\bar{\eta}_T$ assumed here, we finally obtain:

$$\text{For } \bar{\eta}_T = -0{\cdot}1 \begin{cases} \bar{V} = 0{\cdot}468 + 1{\cdot}296\bar{K}_{r\alpha}, \\ h = 0{\cdot}467 - 0{\cdot}356\bar{K}_{r\alpha}, \\ \bar{K}_{r\vartheta} = 0{\cdot}055 + 0{\cdot}153\bar{K}_{r\alpha}. \end{cases} \tag{41}$$

$$\text{For } \bar{\eta}_T = 0{\cdot}1 \quad \begin{cases} \bar{V} = 0{\cdot}675 + 1{\cdot}868\bar{K}_{r\alpha}, \\ h = 0{\cdot}570 - 0{\cdot}072\bar{K}_{r\alpha}, \\ \bar{K}_{r\vartheta} = -(0{\cdot}080 + 0{\cdot}221\bar{K}_{r\alpha}). \end{cases} \tag{42}$$

4.1.2. *Effect of downwash assumptions on required tail volume and c.g. position.* To give some idea of how sensitive the required tail volume and c.g. position are to the particular downwash assumptions made in their calculations, $\bar{V}$ and h have been estimated for the basic design condition, ($\bar{\alpha} = \bar{\eta}_T = 0$) using the downwash equation in the form (22):

$$\epsilon = E_1 C_{L(\alpha)} + E_2 C_{L(\vartheta)}$$

and assigning various pairs of values to the coefficients E_1, E_2. The results are given in equation form in the following table and plotted in Fig. 8.

E_1	E_2	Tail volume $\bar{V}$	c.g. Position: h
0·025	0·025	$0{\cdot}553 + 1{\cdot}53\ \bar{K}_{r\alpha}$	$0{\cdot}509 - 0{\cdot}240\ \bar{K}_{r\alpha}$
0·050	0·050	$0{\cdot}553 + 1{\cdot}53\ \bar{K}_{r\alpha}$	$0{\cdot}422 - 0{\cdot}481\ \bar{K}_{r\alpha}$
0·025	0·020	$0{\cdot}582 + 1{\cdot}606\ \bar{K}_{r\alpha}$	$0{\cdot}524 - 0{\cdot}201\ \bar{K}_{r\alpha}$
0·050	0·040	$0{\cdot}613 + 1{\cdot}692\ \bar{K}_{r\alpha}$	$0{\cdot}443 - 0{\cdot}424\ \bar{K}_{r\alpha}$
0·020	0·025	$0{\cdot}528 + 1{\cdot}458\ \bar{K}_{r\alpha}$	$0{\cdot}514 - 0{\cdot}228\ \bar{K}_{r\alpha}$
0·040	0·050	$0{\cdot}505 + 1{\cdot}393\ \bar{K}_{r\alpha}$	$0{\cdot}438 - 0{\cdot}438\ \bar{K}_{r\alpha}$

4.1.3. *Variation of trimmed incidence and lift coefficient with changes of control settings.* (1) *Variation with tailplane setting* ($\bar{\eta}_T$). Suppose $\bar{V}$ and h have been determined with reference to a specific design condition (Fig. 7) and that it is required to find the variation of trimmed incidence α_s and lift coefficient C_{Ls} as η_T is varied, with λ and ϑ fixed. For a selected value of α_s, values of A_s, B_s, $(\xi_\alpha)_s$, $(\xi_\vartheta)_s$ may be obtained from Figs. 4 to 6 for the appropriate values of λ and ϑ. Values of $C_{L(\alpha)} = A_s\alpha_s$ and $C_{L(\vartheta)} = B_s\vartheta$ may then be calculated and also values of $K_{r\alpha}$, $K_{r\vartheta}$, from Equations (21b). The tail setting $\bar{\eta}_T$ to produce trim at incidence α_s then follows by equating the pitching-moment coefficient C_m (Equation (21a)) to zero; thus

$$\eta_T = \frac{-1}{\bar{V}a_1}(K_{r\alpha}\, C_{L(\alpha)} + K_{r\vartheta}\, C_{L(\vartheta)}). \tag{43}$$

Figs. 9 and 10 give curves of α_s and C_{Ls} versus η_T with λ and ϑ fixed at their design condition values $\bar{\lambda}$ (= 0·3) and $\bar{\vartheta}$ (= 1 rad); Fig. 9 relates to the case $\alpha_s = 0$ when $\eta_T = 0$, Fig. 10 to the case $\alpha_s = 0$ when $\eta_T = -0{\cdot}1$ rad. Fig. 11 shows the variation of α_s and C_{Ls} with η_T when $\lambda = \bar{\lambda} = 0{\cdot}3$, $\vartheta = 0{\cdot}2$ rad ($\neq \bar{\vartheta}$), the design conditions being as for Fig. 9.

(2) *Variation with jet deflection* (ϑ) *and with thrust/weight ratio* (λ). With the downwash assumption of Equation (16), the trim condition (13) may be written

$$[A_s\{h - (\xi_\alpha)_s\} - \bar{V}a_1(1 - EA_s)]\alpha_s + B_s\{h - (\xi_\vartheta)_s + E\bar{V}a_1\}\vartheta - a_1\bar{V}\bar{\eta}_T = 0. \tag{44}$$

If the linear approximations of Equations (39) (*see* also Figs. 4 to 6), are substituted in the above equation, and squares and higher powers of α_s are neglected, the following approximate linear equation for trimmed incidence α_s (valid for small incidences) is obtained:

$$\begin{aligned}[q_1(q_3 - h) + \bar{V}a_1(1 - Eq_1) + \{p_2(q_4 - h - E\bar{V}a_1) + p_4q_2\}\vartheta]\alpha_s \\ = -q_2(q_4 - h - E\bar{V}a_1)\vartheta - \bar{V}a_1\bar{\eta}_T\end{aligned} \tag{45}$$

With $a_1 = 2\pi$, $E = 0{\cdot}025$, $\bar{\eta}_T = 0$, this becomes

where

$$\left.\begin{aligned}&\{Cq_1 + 2\pi\bar{V} + (Dp_2 + p_4q_2)\vartheta\}\alpha_s = -Dq_2\vartheta,\\ &C = q_3 - h - 0{\cdot}157\bar{V},\\ &D = q_4 - h - 0{\cdot}157\bar{V}.\end{aligned}\right\} \tag{46}$$

Since the p's and q's are functions of λ and ϑ only (*see* Figs. 4 to 6), while h and $\bar{V}$ are fixed by the given basic design condition (*see* Fig. 7), Equations (46) may be used to obtain curves of α_s vs. ϑ_s for $\lambda = \bar{\lambda}$ with various values of $\bar{K}_{r\alpha}$, and curves of α_s vs. λ for $\vartheta = \bar{\vartheta}$ with various values of $\bar{K}_{r\alpha}$. Once α_s has been determined, the corresponding $C_{Ls} = A_s\alpha_s + B_s\vartheta$ ($\approx Q + P\alpha_s$) can be calculated, while the values of the restoring margins $K_{r\alpha}$, $K_{r\vartheta}$ follow from Equations (21b).

The above procedure has been followed in deriving Figs. 12 to 16. Figs. 12 and 13 show the variations of trimmed incidence and lift coefficient and of the restoring margins $K_{r\alpha}$, $K_{r\vartheta}$ with jet-flap deflection for various values of the design restoring margin $\bar{K}_{r\alpha}$, (0·05, 0·1, 0·2, 0·3) the tail-plane being fixed at zero incidence and the jet thrust/weight ratio λ fixed at the design value $\bar{\lambda}$. Figs. 14 and 15 provide similar information for the case where the jet-flap deflection is fixed at the

design value $\bar{\vartheta}$ and the jet thrust/weight ratio λ is varied, while Fig.16 gives the variations of trimmed incidence and lift coefficient with flap deflection and thrust/weight ratio for the particular combination of tail volume and c.g. position corresponding to $\overline{K}_{r\alpha} = 0{\cdot}2$.

4.2. *Constant Speed Manoeuvres.* Configurations corresponding to the basic design conditions $\bar{\lambda} = 0{\cdot}3$, $\bar{\vartheta} = 1$ rad, $\bar{\alpha} = \bar{\eta}_T = 0$, $\overline{K}_{r\alpha} = 0{\cdot}05$, $0{\cdot}1$, $0{\cdot}2$ or $0{\cdot}3$ have again been considered, with $a_1 = 2\pi$ and $E = 0{\cdot}025$. To evaluate the control effectiveness parameter $\partial n/\partial\lambda$ (or its inverse, the increment of thrust/weight ratio per g) from Equations (34) or (36) it is necessary to obtain expressions for the partial derivatives of A, B, ξ_α, ξ_ϑ with respect to λ, at constant speed. In the steady circle, initiated from a trimmed condition with lift coefficient C_{Ls}:

$$C_J = \frac{\lambda}{\lambda_s} C_{Js} = \lambda C_{Ls},$$

so that

$$\frac{\partial}{\partial\lambda} = \frac{\partial C_J}{\partial\lambda}\frac{\partial}{\partial C_J} = C_{Ls}\frac{\partial}{\partial C_J}.$$

Hence, from (37) and (38)

$$\left.\begin{aligned} \frac{\partial A}{\partial\lambda} &= C_{Ls}(0{\cdot}576 {C_{Js}}^{-1/2} + 1{\cdot}106 + 0{\cdot}0765 {C_{Js}}^{1/2}), \\ \frac{\partial B}{\partial\lambda} &= C_{Ls}(1{\cdot}773 {C_{Js}}^{-1/2} + 0{\cdot}325 + 0{\cdot}234 {C_{Js}}^{1/2}), \\ \frac{\partial\xi_\alpha}{\partial\lambda} &= -0{\cdot}01 C_{Ls};\ \frac{\partial\xi_\vartheta}{\partial\lambda} = 0{\cdot}0385 C_{Ls}\, {C_{Js}}^{-1/2}. \end{aligned}\right\} \tag{47}$$

4.2.1. *Manoeuvres initiated from the basic design condition.* If the aircraft is initially in trim at zero incidence with $\lambda = \bar{\lambda} = 0{\cdot}3$, $\vartheta = \bar{\vartheta} = 1$ radian, $\eta_T = \bar{\eta}_T = 0$, then $C_{Ls} = \bar{C}_L = 5{\cdot}3$, $B_s = \bar{B} = 5{\cdot}3$, $C_{Js} = 1{\cdot}59$ and from Equations (36) and (47) we obtain

$$\left.\begin{aligned} \frac{\partial n}{\partial\lambda} &= \frac{1}{5{\cdot}3\overline{H}_{m\alpha}}[10{\cdot}746\overline{K}_{r\alpha} - 0{\cdot}859], \\ \frac{\partial n}{\partial\vartheta} &= \frac{\overline{K}_{r\alpha}}{\overline{H}_{m\alpha}}, \\ \frac{\partial n}{\partial\eta_T} &= -\frac{2\pi\overline{V}}{5{\cdot}3\overline{H}_{m\alpha}}, \end{aligned}\right\} \tag{48}$$

where

$$\overline{H}_{m\alpha} = \overline{K}_{r\alpha} - \frac{l_T}{c}\frac{m_q}{\mu_1}.$$

If rotary damping m_q is taken as due to tail only, *i.e.*, $m_q = -\frac{1}{2}a_1(S_T/S)$, then

$$\overline{H}_{m\alpha} = \overline{K}_{r\alpha} + \frac{a_1\overline{V}}{2\mu_1} = \overline{K}_{r\alpha} + \frac{\pi\overline{V}}{\mu_1} \text{ if } a_1 = 2\pi.$$

For illustrative purposes a value of 10π has been assumed for μ_1, giving

$$\bar{H}_{m\alpha} = \bar{K}_{r\alpha} + \frac{\bar{V}}{10},$$

in which case, the control actions per g are given by

$$\left.\begin{aligned} \frac{\partial\lambda}{\partial n} &= \left(\bar{K}_{r\alpha} + \frac{\bar{V}}{10}\right)\Big/(2{\cdot}028\bar{K}_{r\alpha} - 0{\cdot}162), \\ \frac{\partial\vartheta}{\partial n} &= 1 + \frac{\bar{V}}{10\bar{K}_{r\alpha}}, \\ \frac{\partial\eta_T}{\partial n} &= 0{\cdot}8435\left(\bar{K}_{r\alpha} + \frac{\bar{V}}{10}\right)\Big/\bar{V}, \end{aligned}\right\} \tag{49}$$

with

$$\bar{V} = 0{\cdot}553 + 1{\cdot}53\bar{K}_{r\alpha};$$

in accordance with Equation (40).

In Fig. 17, values of the control actions per g, calculated from (49) are exhibited as functions of the design restoring margin $\bar{K}_{r\alpha}$; curves calculated on the assumption of no rotary damping are shown for comparison.

4.2.2. *Manoeuvres initiated from other trimmed conditions.* The basic design condition is essentially a high lift condition corresponding to take-off or landing. For cruising at moderate or low lift coefficients, smaller jet deflections will be employed and it is thus necessary to consider the comparative manoeuvrability, using the various controls, under such conditions. For illustrative purposes, it has been assumed that in trimmed cruising flight the thrust/weight ratio λ retains its basic design value $\bar{\lambda} = 0{\cdot}3$. Equations (34) have been used in conjunction with (47) to calculate $\partial\lambda/\partial n$, $\partial\vartheta/\partial n$ and $\partial\eta_T/\partial n$ for a range of values of ϑ and for various values of the design restoring margin $\bar{K}_{r\alpha}$. The results are shown in Fig. 18 as graphs of the quantities in question against ϑ for the various $\bar{K}_{r\alpha}$. Curves of equal trimmed lift coefficient C_{Ls} are also indicated in the figures.

5. *Discussion.* It has been assumed that from the stability and control point of view, a jet-flapped aircraft would be designed around a certain high-lift condition which has been referred to as the 'basic design condition'. For the purposes of illustration, the values of the jet-flap control parameters λ and ϑ corresponding to this condition have been fixed as $\lambda = \bar{\lambda} = 0{\cdot}3$ and $\vartheta = \bar{\vartheta} = 1$ radian, while for the most part it has been assumed that with these control settings the aircraft will trim at zero incidence with zero tail setting. The combination of tail volume $\bar{V}$ and c.g. position $\bar{h}$, required to achieve this depends (*see* Fig. 7) on the value assigned to the parameter $\bar{K}_{r\alpha}$—the design restoring margin. A suitable value must be selected from a consideration of the trim and manoeuvrability characteristics exhibited in Figs. 9 to 12, 14 and 16 to 18. The choice may be influenced by the consideration of whether the role of the jet-flap is to be simply that of a lift-augmenter, leaving the trimming and manoeuvring to be accomplished by tail controls, or whether the jet-flap controls themselves are to be employed to control the aircraft longitudinally.

With the jet-flap employed purely to augment lift, it is seen from Figs. 9 and 11 that the trim curves have stable slopes for all values of the design restoring margin ($\bar{K}_{r\alpha}$) considered, both in

the high-lift case ($\vartheta = \bar{\vartheta} = 1$ rad) and under cruising conditions with $\vartheta = 0{\cdot}2$ rad. Since the required tail volume increases with $\bar{K}_{r\alpha}$ (Fig. 7) it is desirable to design for the smallest restoring margin consistent with satisfactory manoeuvring characteristics. It is worth noting from Fig. 13 that for a given value of the design restoring margin $\bar{K}_{r\alpha}$, the restoring margin $K_{r\alpha}$ increases as the jet deflection decreases so that if an adequate stability margin is provided in the design condition (high lift), the margin will certainly be adequate in the cruising condition with small jet deflection. Conversely, if the jet-flap deflection is increased beyond the basic design condition value, the α-restoring margin will be reduced and care must therefore be exercised to ensure that it cannot become dangerously small within the useable range of flap deflections. It should also be noted from Fig. 15, that $K_{r\alpha}$ is a decreasing function of the thrust/weight ratio λ and that this may limit the amount by which λ may be increased beyond the basic design value $\bar{\lambda}$.

Figs. 17c and 18c show that the tailplane deflection per g in constant speed manoeuvres increases with $\bar{K}_{r\alpha}$ and in attempting to strike a balance between an excessive value under high lift conditions and too small a value under cruising conditions, we are led to suggest a value for the restoring margin in the range $0{\cdot}1 \leqslant \bar{K}_{r\alpha} \leqslant 0{\cdot}2$ provided that it is not intended to operate with values of ϑ or λ much in excess of the design values $\bar{\vartheta}$ and $\bar{\lambda}$.

If deflection of the jet-flap is used to trim the aircraft with fixed tailplane and fixed throttle setting, the trimmed lift coefficient increases progressively with increasing flap deflection for all values of $\bar{K}_{r\alpha}$ in the range $0{\cdot}05$ to $0{\cdot}30$ (*see* Fig. 12a). There is some variation in the trimmed incidence (Fig. 12b) from the zero value corresponding to the basic design condition. The deviation from zero decreases with increasing $\bar{K}_{r\alpha}$ and for a given value of the restoring margin, attains a maximum for a value of ϑ equal to about $0{\cdot}7\bar{\vartheta}$. Thus, to minimize the variations in trimmed incidence, $\bar{K}_{r\alpha}$ should be made as large as possible. From Fig. 17b it is seen that, provided there is some rotary damping, the jet-flap deflection per g in constant speed manoeuvres (initiated from the basic design condition) tends to infinity as $\bar{K}_{r\alpha}$ tends to zero; clearly, a fairly large restoring margin ($\geqslant 0{\cdot}2$ say) is necessary in order to keep the flap deflection per g reasonably close to the asymptotic value of 1 radian per g in the basic design condition. However, it seems unlikely that jet-flap deflection control would be used in the high-lift case, while under cruising conditions (*see* Fig. 18b) the jet-flap deflection per g is not critically dependent on the value of $\bar{K}_{r\alpha}$.

If throttle (λ) — control is to be used for re-trimming or manoeuvring when the aircraft is initially in the basic design condition, it is clear from Figs. 14 and 17a that a restoring margin $\bar{K}_{r\alpha}$ of at least $0{\cdot}2$ must be achieved. For, on the one hand, if $\bar{K}_{r\alpha}$ is much less than $0{\cdot}2$, the negative incidence acquired as the result of increasing λ will be such as to cause a net reduction in trimmed lift. On the other hand, as can be seen from Fig. 17a, the increment in jet thrust/weight ratio per g ($\partial\lambda/\partial n$) tends to infinity as $\bar{K}_{r\alpha}$ decreases towards a value of (approximately) $0{\cdot}08$. It will be observed that the asymptote for $\partial\lambda/\partial n$ (Fig. 17a) is $\bar{K}_{r\alpha} = 0{\cdot}08$ and not $\bar{K}_{r\alpha} = 0$, as in the case of $\partial\vartheta/\partial n$ (Fig. 17b). This is explained by the presence in the expression for $\partial n/\partial\lambda$ (Equations (36)), of the term involving $\partial\xi_\vartheta/\partial\lambda$, which arises from the fact that ξ_ϑ varies with the jet coefficient C_J (*see* Fig. 3). If the approximation ξ_ϑ = constant had been made at the outset, the term in question would, of course, have disappeared and the asymptote for $\partial\lambda/\partial n$ would then have been $\bar{K}_{r\alpha} = 0$.

To sum up: it may be concluded that if the jet-flap controls are to be used to trim and manoeuvre the aircraft, a value of at least $0{\cdot}2$ should be assigned to the design restoring margin $\bar{K}_{r\alpha}$. If, however, tail controls are to be employed, a value of $0{\cdot}1$ may well be adequate and certainly it should not be necessary to design for a value greater than $0{\cdot}2$.

The following table compares the effectiveness of the various controls on the basis of the respective control actions per g in constant speed manoeuvres, initiated from a high-lift (basic design) condition and from a cruising condition ($C_L = 0{\cdot}3$) respectively.

				High-lift (basic design) condition: $C_L = 5{\cdot}3$ ($\lambda = \bar{\lambda} = 0{\cdot}3$, $\vartheta = \bar{\vartheta} = 57{\cdot}3$ deg, $\eta_T = \bar{\eta}_T = 0$)			Cruise condition $C_L = 0{\cdot}3$ ($\lambda = 0{\cdot}3$, $\vartheta = 12{\cdot}6$ deg)		
Type of control	$\overline{K}_{r\alpha}$	Tail vol. $\overline{V}$	c.g. position h	$\frac{\partial\lambda}{\partial n}$ ($\Delta\lambda$ per g)	$\frac{\partial\vartheta}{\partial n}$ (deg/g)	$\frac{\partial\eta_T}{\partial n}$ (deg/g)	$\frac{\partial\lambda}{\partial n}$ ($\Delta\lambda$ per g)	$\frac{\partial\vartheta}{\partial n}$ (deg/g)	$\frac{\partial\eta_T}{\partial n}$ (deg/g)
Jet-flap	0·2	0·858	0·460	1·17	82	—	0·75	17·2	—
Tail	0·2	0·858	0·460	—	—	16·1	—	—	1·72
	0·1	0·705	0·485	—	—	11·7	—	—	1·5

For the purposes of further argument, let us assume that $\bar{\lambda}/\lambda_{\max} = \bar{\vartheta}/\vartheta_{\max} = 0{\cdot}75$ so that $\lambda_{\max} = 0{\cdot}4$ and $\bar{\vartheta}_{\max} = 76{\cdot}5$ deg, and also that the tailplane travel available for control purposes is $\pm$ 5 deg. Then in the high-lift condition rather less than 1/10 g and 1/4 g could be applied respectively by throttle control ($\Delta\lambda = 0{\cdot}1$) and flap deflection control ($\Delta\vartheta = 19{\cdot}2$ deg) whereas, with tailplane control, more than $3/10g$ could be applied if $\overline{K}_{r\alpha} = 0{\cdot}2$, while with $\overline{K}_{r\alpha}$ reduced to 0·1, this figure would be increased to more than 2/5 g.*

Under cruising conditions ($C_L = 0{\cdot}3$) the maximum available increment 0·1 in λ would produce only 0·133 g, 10 degrees of jet-flap deflection would give 0·58 g while, according as $\overline{K}_{r\alpha} = 0{\cdot}2$ or 0·1, $-$ 5 degrees of tailplane deflection should produce 2·9 g or 3·3 g respectively.

Although the amount of 'g' produced by a specified control action provides a valid basis of comparison between the effectiveness of different controls, it does not, perhaps, give a very clear idea as to the adequacy or otherwise of a particular control, especially at the unusually high C_L's (and hence low speeds) which are under consideration. The radius of turn produced by the given control action may possibly serve as a more useful criterion in these circumstances.

The radius of turn corresponding to unit incremental load factor is given by U^2/g where U, the forward speed, is given by $U^2 = 2\,(W/S)/\sigma\rho_0 C_{Ls}$, σ being the relative air density and $\rho_0 = 0{\cdot}002378$ slugs/ft^3, the standard sea-level density. For low-level flight ($\sigma = 1$) with a wing loading of 35 lb/ft^2 at a lift coefficient of $C_{Ls} = 5{\cdot}3$, the forward speed is 74·5 ft/sec and the radius of turn for unit incremental load factor is 172·5 ft. Thus, in the example cited above for the aircraft with $\overline{K}_{r\alpha} = 0{\cdot}2$, trimmed in the basic design condition, the maximum available increment of thrust $\Delta\lambda = 0{\cdot}1$ would

* The figures are approximate inasmuch as it has been assumed that $\Delta n = \Delta\lambda\, \partial n/\partial\lambda$ etc. for finite increments $\Delta\lambda$ etc., which is not strictly valid. It should also be noted that realization of the figures quoted for tailplane control is dependent on the maintenance of unseparated flow over the aerofoil when positive incidence is acquired as the result of control application (*see* first footnote to Section 3).

produce a radius of turn in the pull-up of about 2000 ft. In 1 second the flight path would turn through about 2 deg, and in covering a forward distance of 74·5 ft, the aircraft would rise about 1·2 ft.

For an aircraft with $\bar{K}_{r\alpha}$ reduced to 0·1 and trimmed to the same high-lift condition, a tailplane deflection of -5 deg would produce a radius of turn of about 400 ft. In a second, the flight path would turn through nearly 11 deg and, in covering a forward distance of 74·5 ft, the aircraft would rise about 6·8 ft.

These calculations are, of course, based on the steady manoeuvring flight condition and take no account of the initial response characteristics, investigation of which lies outside the scope of the present Report.* However, it is evident that on the basis of the ultimate (steady) response achieved, variation of jet thrust alone is not a very effective method of longitudinal control at low speed and in this respect, at least, it would seem to compare unfavourably with tailplane control which, on the same basis, appears to be somewhat superior to jet-flap deflection control for the cruising condition.

It will have been noted from Fig. 17 and the foregoing discussion, that with jet controls (Figs. 17a and b), the manoeuvrability increases with increasing stability whereas with conventional (tail) controls (Fig. 17c) manoeuvrability decreases with increasing stability. This reversal of the usual state of affairs was observed by I. M. Davidson in Ref. 5, and it may be helpful to look a little more closely at the physical reasons which account for it.

Consider the aircraft trimmed in the basic design condition, for which the incidence is zero. Then with the simplifying assumptions made in Section 2, the resultant lift on the *complete* aircraft (L) is simply $L(\vartheta)$, acting through the centre of jet deflection loading N_ϑ, with which, in this condition, the centre of gravity G must clearly coincide (*i.e.*, $K_{r\vartheta}$ must be zero). This is illustrated in Fig. 19a, which may be compared with Fig. 2 for the more general case of non-zero incidence.

Suppose now control is applied by deflecting the jet-flap, with thrust maintained constant. Then, instantaneously, of the two lift components $L(\vartheta)$ and $L(\alpha)$ $(= 0)$, only the former is changed —by an amount $\Delta L(\vartheta)$ say—where the increment $\Delta L(\vartheta)$ acts through N_ϑ.† Motion in a vertical circle now ensues with incremental normal acceleration Δn. If rotary damping forces can be neglected, $\Delta L(\vartheta)$ continues to act through N_ϑ and the balance of forces (including reversed mass-accelerations) is as illustrated in Fig. 19b. At no time are α-forces involved and the normal acceleration produced is independent of the position of N_α, *i.e.*, independent of the design restoring margin $\bar{K}_{r\alpha}$, as we have already observed in Fig. 17b.

The effect of damping forces in the steady circle is to move the point of application of $\Delta L(\vartheta)$ aft, by an amount $\Delta\xi c$, to a point M_ϑ which, by analogy with conventional aircraft manoeuvrability theory, may be called 'the manoeuvre point with respect to jet deflection'. (In general, $\Delta\xi = -(l_T/c)\,(m_q/\mu_1)$ while, if tail damping only is taken into account, $\Delta\xi = a_1\bar{V}/(2\mu_1)$). Since $(\Delta L\vartheta)$ now acts behind the centre of gravity, the aircraft will acquire a negative incidence such that the corresponding (negative) lift increment $\Delta L(\alpha)$ provides the necessary counterbalancing moment to restore equilibrium. The point of application of $\Delta L(\alpha)$ will be M_α, 'the manoeuvre point with respect to incidence', which lies at a distance $\Delta\xi c$ behind N_α, which is itself a distance $\bar{K}_{r\alpha}c$ behind

---

* *Footnote* (1961). The response calculations of Part II indicate a need to modify, in some respects, the conclusions derived from quasi-steady manoeuvrability theory.

† It should be remembered that this takes account of the moment effect due to the tail forces brought into play by the wing lift increment $\Delta L(\vartheta)$.

the c.g. The system of forces is now as shown in Fig. 19c and by taking moments about the c.g. it is easily shown that the net increase in lift is given by

$$\frac{\Delta L}{\Delta L(\vartheta)} = \frac{\Delta L(\vartheta) + \Delta L(\alpha)}{\Delta L(\vartheta)} = \frac{\overline{K}_{r\alpha}}{\overline{K}_{r\alpha} + \Delta\xi}.$$

(It should be noted that this formula is applicable only when the aircraft is trimmed initially in the basic design condition for which $K_{r\vartheta} = 0$). Clearly the effectiveness of the jet-flap deflection control is always reduced by rotary damping, but by an amount that decreases with increasing design restoring margin $\overline{K}_{r\alpha}$. Thus, as already observed, manoeuvrability increases with increasing stability.

Similar arguments may be produced to explain the form of the curves in Fig. 17a, which shows increment in jet thrust/weight ratio per g plotted against $\overline{K}_{r\alpha}$. Here it may be noted that when the thrust is varied, C_J is changed and consequently, in addition to a change in the lift component $C_{L(\vartheta)}$, there is also a shift of the centre of loading N_ϑ. Thus, even in the case where damping is neglected, there will be a moment about the c.g. which results in a change of incidence and the introduction of α-forces, so that manoeuvrability varies with restoring margin whether damping is neglected or included.

6. *Conclusions.* The following are the salient points which emerge from the foregoing discussion:

(1) The present investigation has produced no evidence that would rule out the use of the jet-flap controls (throttle and flap deflection) as an alternative to conventional tail controls for trimming and manoeuvring a jet-flapped aircraft in the longitudinal plane. Nevertheless, on the basis of the steady manoeuvrability criterion (control action per g) jet controls would appear to be less effective than tail controls. For a complete assessment of relative merits, an investigation of dynamic response characteristics must be made (*see* Part II).

(2) Tailplane size and centre of gravity position may probably best be determined to satisfy a prescribed high-lift condition in which the jet thrust/weight ratio λ and the jet-flap deflection ϑ have values of (say) $0{\cdot}75\,\lambda_{max}$ and $0{\cdot}75\,\vartheta_{max}$ respectively. For the purpose of numerical illustration, it has been assumed, in this Report, that with such a combination of control settings, the aircraft is required to trim at zero incidence with zero tail setting. Considerations of trim and manoeuvrability throughout the speed range then suggest that a restoring margin (with respect to incidence changes) $\overline{K}_{r\alpha}$ of at least $0{\cdot}2$ should be provided in this 'basic design condition', if jet controls are to be used. This necessitates a tail volume ratio of about $0{\cdot}86$ with centre of gravity located at $0{\cdot}46c$. To provide a larger restoring margin, the tail volume would have to be increased and the centre of gravity moved forward.

If tail controls are to be used instead of jet controls, a design restoring margin of less than $0{\cdot}2$ will probably suffice. If, for instance, $\overline{K}_{r\alpha} = 0{\cdot}1$, a tail volume of only $0{\cdot}705$ is required with centre of gravity at $0{\cdot}485c$.

(3) For a jet-flapped aircraft, under high-lift conditions, manoeuvrability with jet controls increases with stability (as measured by the design restoring margin $\overline{K}_{r\alpha}$). This is, of course, the reverse of the tendency exhibited by an aircraft of orthodox design and also by a jet-flapped aircraft employing tail controls. Control actions per g in the basic design condition, with jet controls, decrease with increasing $\overline{K}_{r\alpha}$, tending asymptotically to values which compare rather unfavourably with the values of tailplane deflection per g which may be achieved with a reasonably small value (say $0{\cdot}1$)

of $\bar{K}_{r\alpha}$ (*see* Fig. 17). Because of the penalty of increasing tailplane size, it is clearly not profitable to increase $\bar{K}_{r\alpha}$ beyond about 0·3 in the case where jet controls are used, because the improvement in manoeuvrability thereby achieved is no longer worthwhile.

In conclusion, attention must be drawn to the limitations of the present investigation:

(*a*) The analysis has been based on two-dimensional theoretical data so that the results should not be applied to jet-flapped aircraft with low-aspect-ratio wings. For lay-outs of moderately high or high aspect ratio, the conclusions should be at least qualitatively valid.

(*b*) Numerical results depend fairly critically on the assumptions made as regards the downwash at the tail (*see* Fig. 8) even when, as here, the investigation is based on two-dimensional data. Reliable data regarding the downwash field behind three-dimensional jet-flapped wings would be an essential pre-requisite for a stability and control analysis of a jet-flapped aircraft with a moderate or small-aspect-ratio wing.

(*c*) Only trim, static stability and quasi-steady manoeuvrability have been considered here. For a complete appraisal of the relative merits of jet and tail controls, it is necessary to study dynamic response characteristics; this has been done in Part II.

LIST OF SYMBOLS

A, B — Coefficients defined by Equation (1) (functions of C_J only)

C — *See* Equations (46)

C_J — Jet coefficient $= J/\frac{1}{2}\rho U^2 c$

C_L — Total wing lift coefficient

$C_{L(\alpha)}$, $C_{L(\vartheta)}$ — Component lift coefficients (Equation (1)), proportional to α and ϑ respectively for a given C_J.

C_{LT} — Tail lift coefficient

C_m — Pitching-moment coefficient of complete aircraft referred to c.g.

D — *See* Equations (46)

E — Downwash constant (Equation (16))

E_1, E_2 — Downwash constants (Equation (22))

F, G — Defined by Equations (14b)

G_1 — Defined by Equation (17)

$H_{m\alpha} = K_{r\alpha} - \frac{l_T}{c}\frac{m_q}{\mu_1}$ ('α-manoeuvre margin')

J — Gross jet thrust per unit length

$K = \frac{B}{A}$ (Equation (55) of Appendix)

$K_{r\alpha} = -\frac{\partial C_m}{\partial C_{L(\alpha)}}$: aircraft restoring margin with respect to change of incidence

$K_{r\vartheta} = -\frac{\partial C_m}{\partial C_{L(\vartheta)}}$: aircraft restoring margin with respect to jet deflection

N_α, N_ϑ — Aerodynamic centres with respect to incidence and jet deflection respectively, for the complete aircraft

P — Coefficient of α_s in linear approximation for trimmed lift coefficient C_{Ls}: a function of λ and ϑ

Q — Term independent of α_s in linear approximation for C_{Ls}: a function of λ and ϑ

S, S_T — Wing and tailplane areas respectively

U — Free-stream velocity

$\bar{V}$ — Tail volume ratio

W — Weight of aircraft

X		Defined by Equation (59) of the Appendix
a_1		Tailplane lift slope: $\frac{\partial C_{LT}}{\partial \alpha_T}$
c		Wing chord
h		Distance of c.g. from leading edge of chord, as fraction of chord
$h_{r\alpha}$, $h_{r\vartheta}$		Values of h for which $K_{r\alpha}$, $K_{r\vartheta}$ are respectively zero (these correspond to the points N_α, N_ϑ on the aerofoil chord)
l_T		Tail arm measured from c.g. to aerodynamic centre of tailplane
m		Mass of aircraft
m_q	=	$\frac{c}{2l_T}\frac{\partial C_m}{\partial(ql/U)}$, rotary damping derivative
Δng		Additional normal acceleration (relative to steady rectilinear flight)
$p_1, \ldots p_4$		Coefficients of α_s in linear approximations for A_s, B_s, $(\xi_\alpha)_s$, $(\xi_\vartheta)_s$, respectively: functions of λ and ϑ
q		Angular velocity in pitch
$q_1, \ldots q_4$		Terms independent of α_s in linear approximations for A_s, B_s, $(\xi_\alpha)_s$, $(\xi_\vartheta)_s$ respectively: functions of λ and ϑ
α		Wing incidence
γ		Angle of inclination of flight path to horizontal in steady rectilinear flight
ϵ		Angle of downwash at tail
η_T		Tailplane setting relative to wing
ϑ		Angle between jet and wing chord
λ		Jet thrust/weight ratio
μ_1	=	$m/\rho S l_T$, aircraft relative density
ξ_α, ξ_θ		Distances aft of wing leading edge at which component lift coefficients $C_{L(\alpha)}$, $C_{L(\vartheta)}$ respectively act (as fractions of chord)
ρ		Air density
σ		Defined by Equation (54) of the Appendix

Prefix

Δ	increment

Suffix

$_s$	referring to steady rectilinear flight

A bar over a symbol (*e.g.*, $\bar{\vartheta}$) is used to denote the value appropriate to the basic design condition (except in $\bar{V} \equiv$ tail volume ratio).

REFERENCES

No.	*Author*	*Title, etc.*
1	A. S. Taylor	A preliminary examination of the stability and control problems associated with the design of a jet-flap aircraft with conventional tailplane and elevator. A.R.C. 18,208. June, 1955.
2	D. A. Spence	The lift coefficient of a thin jet-flapped wing. *Proc. Roy. Soc.* A. Vol. 238. pp. 46 to 63. 1956.
3	E. C. Maskell and D. A. Spence	A theory of the jet-flap in three-dimensions. *Proc. Roy. Soc.* A. Vol. 251. pp. 407 to 425. 1959.
4	A. J. Ross	The theoretical evaluation of the downwash behind jet-flapped wings. A.R.C. R. & M. 3119. January, 1958.
5	I. M. Davidson	Some notes on the shrouded jet-flap and flight without incidence. A.R.C. 16,139. August, 1953.

APPENDIX

An Alternative Formulation of the Trim and Manoeuvrability Analysis

The following method of analysis has been suggested by S. B. Gates.

If it is assumed that the downwash at the tailplane is given by the simple relationship

$$\epsilon = E\,C_L = E(C_{L(\alpha)} + C_{L(\vartheta)}), \tag{50}$$

where

$$C_{L(\alpha)} = A\alpha;\ C_{L(\vartheta)} = B\vartheta; \tag{51}$$

then using Equations (21) of the main text, we may write the trim equation as

$$K_{r\alpha}\,C_L + \sigma\vartheta + a_1\bar{V}\eta_T = 0, \tag{52}$$

where

$$K_{r\alpha} = \xi_\alpha - h + \frac{a_1\bar{V}}{A}(1-EA) \tag{53}$$

and

$$\begin{aligned}\sigma &= B(K_{r\vartheta} - K_{r\alpha}) \\ &= B(\xi_\vartheta - \xi_\alpha) - a_1\bar{V}K,\end{aligned} \tag{54}$$

with

$$K = \frac{B}{A}. \tag{55}$$

For a given design, $K_{r\alpha}$ and σ are functions of C_J only, where

$$C_J = \lambda C_L \tag{56}$$

in steady rectilinear flight.

Differentiating (52) and (56) we have

$$K_{r\alpha}\delta C_L + C_L K_{r\alpha}{}'\delta C_J + \sigma\delta\vartheta + \vartheta\sigma'\delta C_J + a_1\bar{V}\delta\eta_T = 0,$$

$$\delta C_J = \lambda\delta C_L + C_L\delta\lambda,$$

where primes denote differentiation with respect to C_J. Elimination of δC_J and collection of terms leads to

$$\{K_{r\alpha} + \lambda(K_{r\alpha}{}'C_L + \sigma'\vartheta)\}\,\delta C_L + (K_{r\alpha}{}'C_L + \sigma'\vartheta)C_L\delta\lambda + \sigma\delta\vartheta + a_1\bar{V}\delta\eta_T = 0, \tag{57}$$

giving

$$\left.\begin{aligned}\frac{\partial C_L}{\partial\lambda} &= -\frac{C_L}{\lambda}\frac{X}{K_{r\alpha}+X}, \\ \frac{\partial C_L}{\partial\vartheta} &= -\frac{\sigma}{K_{r\alpha}+X}, \\ \frac{\partial C_L}{\partial\eta_T} &= -\frac{a_1\bar{V}}{K_{r\alpha}+X},\end{aligned}\right\} \tag{58}$$

where

$$X = K_{r\alpha}{}'C_J + \sigma'\lambda\vartheta \tag{59}$$

is a function of C_J, $\lambda\vartheta$ for a given design.

the controls can be obtained. To illustrate the procedure, some sample calculations have been made with $\bar{V} = 0{\cdot}859$, $h = 0{\cdot}461$, $E = 0{\cdot}025$, $a_1 = 2\pi$, which correspond to a 'basic design condition' (*see* Section 3 of main text) defined by $\bar{\lambda} = 0{\cdot}3$, $\bar{\vartheta} = 1$ radian, $\bar{\alpha} = \bar{\eta}_T = 0$, $\bar{K}_{r\alpha} = 0{\cdot}2$.

The basic trim diagram for this case is shown in Fig. 20. It will be seen at once, that in this form, the diagram is not very convenient for interpolation. In practice we shall want to know how C_J (and hence C_L and α) vary when, with two of the controls held fixed, the third control is varied. For this purpose, diagrams of the form shown in Figs. 21, 22 and 23 (obtained by cross-plotting from Fig. 20) are probably more suitable.*

In Fig. 21 C_J is plotted against $\lambda\vartheta$ for various values of $\lambda\eta_T$; this form of the diagram is most useful when λ, η_T are the fixed controls and ϑ is the variable control.

In Fig. 22, C_J is plotted against $\lambda\eta_T$ for various values of $\lambda\vartheta$; this form is most useful when λ, ϑ are the fixed controls and η_T is varied.

If λ is used as the trimming control, with ϑ and η_T fixed, then both $\lambda\vartheta$ and $\lambda\eta_T$ vary and neither Fig. 21 nor Fig. 22 is very convenient for studying how C_J varies with λ. In this case, however, η_T/ϑ remains constant and Fig. 23, in which C_J is plotted against $\lambda\vartheta$ for various values of η_T/ϑ is more useful.

To evaluate the partial trimming slopes (Equations (58)) and also the quantity $\partial n/\partial\lambda$ (Equation (61)(i)) the function X is required. From (59), this is seen to be a linear function of $\lambda\vartheta$ for a given value of C_J and Fig. 24 shows the straight lines X versus $\lambda\vartheta$ for a range of values of C_J, calculated for $\bar{V} = 0{\cdot}859$, as before.†

(*b*) *Determination of c.g. position and tail volume to satisfy a specified design condition.* If it is specified that a trimmed lift coefficient $\bar{C}_L$ is to be produced with control settings $\bar{\lambda}$, $\bar{\vartheta}$, $\bar{\eta}_T$ and that the restoring margin in this condition is to be $\bar{K}_{r\alpha}$ then $\bar{C}_J$, $(= \bar{\lambda}\bar{C}_L)\bar{A}$, $\bar{B}$, $\bar{K}$, $\bar{\alpha}$, $\bar{\xi}_\alpha$ and $\bar{\xi}_\vartheta$ are all known and Equations (52) and (53) may be written

$$a_1\bar{V}\{\bar{K}\bar{\vartheta} - \bar{\eta}_T\} = \bar{K}_{r\alpha}\bar{C}_L + \bar{B}\bar{\vartheta}(\bar{\xi}_\vartheta - \bar{\xi}_\alpha), \tag{66}$$

$$h - \frac{a_1\bar{V}}{\bar{A}}(1 - E\bar{A}) = \bar{\xi}_\alpha - \bar{K}_{r\alpha} \tag{67}$$

and solved for h and $\bar{V}$.

For the 'basic design condition' discussed in the main text it was assumed that $\bar{\eta}_T = \bar{\alpha} = 0$ in which case $\bar{C}_L = \bar{B}\bar{\vartheta}$. Equation (66) then becomes

$$\bar{V} = \frac{\bar{A}}{a_1}(\bar{K}_{r\alpha} + \bar{\xi}_\vartheta - \bar{\xi}_\alpha) \tag{68}$$

and (67) simplifies to

$$h = \bar{\xi}_\vartheta - E\bar{A}(\bar{K}_{r\alpha} + \bar{\xi}_\vartheta - \bar{\xi}_\alpha) = \bar{\xi}_\vartheta - Ea_1\bar{V}. \tag{69}$$

Equations (68) and (69) are identical with the first two of Equations (35) of the main text.

The range of applicability of Figs. 20 to 23. The basic trim diagram of Fig. 20 has been plotted for a range of values of C_J, extending up to 10, for which the interpolation formulae for A and B (Equations (37) of main text) are theoretically valid. Similarly, in cross-plotting the data to obtain Figs. 21 to 23, the full range of C_J up to 10 has been used.

---

* Some remarks on the range of applicability of these figures are made at the end of this Appendix.

† X depends (through $K_{r\alpha}'$ and σ') on the value of $\bar{V}$ but is independent of the value of h.

It must not be inferred, however, that all points coming within the scope of the various trim diagrams necessarily represent trimmed conditions which are realisable in practice. For it may well be that the trimmed incidence which corresponds theoretically to a given point of the trim diagram is, in fact, outside the range for which the linear theory is valid; such a point has no practical significance. On the basis of such considerations, it seems probable that the upper branches of the curves in Figs. 21 and 23 and the corresponding parts of the curves of Fig. 22, for which $C_J > 3 \cdot 47$, may be disregarded for practical purposes.

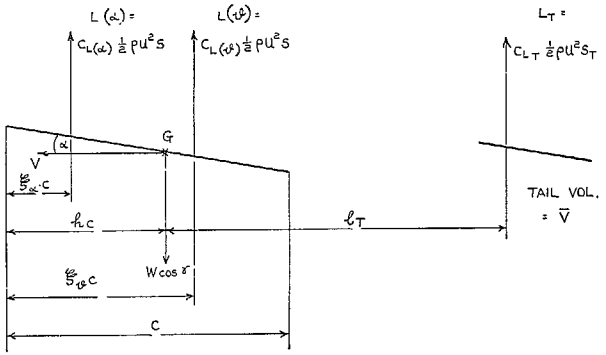

FIG. 1. System of forces acting normally to the flight path of a jet-flapped aircraft with tail.

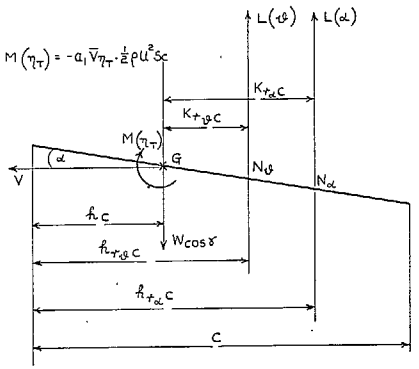

FIG. 2. An equivalent force and moment system.

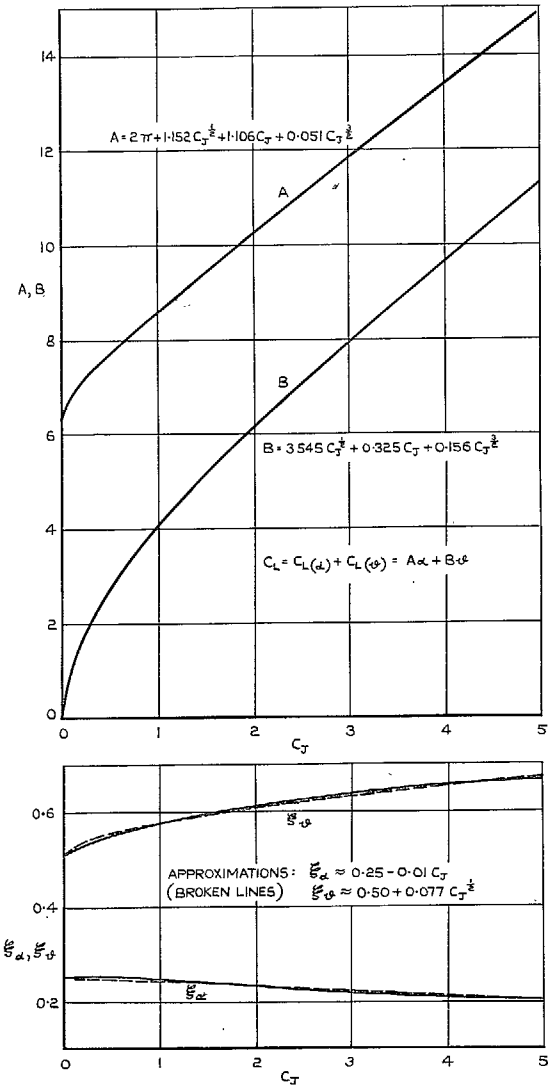

FIG. 3. Theoretical values of A, B, ξ_α and ξ_ϑ (Spence).

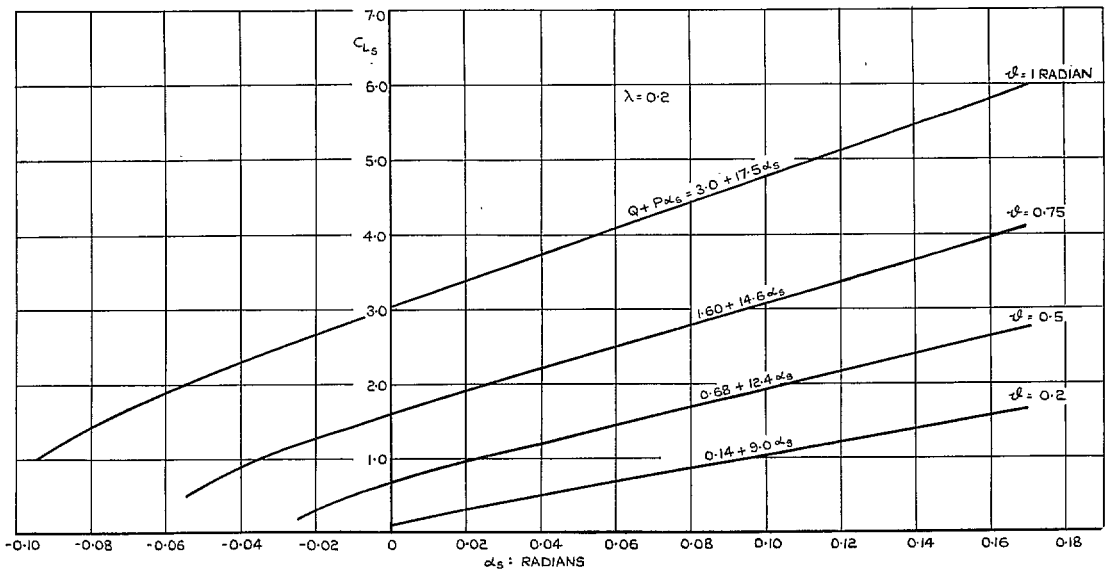

FIG. 4a. Total lift coefficient $C_{L\,s}$ in trimmed rectilinear flight with $\lambda = 0{\cdot}2$.

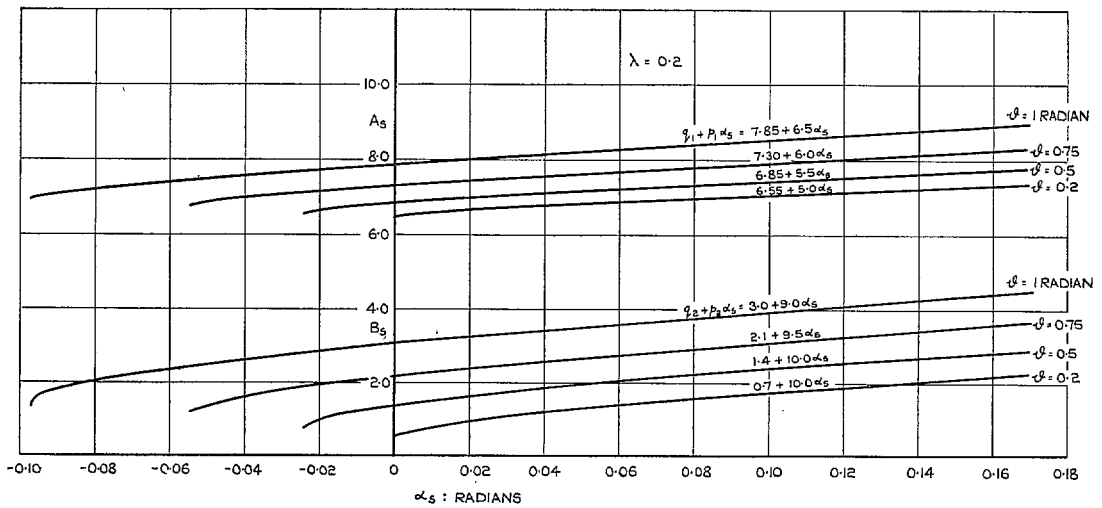

FIG. 4b. The coefficients A_s, B_s in trimmed rectilinear flight with $\lambda = 0{\cdot}2$.

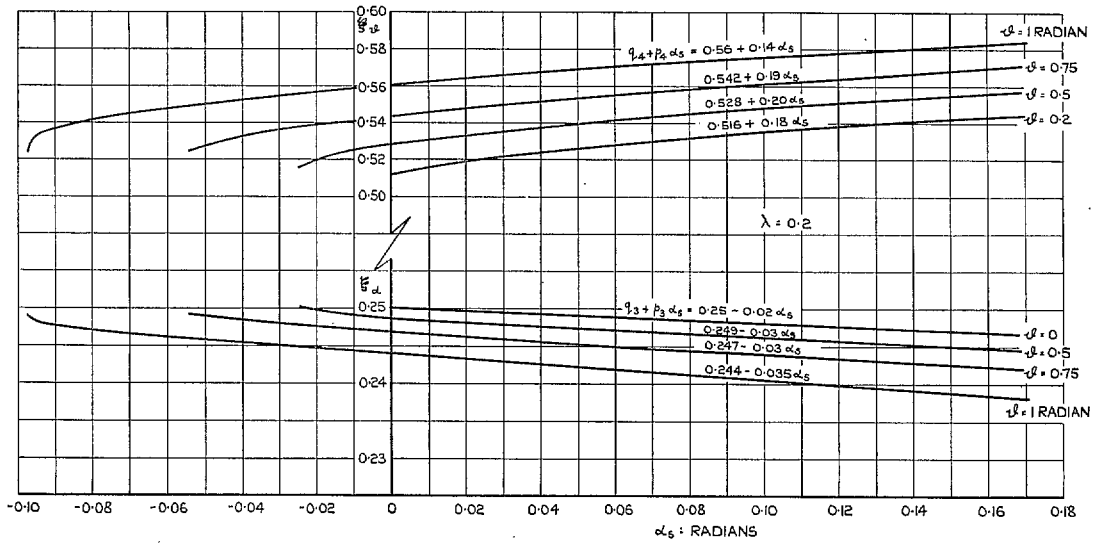

FIG. 4c. The coefficients ξ_α, ξ_ϑ in trimmed rectilinear flight with $\lambda = 0{\cdot}2$.

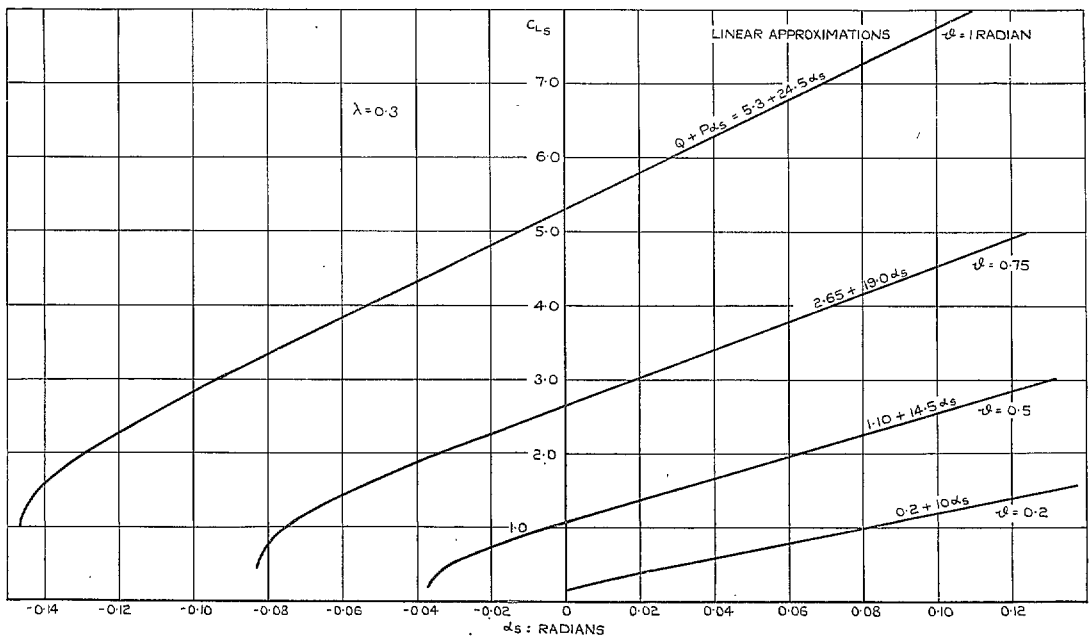

FIG. 5a. Total lift coefficient $C_{L\,s}$ in trimmed rectilinear flight with $\lambda = 0{\cdot}3$.

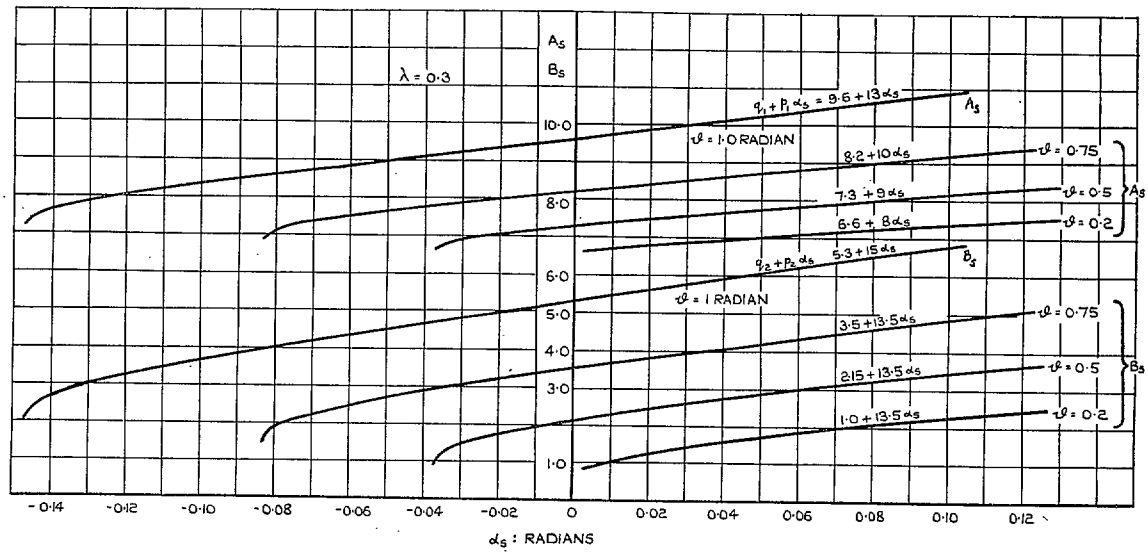

FIG. 5b. The coefficients A_s, B_s in trimmed rectilinear flight with $\lambda = 0·3$.

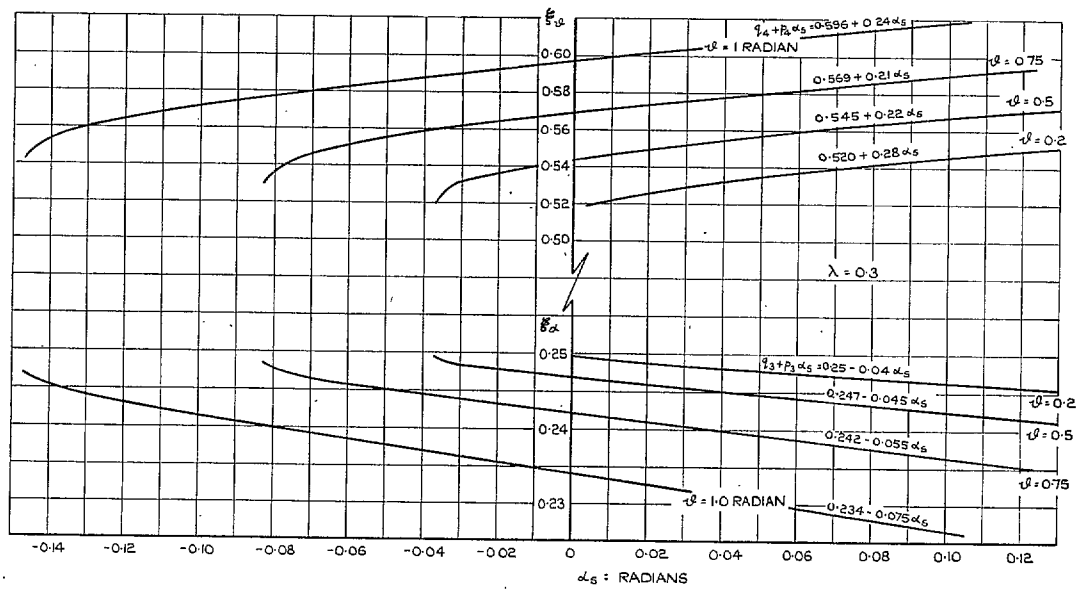

FIG. 5c. The coefficients ξ_α, ξ_ϑ in trimmed rectilinear flight with $\lambda = 0·3$.

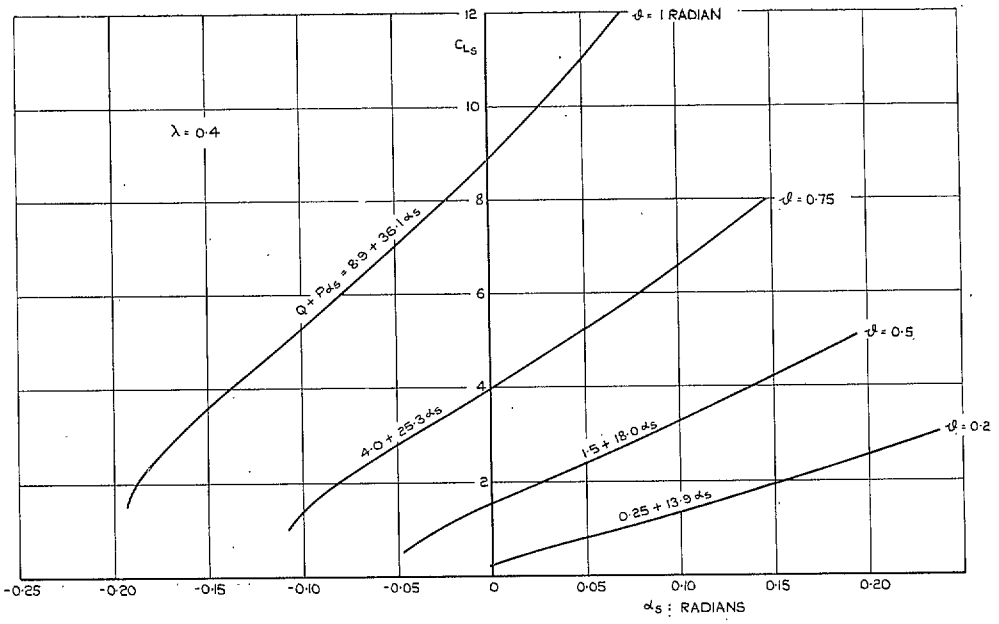

FIG. 6a. Total lift coefficient $C_{L\,s}$ in trimmed rectilinear flight with $\lambda = 0{\cdot}4$.

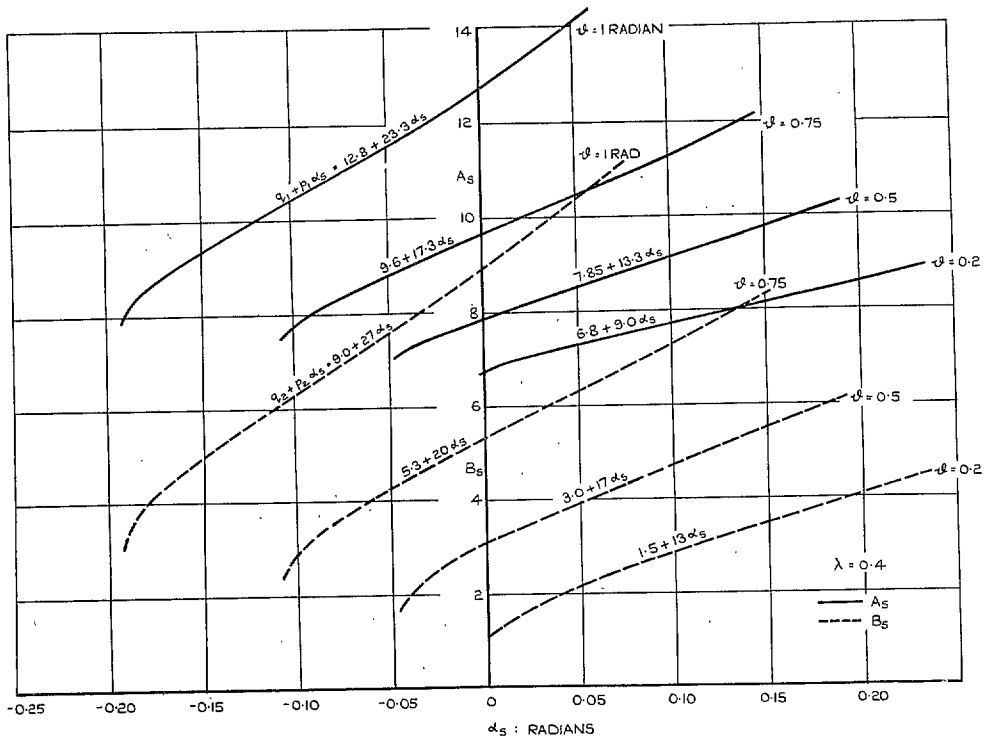

FIG. 6b. The coefficients A_s, B_s in trimmed rectilinear flight with $\lambda = 0{\cdot}4$.

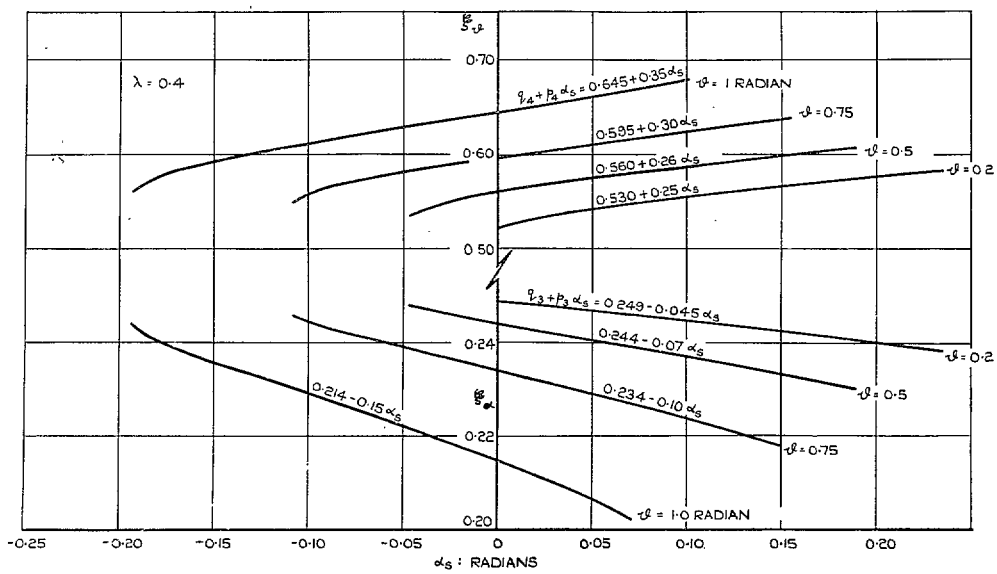

FIG. 6c. The coefficients ξ_α, ξ_ϑ in trimmed rectilinear flight with $\lambda = 0{\cdot}4$.

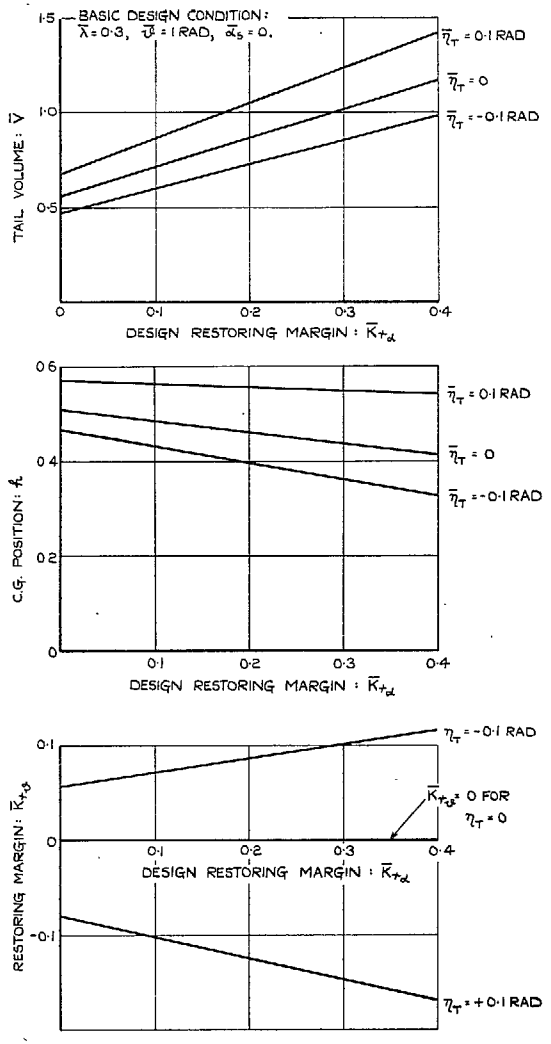

FIG. 7. Tail volume and c.g. position as determined by basic design conditions.

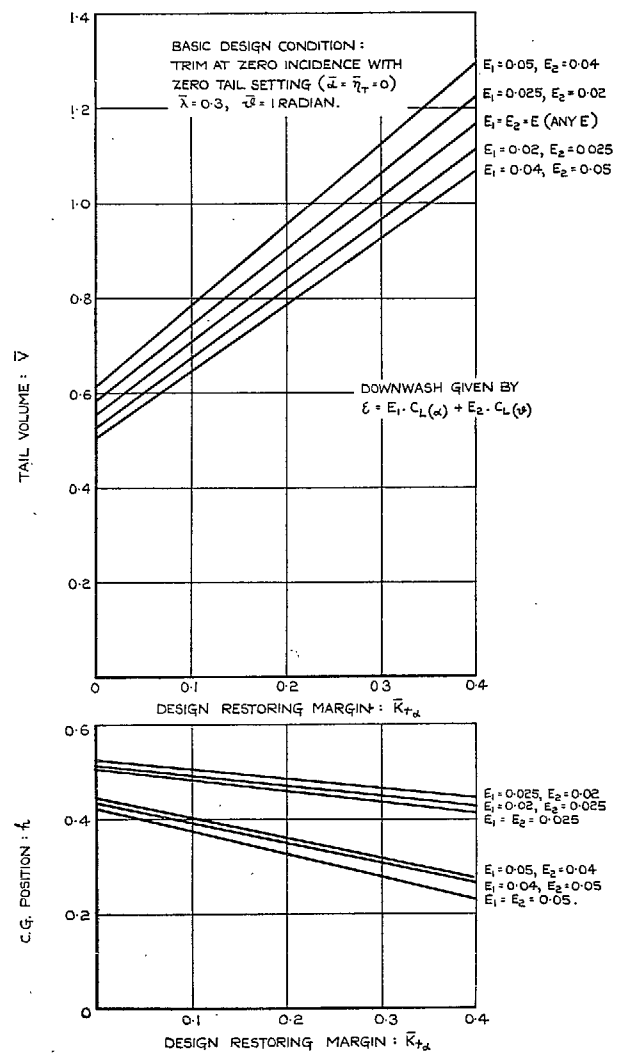

FIG. 8. Effect of downwash assumptions on required tail volume and c.g. position.

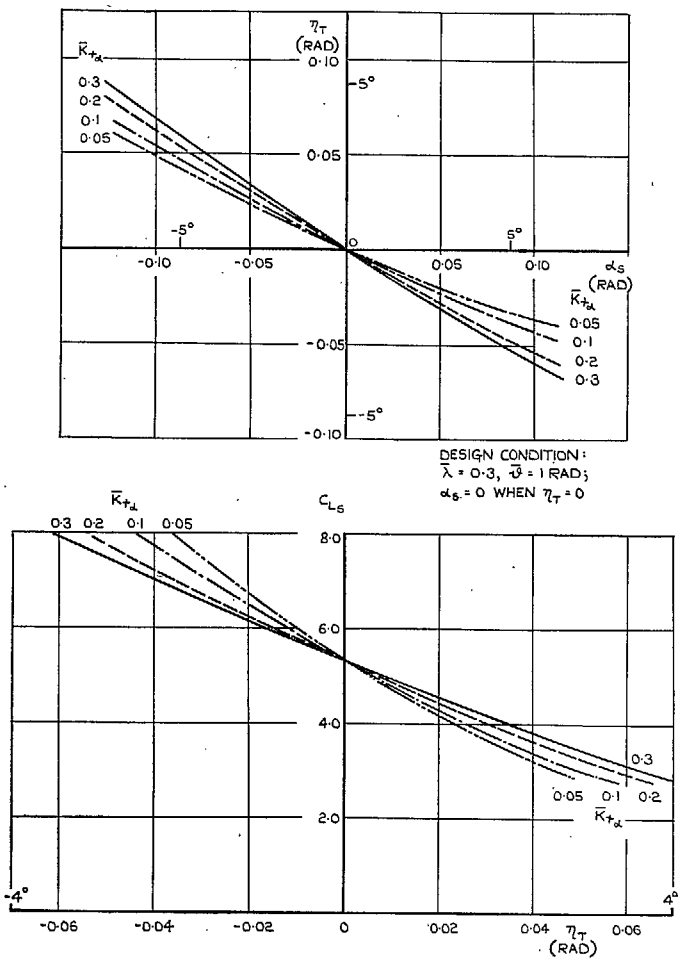

FIG. 9. Variation of trimmed incidence and lift coefficient with tailplane setting: $\vartheta = \bar{\vartheta}$, $\lambda = \bar{\lambda}$; $\bar{\eta}_T = 0$.

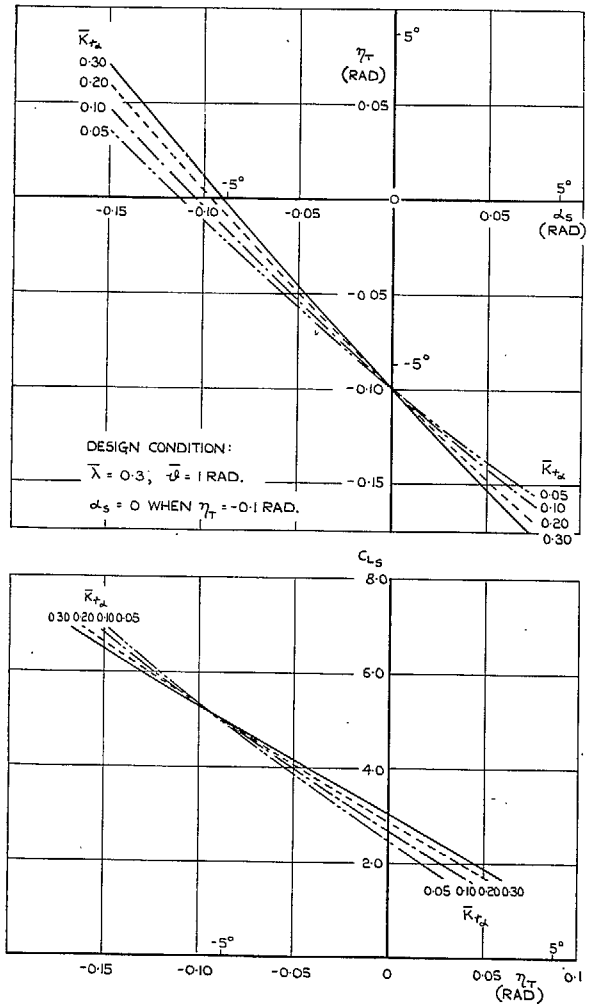

FIG. 10. Variation of trimmed incidence and lift coefficient with tailplane setting: $\vartheta = \bar{\vartheta}$, $\lambda = \bar{\lambda}$; $\bar{\eta}_T = -0{\cdot}1$ radian.

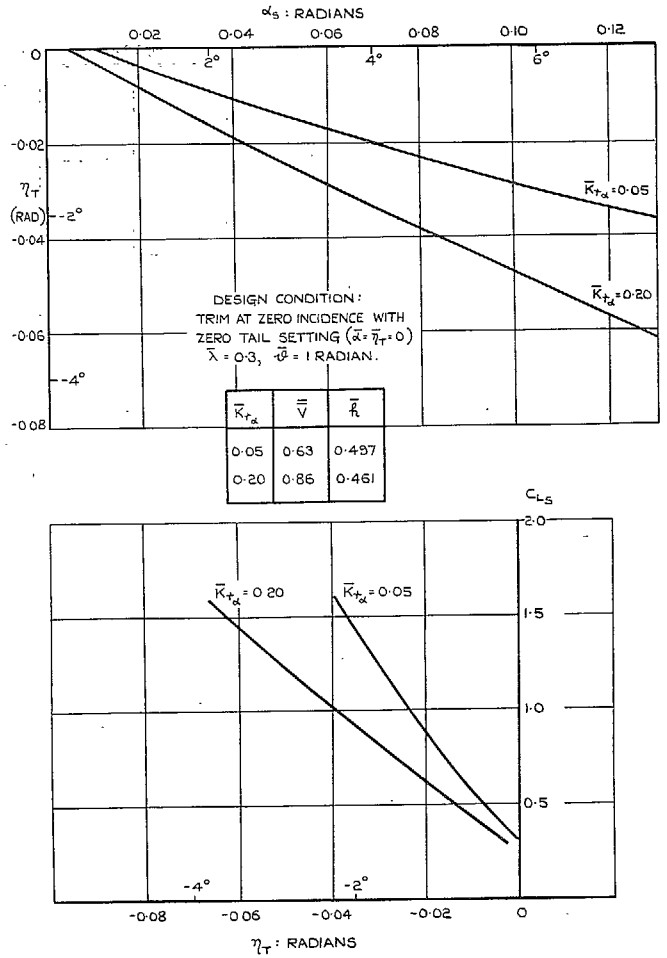

FIG. 11. Variation of trimmed incidence and lift coefficient with tailplane setting: $\lambda = 0{\cdot}3$, $\vartheta = 0{\cdot}2$ radian; $\bar{\eta}_T = 0$.

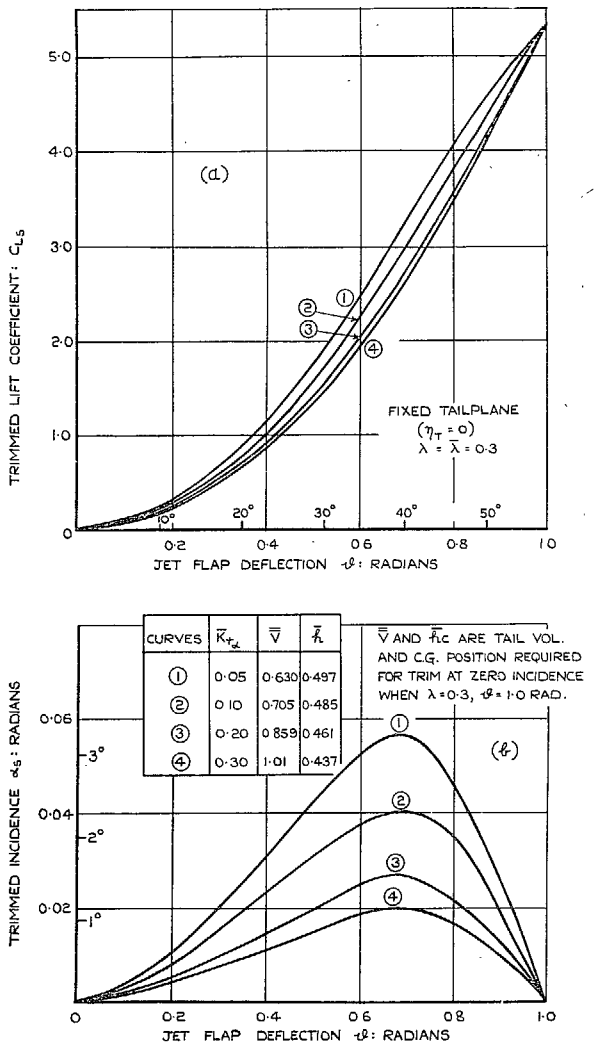

FIG. 12. Variation of trimmed incidence and lift coefficient with jet-flap deflection.

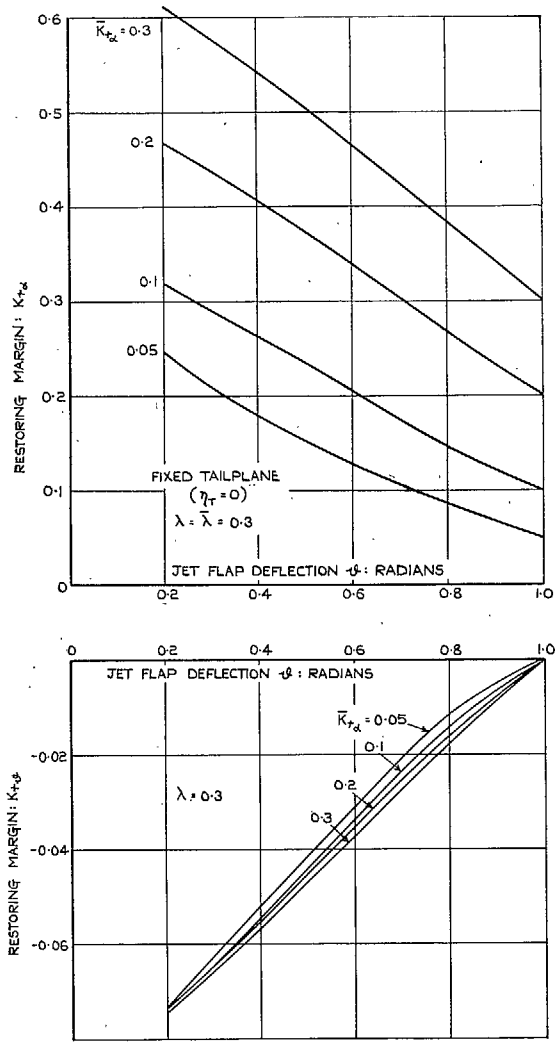

FIG. 13. Variation of restoring margins $K_{r\,\alpha}$, $K_{r\,\vartheta}$ with jet-flap deflection.

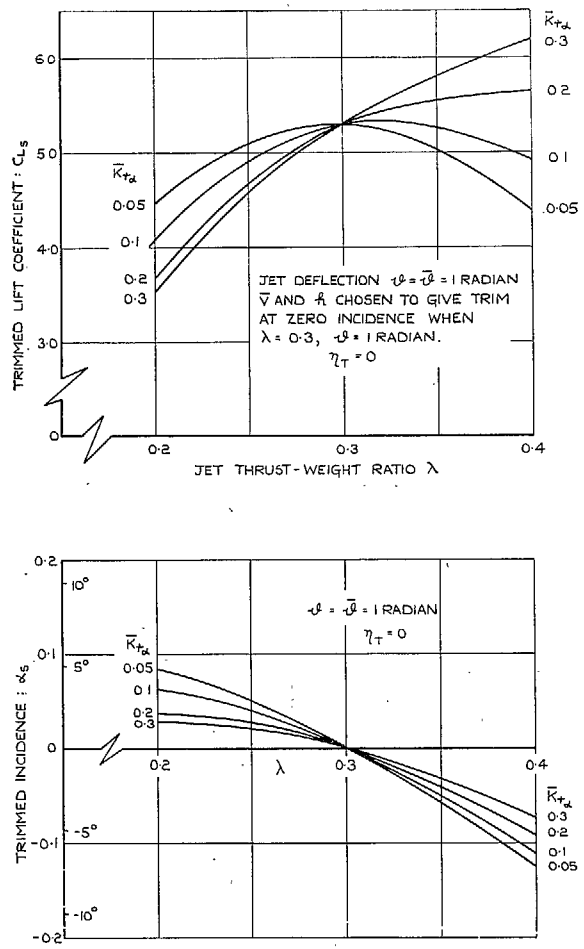

FIG. 14. Variation of trimmed incidence and lift coefficient with jet thrust.

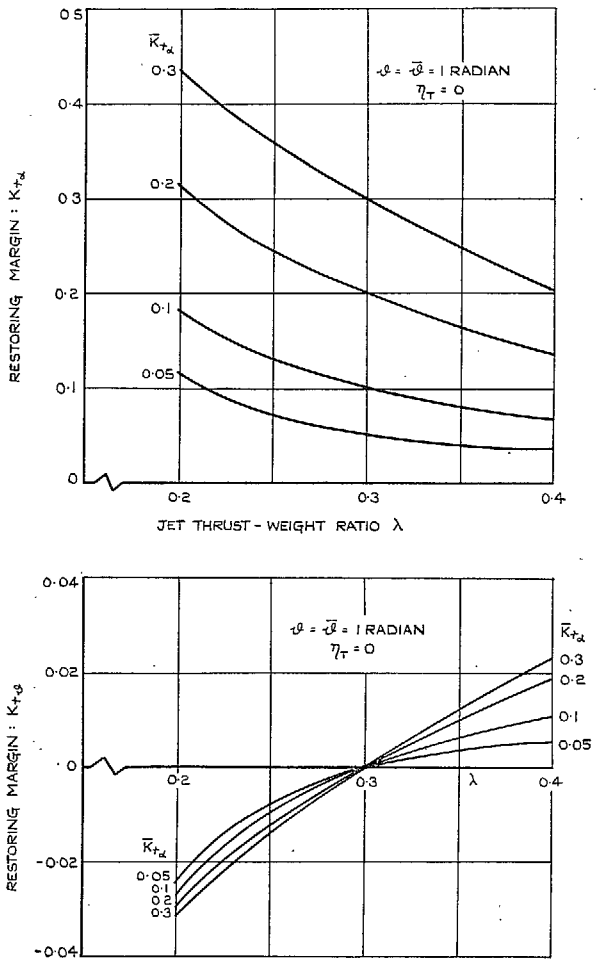

FIG. 15. Variation of restoring margins $K_{r\,\alpha}$, $K_{r\,\vartheta}$ with jet thrust.

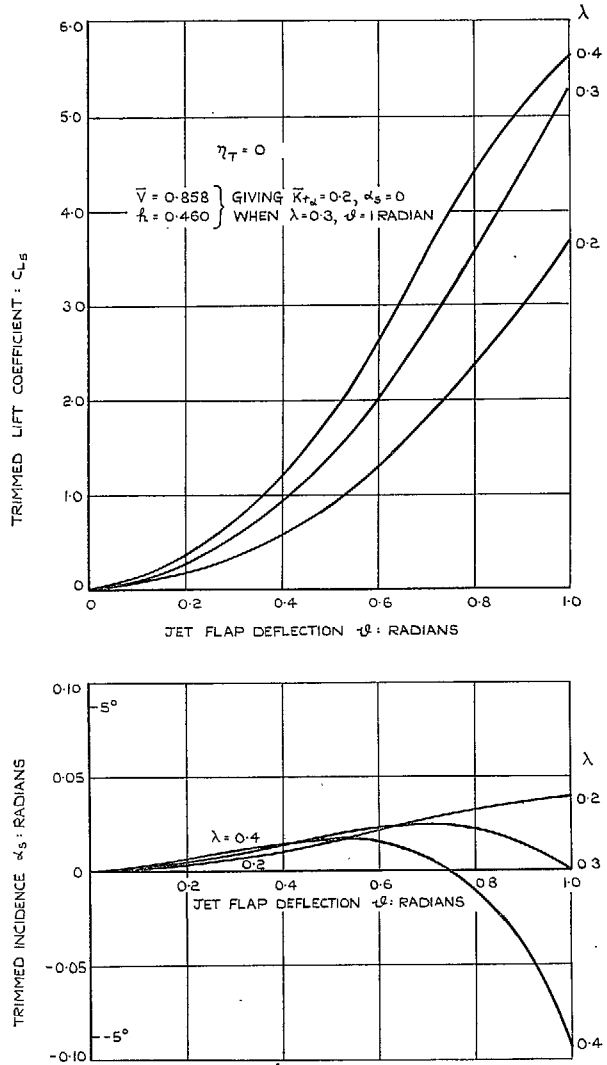

FIG. 16. Variation of trimmed incidence and lift coefficient with jet-flap deflection and jet thrust for a particular combination of tail volume and c.g. position.

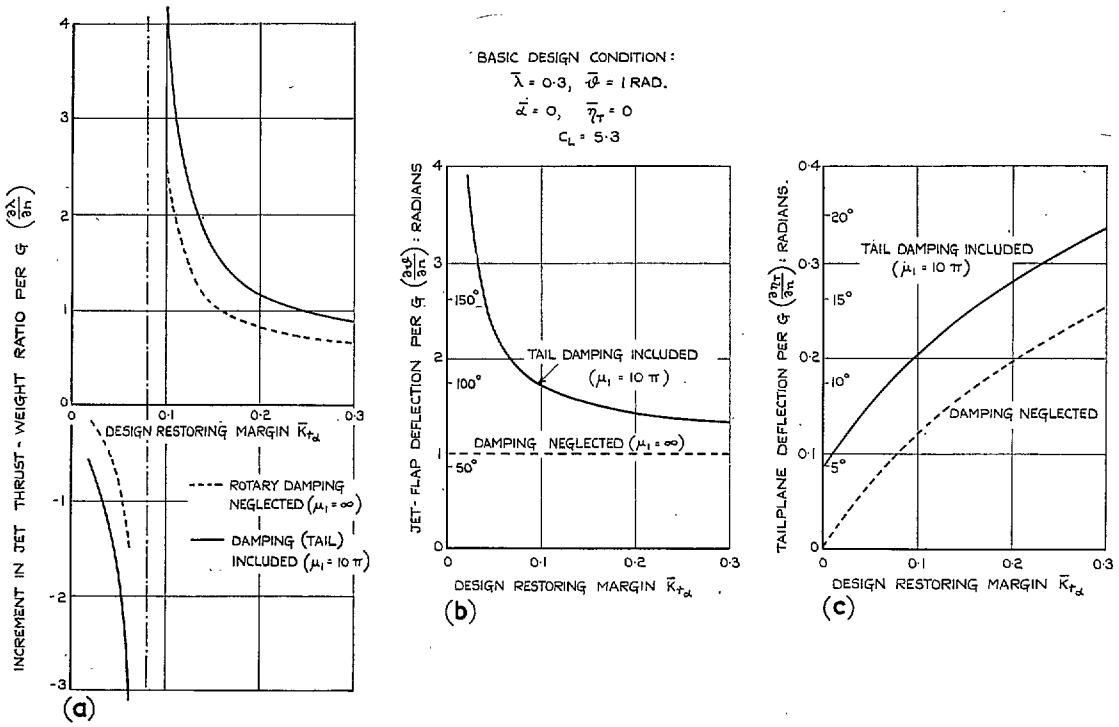

FIG. 17a to c. Control actions per g in constant speed manoeuvres initiated from the basic design condition.

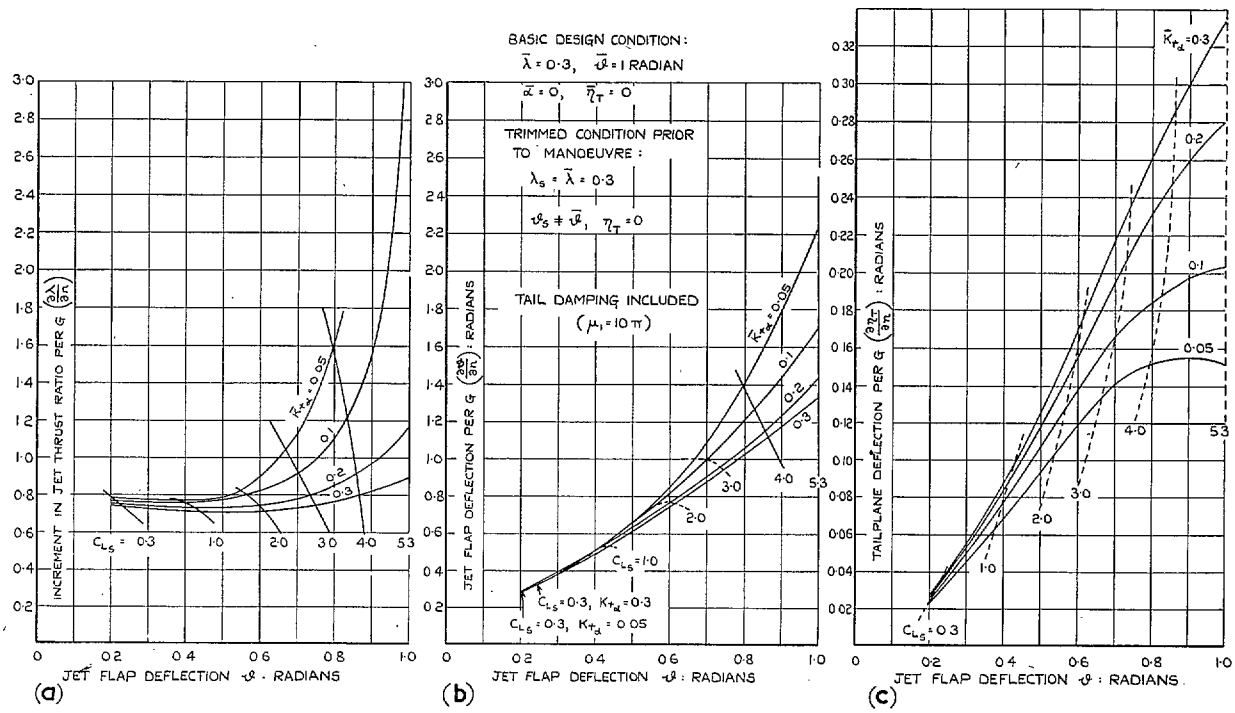

FIG. 18a to c. Control actions per g in constant speed manoeuvres initiated from trimmed conditions with $\lambda_s = \bar{\lambda}$, $\vartheta_s \neq \bar{\vartheta}$.

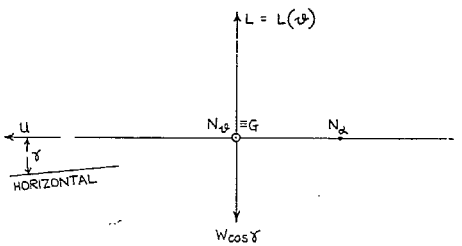

(a) TRIMMED RECTILINEAR FLIGHT IN THE BASIC DESIGN CONDITION.

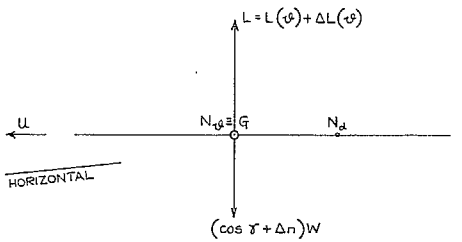

(b) MOTION IN STEADY CIRCLE FOLLOWING APPLICATION OF JET-FLAP DEFLECTION CONTROL: DAMPING NEGLECTED.

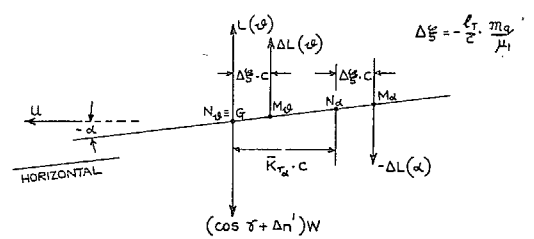

(c) MOTION IN STEADY CIRCLE FOLLOWING APPLICATION OF JET-FLAP DEFLECTION CONTROL: DAMPING INCLUDED.

FIG. 19a to c. Balance of forces in manoeuvring flight initiated by jet-flap deflection.

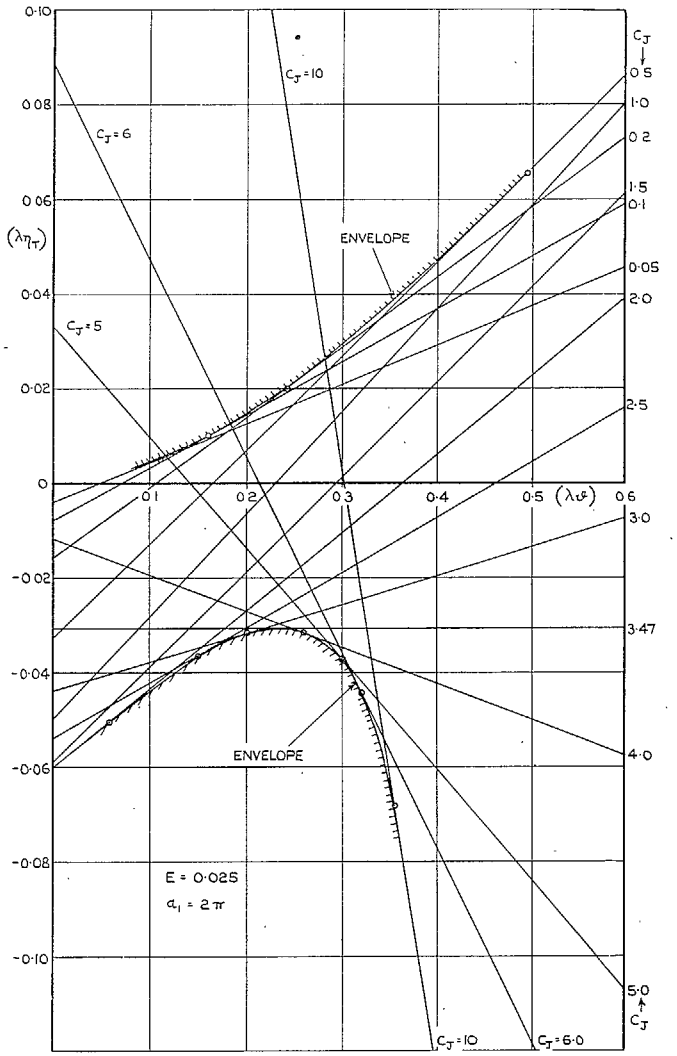

FIG. 20. The basic trim diagram for $\overline{V} = 0{\cdot}859$, $h = 0{\cdot}461$.

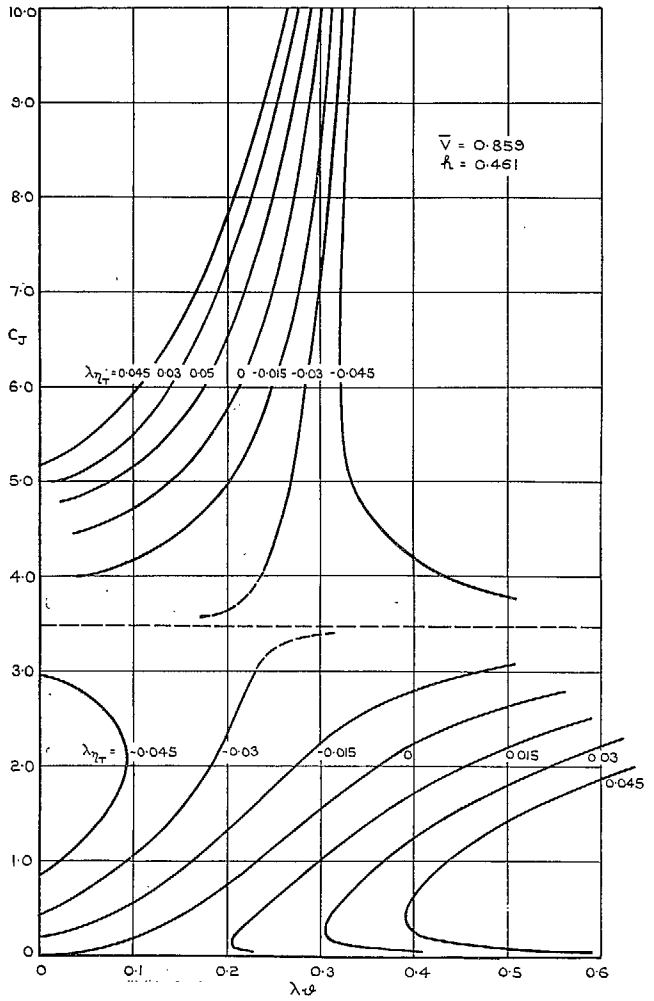

FIG. 21. Alternative form of trim diagram for use when λ and η_T controls are fixed.

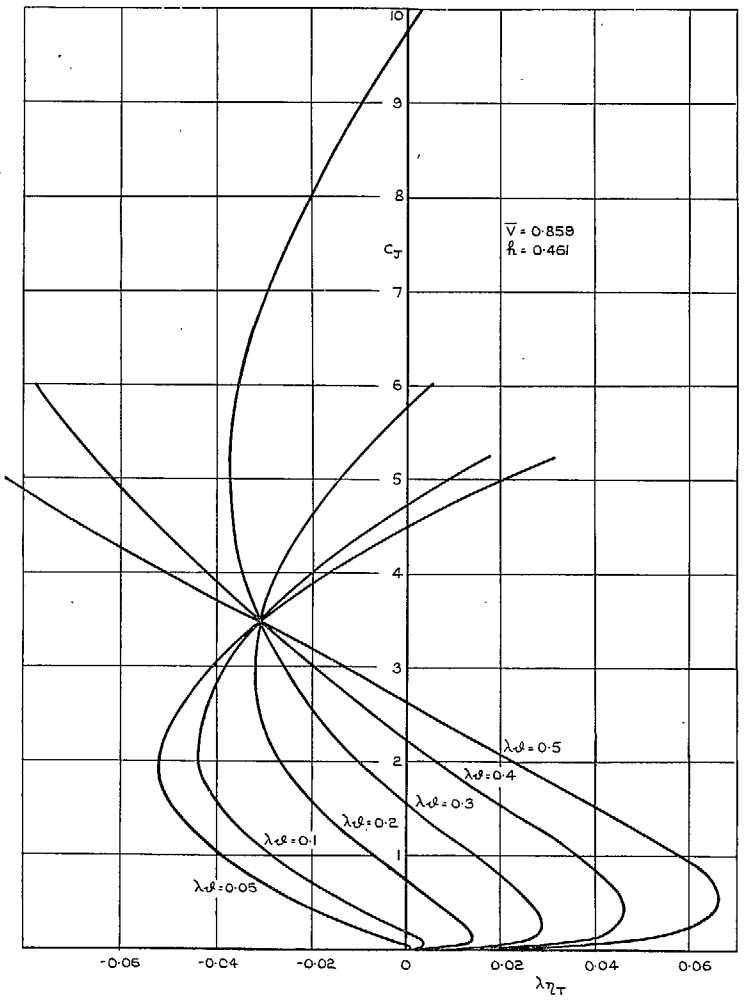

FIG. 22. Alternative form of trim diagram for use when λ and ϑ controls are fixed.

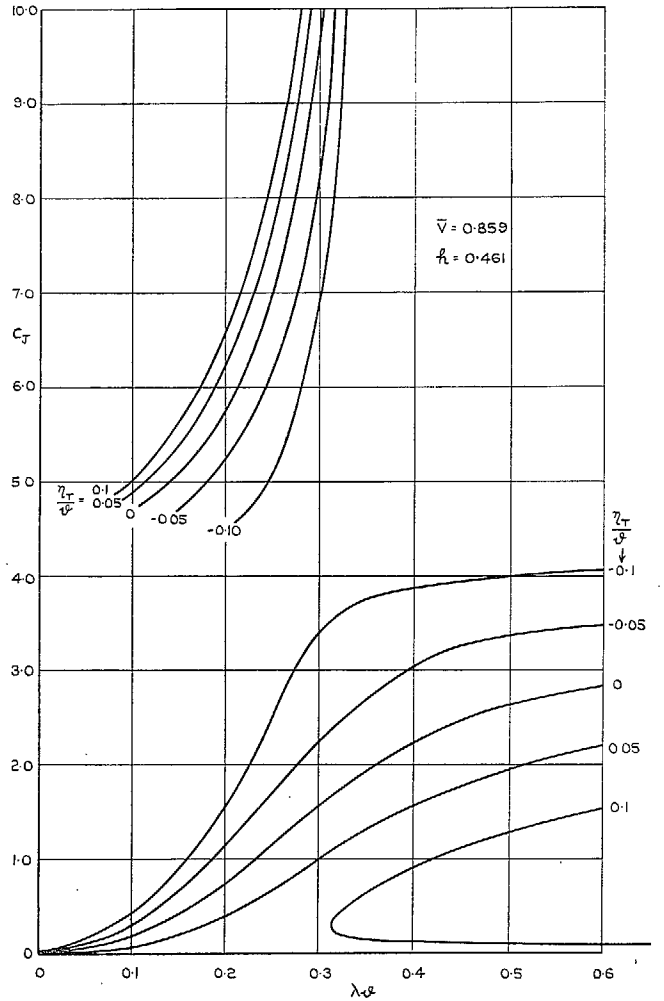

FIG. 23. Alternative form of trim diagram for use when ϑ and η_T controls are fixed.

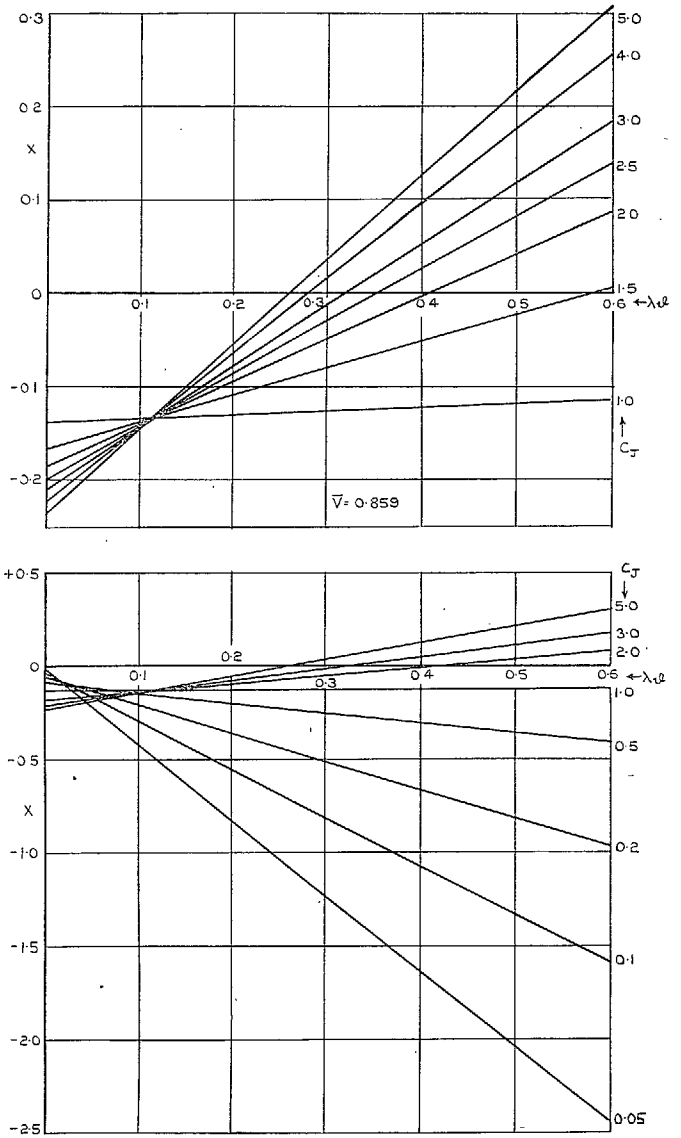

FIG. 24. The function X.

Part II

Dynamic Longitudinal Stability and Response Characteristics of Jet-Flap Aircraft

Summary. The generalized stability and control investigation, based on Spence's two-dimensional theoretical data, which was begun in Part I with considerations of trim, static stability and quasi-steady manoeuvrability, is extended by a study of dynamic stability and of comparative response characteristics for step-inputs of tail and jet controls.

From numerical examples it is concluded that in the 'basic design' (high lift) condition, the quasi-steady manoeuvrability criterion is not a valid basis of comparison of control effectiveness, because a divergent phugoid of relatively short period, coupled with a rapid oscillation of relatively long period, prevents the establishment of a quasi-steady condition. Because initial response is much slower for tail control than for jet controls, it now appears that jet deflection control may be more effective than tail control for this case.

The manoeuvrability criterion is shown to remain substantially valid for the cruising condition, however, and the superiority of tail over jet controls in this case is confirmed.

---

1. *Introduction.* In Ref. 1 the author made a preliminary examination of some of the stability and control problems associated with the design of a jet-flapped aircraft, stabilized and controlled longitudinally by a conventional tailplane and elevator (or all-moving tailplane). In Part I of the present Report, the possibility of using the jet controls (throttle and jet-flap deflection) to trim and manoeuvre the aircraft was examined. Both of these investigations were restricted to considerations of trim, static longitudinal stability and quasi-steady manoeuvrability criteria although, as pointed out in the conclusions of Part I, it is necessary, in attempting a complete appraisal of the relative merits of jet and tail controls, to study dynamic stability and response characteristics. It is the purpose of this Part of the Report to fulfil this need.

The relevant mathematical theory is developed in Section 2, where the standard equations of disturbed longitudinal motion with deflected controls[2] are adapted and extended for application to the jet-flapped aircraft. The generalized form of the stability quartic governing the motion is derived in Section 2.2 and operational solutions for the responses to control application are given in Section 2.3. Only step-function inputs of the three controls have been considered, because of uncertainty as to the respective modes of application that will be realizable in practice.

The calculation of the aerodynamic derivatives required for response calculations is discussed in Section 2.4. For reasons given there, calculations have been based on the early version of Spence's two-dimensional theory[7], which was used as the basis of the investigations described in Part I. Formulae obtained for the derivatives are collected together in Table 1; their derivation is given in full in Appendix I.

To ensure self-consistency of the dynamic analysis, which must take account of changes in the longitudinal (thrust and drag) forces, it has been necessary to revise the trim and static stability analysis of Part I which neglected the effects of such forces. It has been found that the inclusion of such effects results in appreciable changes in the tail volume ratio and c.g. position required to satisfy specified design conditions.

The numerical work performed in connection with this investigation is described in Section 3 and the results, given in Tables 2 to 6 and Figs. 2 to 15, have been used to re-assess the comparative effectiveness of jet and tail controls. It appears that the conclusions arrived at in Part I, on the basis of quasi-steady manoeuvrability theory, need modification in respect of the 'basic design' (high lift) condition, but remain essentially valid for the cruising condition.

An extended summary of the work described in this Part, together with a discussion of the results and the conclusions to be drawn therefrom, is given in Section 4. Possible future developments are briefly discussed in Section 5.

Acknowledgement. Acknowledgement is due to Miss F. M. Ward and Miss B. E. Mills for their assistance in performing numerical work and preparing figures for this Part.

2. *Mathematical Theory.* 2.1. *Equations of Disturbed Longitudinal Motion with Deflected Controls.* The jet-flapped aircraft may be considered to have three possible longitudinal controls: tail control, (elevator or all-moving tailplane) jet-flap deflection control and jet thrust/weight ratio control (exercised *via* the throttle).

If the (small) deflections of these three controls from their steady-flight settings η_{Ts}, ϑ_s and λ_s are denoted by $\hat{\eta}_T$, $\hat{\vartheta}$ and $\hat{\lambda}$ respectively, and if the general notation of Ref. 2 is adopted (except that $m_{\dot{u}}$, $m_{\dot{w}}$ are written for $\overline{m}_{\dot{u}}$, $\overline{m}_{\dot{w}}$) the equations of motion may be written

$$\left.\begin{aligned}
\left(\frac{d}{d\tau}-x_u\right)\frac{u}{U_s} \quad & -x_w\frac{w}{U_s} \quad -\frac{x_q}{\mu_1}q\hat{t}+k_L\theta- \\
& -x_{\eta_T}\hat{\eta}_T \quad -x_\vartheta\hat{\vartheta} \quad -x_\lambda\hat{\lambda}=0, \\
-z_u\frac{u}{U_s} \quad & +\left(\frac{d}{d\tau}-z_w\right)\frac{w}{U_s} \quad -\left(1+\frac{z_q}{\mu_1}\right)q\hat{t}-k'\theta- \\
& -z_{\eta_T}\hat{\eta}_T \quad -z_\vartheta\hat{\vartheta} \quad -z_\lambda\hat{\lambda}=0, \\
\left(-\frac{m_{\dot{u}}}{i_B}\frac{d}{d\tau}-\frac{\mu_1 m_u}{i_B}\right)\frac{u}{U_s}+\left(-\frac{m_{\dot{w}}}{i_B}\frac{d}{d\tau}-\frac{\mu_1 m_w}{i_B}\right)\frac{w}{U_s}+\left(\frac{d}{d\tau}-\frac{m_q}{i_B}\right)q\hat{t}- & \\
-\frac{\mu_1 m_{\eta_T}}{i_B}\hat{\eta}_T-\frac{\mu_1 m_\vartheta}{i_B}\hat{\vartheta}-\frac{\mu_1 m_\lambda}{i_B}\hat{\lambda}=0, & \\
-q\hat{t}+\frac{d\theta}{d\tau}=0. &
\end{aligned}\right\} \tag{1}$$

The terms involving x_q, z_q may, in conformity with common practice, be neglected in the present investigation. Then introducing Neumark's subsidiary notation[3] with some additions:

$$\left.\begin{aligned}
\omega &= -\frac{\mu_1 m_w}{i_B}, & \nu &= -\frac{m_q}{i_B}, & \chi &= -\frac{m_{\dot{w}}}{i_B}, \\
\Upsilon &= -\frac{m_{\dot{u}}}{i_B}, & \kappa &= -\frac{\mu_1 m_u}{i_B}, & & \\
\delta_{\eta_T} &= -\frac{\mu_1 m_{\eta_T}}{i_B}, & \delta_\vartheta &= -\frac{\mu_1 m_\vartheta}{i_B}, & \delta_\lambda &= -\frac{\mu_1 m_\lambda}{i_B},
\end{aligned}\right\} \tag{2}$$

writing

$$\frac{u}{U_s}=\hat{u}, \qquad \frac{w}{U_s}=\hat{w} \tag{3}$$

and using the last of Equations (1) to eliminate q from the remaining three, we may write these in the form

$$\left.\begin{aligned}
\left(\frac{d}{d\tau}-x_u\right)\hat{u} \qquad -x_w\hat{w} \qquad +k_L\theta - x_{\eta_T}\hat{\eta}_T - x_\vartheta\hat{\vartheta} - x_\lambda\hat{\lambda} &= 0,\\
-z_u\hat{u} \;+\left(\frac{d}{d\tau}-z_w\right)\hat{w} \;-\left(\frac{d}{d\tau}+k'\right)\theta - z_{\eta_T}\hat{\eta}_T - z_\vartheta\hat{\vartheta} - z_\lambda\hat{\lambda} &= 0,\\
\left(\Upsilon\frac{d}{d\tau}+\kappa\right)\hat{u} + \left(\chi\frac{d}{d\tau}+\omega\right)\hat{w} + \frac{d}{d\tau}\left(\frac{d}{d\tau}+\nu\right)\theta + \delta_{\eta_T}\hat{\eta}_T + \delta_\vartheta\hat{\vartheta} + \delta_\lambda\hat{\lambda} &= 0.
\end{aligned}\right\} \tag{4}$$

In these equations $\hat{\eta}_T$, $\hat{\vartheta}$ and $\hat{\lambda}$ are to be regarded as arbitrary functions of τ and to obtain the responses to particular control inputs, use may be made of the operational calculus. If the Heaviside method (*see*, for example, Ref. 4) is employed, the subsidiary equations corresponding to (4) will be

$$\left.\begin{aligned}
(D-x_u)\hat{u}(D) \qquad -x_w\hat{w}(D) \qquad +k_L\theta(D) &= x_{\eta_T}\hat{\eta}_T(D) + x_\vartheta\hat{\vartheta}(D) + x_\lambda\hat{\lambda}(D) + \hat{u}_0 D,\\
-z_u\hat{u}(D) \;+(D-z_w)\hat{w}(D) \;-(D+k')\theta(D) &= z_{\eta_T}\hat{\eta}_T(D) + z_\vartheta\hat{\vartheta}(D) + z_\lambda\hat{\lambda}(D) +\\
&\qquad + \hat{w}_0 D - \theta_0 D,\\
(\Upsilon D+\kappa)\hat{u}(D) + (\chi D+\omega)\hat{w}(D) + D(D+\nu)\theta(D) &= -\delta_{\eta_T}\hat{\eta}_T(D) - \delta_\vartheta\hat{\vartheta}(D) - \delta_\lambda\hat{\lambda}(D) +\\
&\qquad + \Upsilon\hat{u}_0 D + \chi\hat{w}_0 D + \theta_0 D(D+\nu) + \dot{\theta}_0 D,
\end{aligned}\right\} \tag{5}$$

where $\hat{u}(D)$, $\hat{w}(D)$, $\theta(D)$, $\hat{\eta}_T(D)$, $\hat{\vartheta}(D)$, $\hat{\lambda}(D)$ are the (Heaviside) operational equivalents of $\hat{u}$, $\hat{w}$, θ, $\hat{\eta}_T$, $\hat{\vartheta}$ and $\hat{\lambda}$ respectively and $\hat{u}_0$, $\hat{w}_0$, θ_0 and $\dot{\theta}_0$ are the initial values of $\hat{u}$, $\hat{w}$, θ and $d\theta/d\tau$ respectively. For control inputs $\hat{\eta}_T$ etc., which are elementary functions of τ, the operational equivalents $\eta_T(D)$ etc., will be readily obtainable from Ref. 4 or otherwise and Equations (5) may then be solved for $\hat{u}(D)$, $\hat{w}(D)$ and $\theta(D)$. It then remains only to determine the functions whose operational equivalents are $\hat{u}(D)$ etc. and the response problem is solved. The last stage of the work may be much facilitated by use of the tables of Ref. 4.

2.2. *The Stability Quartic.* The stability equation, obtained by equating to zero the determinant of coefficients on the left-hand sides of Equations (5) is a quartic

$$F(D) \equiv D^4 + B_1 D^3 + C_1 D^2 + D_1 D + E_1 = 0, \tag{6}$$

where

$$\left.\begin{aligned}
B_1 &= N_1 + \nu \qquad + \chi,\\
C_1 &= P_1 + \nu N_1 + \chi Q_1 + \omega \qquad - \Upsilon S_1,\\
D_1 &= \qquad \nu P_1 + \chi R_1 + \omega Q_1 + \Upsilon T_1 + \kappa S_1,\\
E_1 &= \qquad\qquad\quad \omega R_1 \qquad\quad + \kappa T_1,
\end{aligned}\right\} \tag{7}$$

and

$$\left.\begin{aligned}
N_1 &= -(x_u + z_w); & R_1 &= -(k'x_u + k_L z_u);\\
P_1 &= x_u z_w - x_w z_u; & S_1 &= x_w - k_L;\\
Q_1 &= -(x_u - k'); & T_1 &= k_L z_w + k' x_w.
\end{aligned}\right\} \tag{8}$$

2.3. *Response to Individual Control Actions.* It is hardly possible at this stage of development, to specify realistic modes of application for the three types of control. This is true in particular of the λ-type control, characteristics of which will be bound up with the question of the response of the jet engine itself to throttle setting. In such a state of ignorance it would appear pointless to attempt more than a crude comparison of the response characteristics resulting from simple step-function inputs of each control in turn.

2.3.1. *Response to step-function inputs of the three controls.* Let $\hat{\eta}_r$, $r = 1, 2, 3$, denote increments of tail-, jet deflection- and jet thrust-control settings respectively,
i.e.,

$$\hat{\eta}_1 \equiv \hat{\eta}_T; \qquad \hat{\eta}_2 \equiv \hat{\vartheta}; \qquad \hat{\eta}_3 \equiv \hat{\lambda}. \tag{9}$$

Then for a step-function input of the rth control we have

$$\left.\begin{aligned} &\hat{\eta}_r(\tau) = \hat{\eta}_{r0} = \text{constant} \\ \text{and} \quad &\hat{\eta}_s(\tau) = 0, \quad s \neq r, \end{aligned}\right\} \tag{10}$$

whence

$$\left.\begin{aligned} &\hat{\eta}_r(D) = \hat{\eta}_{r0} \\ \text{and} \quad &\hat{\eta}_s(D) = 0, \quad s \neq r. \end{aligned}\right\} \tag{11}$$

Initial conditions are

$$\hat{u}_0 = \hat{w}_0 = \theta_0 = \dot{\theta}_0 = 0. \tag{12}$$

The right-hand sides of Equations (5) reduce to $x_{\eta r}\hat{\eta}_{r0}$, $z_{\eta r}\hat{\eta}_{r0}$ and $-\delta_{\eta r}\hat{\eta}_{r0}$ respectively, and their solutions may be written down as

$$\frac{\hat{u}(D)}{\hat{\eta}_{r0}} = \frac{F_u^{(r)}(D)}{F(D)}; \quad \frac{\hat{w}(D)}{\hat{\eta}_{r0}} = \frac{F_w^{(r)}(D)}{F(D)}; \quad \frac{\theta(D)}{\hat{\eta}_{r0}} = \frac{F_\theta^{(r)}(D)}{F(D)}, \tag{13}$$

where $F(D)$ is given by (6) and

$$\left.\begin{aligned} F_u^{(r)}(D) &= B_u^{(r)}D^3 + C_u^{(r)}D^2 + D_u^{(r)}D + E_u, \\ F_w^{(r)}(D) &= B_w^{(r)}D^3 + C_w^{(r)}D^2 + D_w^{(r)}D + E_w, \\ F_\theta^{(r)}(D) &= \qquad C_\theta^{(r)}D^2 + D_\theta^{(r)}D + E_\theta. \end{aligned}\right\} \tag{14}$$

The coefficients of the first of Equations (14) are

$$\left.\begin{aligned} B_u^{(r)} &= x_{\eta r}, \\ C_u^{(r)} &= (-z_w + \nu + \chi)x_{\eta r} + x_w z_{\eta r}, \\ D_u^{(r)} &= S_3 x_{\eta r} + S_2 z_{\eta r} - S_1\delta_{\eta r}, \\ E_u^{(r)} &= k'\omega x_{\eta r} + k_L\omega z_{\eta r} - T_1\delta_{\eta r}, \end{aligned}\right\} \tag{15}$$

where

$$\left.\begin{aligned} S_2 &= \nu x_w + k_L\chi, \\ S_3 &= -\nu z_w + k'\chi + \omega \end{aligned}\right\} \tag{16}$$

and S_1, T_1 are defined by (8).

In the second of Equations (14),

$$\left.\begin{aligned} B_w^{(r)} &= z_{\eta r}, \\ C_w^{(r)} &= (z_u - \Upsilon)x_{\eta r} + (\nu - x_u)z_{\eta r} - \delta_{\eta r}, \\ D_w^{(r)} &= Q_3 x_{\eta r} + Q_2 z_{\eta r} - Q_1 \delta_{\eta r}, \\ E_w^{(r)} &= -k'\kappa x_{\eta r} - k_L \kappa z_{\eta r} - R_1 \delta_{\eta r}, \end{aligned}\right\} \tag{17}$$

where

$$\left.\begin{aligned} Q_2 &= -\nu x_u - k_L \Upsilon, \\ Q_3 &= \nu z_u - k'\Upsilon - \kappa \end{aligned}\right\} \tag{18}$$

and Q_1, R_1 are defined by (8).

In the last of Equations (14),

$$\left.\begin{aligned} C_\theta^{(r)} &= -\Upsilon x_{\eta r} - \chi z_{\eta r} - \delta_{\eta r}, \\ D_\theta^{(r)} &= N_3 x_{\eta r} + N_2 z_{\eta r} - N_1 \delta_{\eta r}, \\ E_\theta^{(r)} &= P_3 x_{\eta r} + P_2 z_{\eta r} - P_1 \delta_{\eta r}, \end{aligned}\right\} \tag{19}$$

where

$$\left.\begin{aligned} P_2 &= \omega x_u - \kappa x_w, \\ P_3 &= -\omega z_u + \kappa z_w, \\ N_2 &= \chi x_u - \Upsilon x_w - \omega, \\ N_3 &= -\chi z_u + \Upsilon z_w - \kappa \end{aligned}\right\} \tag{20}$$

and N_1, P_1 are defined by (8).

2.3.2. *Interpretation of the operational solutions.* The solutions $\hat{u}(D)$ etc., of the subsidiary equations are, in all cases, algebraic fractions in which the denominator is a quartic in D, while the numerators are of third or smaller order in D. The corresponding solutions $\hat{u}(\tau)$ etc., of the original equations of motion (4) are therefore readily obtainable from Table 3 (Item No. 126) of Ref. 4 and are of the general form

$$\hat{u} \text{ etc.} = A + \left(L \cos J\tau + N \frac{\sin J\tau}{J}\right) e^{-R\tau} + \\ + \left(l \cos j\tau + n \frac{\sin j\tau}{j}\right) e^{-r\tau}, \tag{21}$$

where $-R \pm iJ$, $-r \pm ij$ are the (complex) roots of the determinantal equation $F(D) = 0$ (Equation (6)) and A, L, N, l, n are constants.

2.4. *Basic Assumptions for the Estimation of the Aerodynamic Forces, Moments and Derivatives.* At this stage we must consider on what basis the aerodynamic derivatives appearing in the response equations are to be estimated. At the same time, it must be borne in mind that the study of disturbed motion involves the specification of the steady trimmed state about which the disturbance occurs. Clearly these two interlinked problems must be studied on the basis of the same aerodynamic assumptions.

Any practical application of the jet-flap principle will, of course, involve a jet-flapped wing of finite aspect ratio and, in the study of a specific project, the values of the aerodynamic forces and

derivatives used in the trim, stability and response analyses should, as far as possible, be derived from model tests or three-dimensional theory. However, the work described here was conceived as part of a generalized investigation, begun in Part I, of which the professed aim was a qualitative, rather than a precise quantitative, assessment of the effects under consideration. At the outset of this work, the final versions of Spence's two-dimensional theory[5] and Maskell and Spence's three-dimensional theory[6] had not been published. From a preview of the latter, at the time of writing Part I, however, the present author had concluded that the use of the three-dimensional theoretical results would render the trim analysis too complicated for the purpose in mind, and the decision was made to base the whole investigation on the early version of Spence's two-dimensional theory[7], which accordingly has been employed in developing the trim analysis of the present Paper (Section 2.5) and in obtaining expressions for the aerodynamic derivatives (Section 2.6).

In the latter connection, no account has been taken of unsteady flow effects as regards the forces and moments acting on the wing and assessment of the derivatives $m_{\dot{u}}$ and $m_{\dot{w}}$ has been based on the concept of downwash delay at the tailplane. The rotary damping of the wing has been neglected in comparison with that of the tailplane.

Further aerodynamic assumptions are noted in the following Section, where the trim analysis of Part I is re-worked, taking account of the effects of thrust and drag forces which were previously neglected.

2.5. *The Determination of Trimmed Conditions.* 2.5.1. *Trim and stability equations.* Fig. 1 shows the configuration of the aircraft and the system of forces acting on it, following small disturbances from the condition of steady rectilinear flight at speed U_s and incidence α_s, along a path inclined at an angle γ_s to the horizontal. Gx, Gz are axes fixed in the aircraft, Gx coinciding with the direction of motion in undisturbed flight.

In accordance with Spence's theory[7], the lift coefficient for the wing may be written

$$C_L = C_{L(\alpha)} + C_{L(\vartheta)} = A\alpha + B\vartheta, \tag{22}$$

with the corresponding forces $L(\alpha)$, $L(\vartheta)$ acting at distances $\xi_\alpha c$, $\xi_\vartheta c$ respectively from the leading edge, where A, B, ξ_α and ξ_ϑ are functions of the jet coefficient C_J only*.

---

* It may be pointed out here that although in the three-dimensional theory[6] the lift coefficient may be expressed in the form (22), the coefficients A and B in that case are functions not of C_J only, but of C_J, α, ϑ and aspect ratio A_R; *i.e.*, the contributions due to incidence and jet deflection are not, in fact, separable. Consequently, a trim and stability analysis based on the full three-dimensional formulae for C_L given in Sections 5.3 and 5.4 of Ref. 6 would be prohibitively complicated. However, from a limited amount of numerical work, it appears likely that over the practical range of parameters, the three-dimensional lift coefficient $C_L{}^{(3)}$ might be reasonably well approximated by the relationship

$$C_L{}^{(3)}/C_L{}^{(2)} = G(A_R, C_J)$$

with $G(A_R, C_J)$ given by Equation (67) of Ref. 6:—

$$G = (A_R + 0{\cdot}637\ C_J)/(A_R + 2 + 0{\cdot}604\ C_J{}^{1/2} + 0{\cdot}876\ C_J)$$

Thus, for a specified value of the aspect ratio, it would be possible to express $C_L{}^{(3)}$ in the form (22), with A and B depending on C_J only, albeit in a more complicated fashion than in the two-dimensional case.

To simplify the analysis it is assumed, when considering the balance of normal forces, that the lift provided by the tailplane is negligible in comparison with the wing lift so that the wing lift coefficient given by (22) may be taken as the total lift coefficient for the aircraft. The coefficient of resultant force in the direction of motion, C_F, may be expressed as

$$C_F = C_T - C_{D0}, \tag{23}$$

where C_{D0} is the skin-friction drag coefficient and C_T is the total thrust coefficient which, according to Spence, may be broken down into internal (direct) and external (induced) components C_{TI} and C_{Tc} respectively, where

$$C_{TI} = C_J \cos(\alpha+\vartheta) \tag{24}$$

and where, according to inviscid flow theory

$$C_{Tc} = C_J\{1 - \cos(\alpha+\vartheta)\}, \tag{25a}$$

so that

$$C_T = C_J. \tag{26a}$$

In practice, it is unlikely that the full value of the induced thrust, as given by (25a) will be attained and it is preferable to write

$$C_{Tc} = k_T C_J\{1 - \cos(\alpha+\vartheta)\}; \quad k_T \leqslant 1 \tag{25b}$$

and hence

$$C_T = C_J\{(1-k_T)\cos(\alpha+\vartheta) + k_T\}. \tag{26b}$$

On the assumption that the coefficients ξ_α, ξ_ϑ, defining the points of application of $L(\alpha)$, $L(\vartheta)$ respectively, have been chosen so as to give the correct pitching moment about the leading edge (*i.e.*, in accordance with Spence's theory) the thrust corresponding to C_T, as defined by (26b), must be assumed to act through the leading edge. The skin-friction drag will be assumed to act at the same position as does the lift when $C_J = 0$, *i.e.*, at $\xi_\alpha(0)c$. To simplify the analysis it will be further assumed that the wing zero-lift pitching moment and the body pitching moment are zero.

With the above assumptions, the pitching-moment coefficient for the complete aircraft, referred to the c.g., located at distance hc behind the wing leading edge, may be written as

$$\begin{aligned} C_m = {} & C_{L(\alpha)}(h-\xi_\alpha) + C_{L(\vartheta)}(h-\xi_\vartheta) + C_{D0}\{h-\xi_\alpha(0)\}\alpha - C_T h\alpha - \\ & - a_1\overline{V}\{\alpha - \epsilon(t) + \eta_T + ql_T/U\}. \end{aligned} \tag{27}$$

The 'α-restoring margin' $K_{r\alpha}$ and 'ϑ-restoring margin' $K_{r\vartheta}$ are given respectively by

$$\begin{aligned} K_{r\alpha} = {} & -\frac{\partial C_m}{\partial\alpha}\Big/\frac{\partial C_L}{\partial\alpha} \\ = {} & \xi_\alpha - h + \frac{\overline{V}a_1}{A}\left(1 - \frac{\partial\epsilon}{\partial\alpha}\right) - \frac{C_{D0}}{A}\{h - \xi_\alpha(0)\} + \\ & + \frac{C_T}{A}h - \frac{C_J}{A}h\alpha(1-k_T)\sin(\alpha+\vartheta) \end{aligned} \tag{28}$$

and

$$\begin{aligned} K_{r\vartheta} = {} & -\frac{\partial C_m}{\partial\vartheta}\Big/\frac{\partial C_L}{\partial\vartheta} \\ = {} & \xi_\vartheta - h - \frac{a_1\overline{V}}{B}\frac{\partial\epsilon}{\partial\vartheta} - \frac{C_J}{B}h\alpha(1-k_T)\sin(\alpha+\vartheta). \end{aligned} \tag{29}$$

For trimmed rectilinear flight at a small angle γ to the horizontal ($\cos\gamma \approx 1$) we have $C_m = q = 0$, so that if symbols appropriate to this condition are distinguished by the suffix 's' and if the thrust/weight ratio J/W is denoted by λ, the conditions of equilibrium of normal forces and pitching moments, used in conjunction with (22), lead to the equations

$$C_{J\,s} = \lambda C_{L\,s}, \tag{30}$$

where

$$C_{L\,s} = A_s\alpha_s + B_s\vartheta_s \tag{31}$$

and

$$\left[A_s\left\{h - (\xi_\alpha)_s - \frac{a_1\bar{V}}{A_s}\right\} - C_{T\,s}h + C_{D\,0}\{h - \xi_\alpha(0)\}\right]\alpha_s + \\ + B_s\{h - (\xi_\vartheta)_s\}\vartheta_s + a_1\bar{V}\epsilon_s - a_1\bar{V}(\eta_T)_s = 0. \tag{32}$$

It has been shown in Part I that $C_{L\,s}$, A_s, B_s $(\xi_\alpha)_s$, $(\xi_\vartheta)_s$ can be well approximated by linear relationships

$$\left.\begin{aligned} C_{L\,s} &= P\alpha_s + Q\,; \\ A_s &= p_1\alpha_s + q_1\,; \qquad (\xi_\alpha)_s = p_3\alpha_s + q_3\,; \\ B_s &= p_2\alpha_s + q_2\,; \qquad (\xi_\vartheta)_s = p_4\alpha_s + q_4\,; \end{aligned}\right\} \tag{33}$$

where P, Q, p_1, q_1, etc. are functions of λ and ϑ only. Thus, for a given aircraft, whose tail volume ($\bar{V}$) and c.g. position have been fixed, Equation (32) may be regarded as an equation for determining the trimmed incidence α_s, corresponding to a prescribed combination of control settings λ, ϑ, η_T, while (28) and (29) give the values of the two restoring margins.

2.5.2. *Tail volume and c.g. position as determined by basic design conditions.* The trim Equation (32) may be written in the form

$$[\{A_s - (C_{T\,s} - C_{D\,0})\}\alpha_s + B_s\vartheta_s]h - \bar{V}a_1\{\alpha_s - \epsilon_s + (\eta_T)_s\} \\ = \{A_s(\xi_\alpha)_s + C_{D\,0}\xi_\alpha(0)\}\alpha_s + B_s\vartheta_s(\xi_\vartheta)_s. \tag{34}$$

Then if (28) is rearranged thus for the steady condition:

$$\left\{1 - \frac{C_{T\,s} - C_{D\,0}}{A_s} + \frac{C_{J\,s}}{A_s}\alpha_s(1-k_T)\sin(\alpha_s+\vartheta_s)\right\}h - \\ - \frac{\bar{V}a_1}{A_s}\left\{1 - \left(\frac{\partial\epsilon}{\partial\alpha}\right)_s\right\} = \xi_{\alpha\,s} - K_{r\alpha\,s} + \frac{C_{D\,0}}{A_s}\xi_\alpha(0), \tag{35}$$

we have two equations from which the tail volume $\bar{V}$ and c.g. position hc, required to satisfy a specified design condition, may be determined. It will be assumed that $\alpha_s = \eta_{T\,s} = 0$, in the 'basic design condition' (*see* Part I) for which, with a combination of jet control settings $\vartheta = \bar{\vartheta}$, $\lambda = \bar{\lambda}$, the aircraft is required to have an α-restoring margin $K_{r\alpha}$. If it is further assumed that the downwash angle at the tail ϵ, may be expressed as

$$\epsilon = EC_L = E(A\alpha + B\vartheta) \tag{36}$$

and if the small term $(C_{D\,0}/A_s)\xi_\alpha(0)$ in (35) is neglected, Equations (34) and (35) may be simplified and solved to give

$$\left.\begin{aligned} \bar{V} &= \frac{\bar{A}}{a_1(1-E\bar{C}_F)}\left\{\left(1 - \frac{\bar{C}_F}{\bar{A}}\right)\bar{\xi}_\vartheta - \bar{\xi}_\alpha + \bar{K}_{r\alpha}\right\}, \\ h &= \bar{\xi}_\vartheta - \frac{E\bar{A}}{1-E\bar{C}_F}\left\{\left(1 - \frac{\bar{C}_F}{\bar{A}}\right)\bar{\xi}_\vartheta - \bar{\xi}_\alpha + \bar{K}_{r\alpha}\right\}, \end{aligned}\right\} \tag{37}$$

where $C_F = C_T - C_{D0}$ (Equation (23)) and 'barred' symbols are appropriate to the basic design condition. (Equations (37) may be compared with Equations (25) of Part I from which they differ because of the inclusion in the present analysis of thrust and drag forces whose effect on trim was neglected in the earlier work.)

With the assumption (36), the expressions (28) and (29) for the restoring margins become

$$\left.\begin{aligned} K_{r\alpha} &= \xi_\alpha - h + \frac{\bar{V}a_1}{A}(1-EA) - \frac{C_{D0}}{A}\{h - \xi_\alpha(0)\} + \frac{C_T}{A}h - \frac{C_J}{A}h\alpha(1-k_T)\sin(\alpha+\vartheta), \\ K_{r\vartheta} &= \xi_\vartheta - h - E\bar{V}a_1 - \frac{C_J}{B}h\alpha(1-k_T)\sin(\alpha+\vartheta). \end{aligned}\right\} \quad (38)$$

2.5.3. *Variation of trimmed incidence and lift coefficient with changes of control settings.* The aircraft may be trimmed to conditions other than those of 'basic design' by varying the control settings η_T, ϑ and λ, either singly or in combination and a complete trim analysis might be developed along the lines of Section 4.1.3 of Part I or of the Appendix thereto. However, in view of the limited computational effort available for this investigation, consideration has been given here only to the case where the aircraft has been trimmed by variation of the jet deflection ϑ, the thrust/weight ratio λ and the tailplane setting η_T remaining fixed at their basic design condition values ($\lambda = \bar{\lambda}$, $\eta_T = \bar{\eta}_T = 0$). In this case, if use is made of Equations (26b), (30) and (36), the equation for trimmed incidence is obtained from (32) as

$$\begin{aligned} &[A_s\{h - (\xi_\alpha)_s\} - \bar{V}a_1(1-EA_s) - \lambda C_{Ls}\{(1-k_T)\cos(\alpha_s+\vartheta_s) + k_T\} + \\ &\quad + C_{D0}\{h - \xi_0(0)\}]\,\alpha_s + B_s\{h - (\xi_\vartheta)_s + E\bar{V}a_1\}\vartheta_s = 0. \end{aligned} \quad (39)$$

If the linear approximations of (33) are substituted in the last equation, and squares and higher powers of α_s are neglected, the following approximate linear equation for trimmed incidence α_s (valid for small incidences) is obtained:

$$\begin{aligned} &[q_1(h-q_3) - \bar{V}a_1(1-Eq_1) - \bar{\lambda}Q\{(1-k_T)\cos\vartheta_s + k_T\} + C_{D0}\{h - \xi_\alpha(0)\} + \\ &\quad + \{p_2(h-q_4+E\bar{V}a_1) - p_4q_2\}\vartheta_s]\,\alpha_s = -q_2(h-q_4+E\bar{V}a_1)\vartheta_s. \end{aligned} \quad (40)$$

Values of Q and of the p's and q's appropriate to $\lambda = \bar{\lambda}$ and $\vartheta = \vartheta_s$ may be determined from Figs. 4 to 6 of Part I. Once α_s has been calculated, the corresponding $C_{Ls} = A_s\alpha_s + B_s\vartheta_s$ can also be calculated.

2.6. *Formulae for the Aerodynamic Derivatives.* Details of the derivation of formulae for the aerodynamic derivatives appropriate to disturbed flight are given in Appendix I; the formulae themselves are set out in Table 1.

3. *Numerical Examples.* 3.1. *Data and Assumptions.* As in Part I, all calculations have been based on the following formulae for the coefficients A, B, ξ_α, ξ_ϑ, derived from Spence's original two-dimensional work[7]:

$$\left.\begin{aligned} A &= 2\pi + 1{\cdot}152C_J^{1/2} + 1{\cdot}106C_J + 0{\cdot}051C_J^{3/2}, \\ B &= \quad 3{\cdot}545C_J^{1/2} + 0{\cdot}325C_J + 0{\cdot}156C_J^{3/2}, \\ \xi_\alpha &= 0{\cdot}25 - 0{\cdot}01C_J, \\ \xi_\vartheta &= 0{\cdot}50 + 0{\cdot}077C_J^{1/2}. \end{aligned}\right\} \quad (41)$$

Values for certain other coefficients and parameters have been assumed as follows:

Tailplane lift slope	a_1	=	2π
Downwash coefficient	E	=	$0{\cdot}025$
Skin-friction drag coefficient	C_{D0}	=	$0{\cdot}1$
Pitching inertia coefficient	i_B	=	$0{\cdot}1$
Tail arm ratio	l_T/c	=	$3{\cdot}5$
Aircraft wing loading	W/S	=	35 lb/ft^2
Aircraft relative density	μ_1	=	25
Air relative density (corresponding to operating height of 5000 ft)	σ	=	$0{\cdot}862$
The last four assumptions imply:			
Tail arm	l_T	=	$21{\cdot}2$ ft
Wing chord	c	=	$6{\cdot}05$ ft

The 'basic design condition' has been taken as:

Aircraft to trim at zero incidence with 'α-restoring margin' $\bar{K}_{r\alpha}$ (disposable parameter) when $\lambda = \bar{\lambda} = 0{\cdot}3$, $\vartheta = \bar{\vartheta} = 1$ radian and $\eta_T = \bar{\eta}_T = 0$.

The induced thrust factor k_T (introduced in Equation (25b)) will have a value between 0 and 1 and in order to assess the sensitivity of the results to variations in this parameter some of the initial calculations have been performed for $k_T = 0$ and $k_T = 1$. As these calculations indicated a relatively small effect the remainder of the calculations have been based on the assumption $k_T = 1$.

3.2. *Tail Volume and c.g. Position as Determined by Basic Design Conditions.* As in the numerical examples of Part I, the basic design condition provides a lift coefficient $\bar{C}_L = 5{\cdot}3$, with $\bar{A} = 9{\cdot}6$, $\bar{B} = 5{\cdot}3$, $\bar{C}_J = 1{\cdot}59$ $\bar{\xi}_\alpha = 0{\cdot}234$ and $\bar{\xi}_\vartheta = 0{\cdot}596$. The value of $\bar{C}_F$ is $1{\cdot}49$ if $k_T = 1$ or $0{\cdot}758$ if $k_T = 0$.

Equations (37) give

For

$$\left.\begin{aligned} k_T = 1, \qquad \bar{V} &= 0{\cdot}426 + 1{\cdot}585\bar{K}_{r\alpha}, \\ h &= 0{\cdot}529 - 0{\cdot}2495\bar{K}_{r\alpha}. \end{aligned}\right\} \tag{42a}$$

For

$$\left.\begin{aligned} k_T = 0, \qquad \bar{V} &= 0{\cdot}367 + 1{\cdot}556\bar{K}_{r\alpha}, \\ h &= 0{\cdot}538 - 0{\cdot}245\bar{K}_{r\alpha}. \end{aligned}\right\} \tag{42b}$$

$\bar{V}$ and h have been calculated from these equations and plotted in Fig. 2 which also reproduces the corresponding curves from Fig. 7 of Part I, in order to demonstrate the appreciable effect of including in the present analysis, thrust and drag forces which were neglected in the earlier work. The effect of varying k_T between 0 and 1 is seen to be quite small.

3.3. *Dynamic Stability in the Basic Design Condition.* 3.3.1. *Effect of the factor k_T on stability characteristics.* As a further check on the degree of importance of the factor k_T, the stability quartic

for the basic design condition with $\bar{K}_{r\alpha} = 0{\cdot}2$ has been set up and solved for the two cases $k_T = 1$ and $k_T = 0$, which correspond respectively to steady flight conditions of 78·9 ft/sec at 15·6 deg to the horizontal and 79·8 ft/sec at 8·2 deg to the horizontal.

Values of the derivatives as calculated from the formulae of Table 1 and Equations (2) (using the data of Section 3.1), for the two values of k_T, are given in Table 2, while the characteristics of the motion for the two cases are compared in Table 3.

From a perusal of Tables 2 and 3 it is clear that variation of k_T within the extreme limits 0 to 1 does not have a profound effect on the calculated characteristics; accordingly k_T has been taken equal to 1 throughout the remainder of the numerical work. Since in practice typical values of k_T are likely to be of the order 0·7 to 0·8, the effect of this assumption should be negligible.

3.3.2. *Effect of the design restoring margin $\bar{K}_{r\alpha}$ on dynamic stability characteristics.* The characteristics of disturbed longitudinal motion, initiated from the basic design condition, have been evaluated for a range of values of the design restoring margin $\bar{K}_{r\alpha}$ and the results are shown in Figs. 3a, b, c.

It will be seen that as $\bar{K}_{r\alpha}$ is reduced, the period of the short-period mode increases while that of the long-period mode decreases; thus while at $\bar{K}_{r\alpha} = 0{\cdot}4$ the long-period is nearly five times the short-period, at $\bar{K}_{r\alpha} = 0{\cdot}1$ the ratio between the periods is not much more than two.

The short period mode is well-damped throughout the range of $\bar{K}_{r\alpha}$ considered; the absolute time to halve the amplitude increases as $\bar{K}_{r\alpha}$ is reduced but the number of cycles decreases.

The long-period mode is an increasing oscillation for which the time to double amplitude (both in seconds and in cycles) decreases as $\bar{K}_{r\alpha}$ is reduced.

3.4. *Variation of Dynamic Stability Characteristics with Trimmed Lift Coefficient.* 3.4.1. *Variation of the stability derivatives.* Equation (40) has been used to estimate the trimmed incidence α_s, and hence the trimmed lift coefficient C_{Ls}, for a range of values of the jet-flap deflection ϑ_s, the other control settings being fixed at their basic design values ($\lambda = \bar{\lambda} = 0{\cdot}3$, $\eta_T = \bar{\eta}_T = 0$) and a value of 0·2 having been assumed for $\bar{K}_{r\alpha}$*. The results are exhibited in Fig. 4, which also shows the variation of trimmed speed with ϑ, calculated for the assumed height of 5000 ft with a wing loading of 35 lb/ft².

Values of the stability derivatives corresponding to the same range of trimmed conditions have been calculated from the formulae of Table 1 and Equations (2) (with $i_B = 0{\cdot}1$, $\mu_1 = 25$), and the results are shown in Figs. 5a, b.

3.4.2. *Variation of the periods and dampings.* The stability quartic has been solved for several trimmed conditions in the range covered by Figs. 4 and 5 and the results are given in Fig. 6a, which shows the periods of oscillation of the two modes, and in Figs. 6b and c which show the corresponding damping characteristics.

It will be observed that as the trimmed lift coefficient is increased, the long period decreases while the short period increases. Thus, while at $C_{Ls} \approx 0{\cdot}25$ the long period is about eighty times the short period, at $C_{Ls} = 5{\cdot}3$ the ratio of the two periods is little more than three. The short-period mode is well damped over the complete range of trimmed conditions considered; the actual time to halve the amplitude increases as C_{Ls} increases, although the corresponding number of cycles

* It was concluded in Part I from trim and manoeuvrability considerations that if jet controls are to be used, $\bar{K}_{r\alpha}$ should not be less than 0·2. For tail control, $\bar{K}_{r\alpha}$ could be reduced down to about 0·1.

decreases slightly. The long-period mode is (positively) damped at low values of C_{Ls} but becomes unstable for a C_{Ls} of order 1·0; it becomes progressively more unstable as C_{Ls} is increased until, at the basic design value of $C_{Ls} = 5{\cdot}3$, the amplitude of the oscillation doubles in rather less than one cycle.

The manner in which the stability characteristics vary with C_{Ls} for the jet-flap aircraft is not fundamentally different from the case of a conventional aircraft. Thus, it is usual for the phugoid- and short-periods to tend towards one another as C_{Ls} increases and for the phugoid damping to deteriorate at the same time. However, the fact that much higher values of C_{Ls} are attainable with the jet-flap aircraft than with a conventional one, means that, within the practicable range of that parameter, the two periods may be brought much closer together than usual, while the phugoid damping can deteriorate well beyond the point where the mode becomes unstable.

3.5. *Response Calculations.* 3.5.1. *Basis of Calculations.* In view of the difficulty (already alluded to in Section 2.3) of specifying realistic modes of application for the three types of longitudinal control, responses have been computed only for simple step-function inputs of each control. Two initial trim conditions have been considered:

(*a*) Basic design condition ($\bar{\lambda} = 0{\cdot}3$, $\bar{\vartheta} = 1$ radian, $\bar{\eta}_T = \bar{\alpha} = 0$, $\bar{K}_{r\alpha} = 0{\cdot}2$, giving $C_{Ls} = 5{\cdot}3$, $U_s = 78{\cdot}9$ ft/sec, $\gamma_s = 15{\cdot}6$ deg).

(*b*) Cruise condition ($\lambda = 0{\cdot}3$, $\vartheta = 0{\cdot}2$ radian, $\eta_T = 0$, giving $C_{Ls} = 0{\cdot}268$, $U_s = 357$ ft/sec, $\gamma_s = -4{\cdot}2$ deg).

The basic response quantities $\hat{u}$, $\hat{w}$ and θ have been evaluated by application of the analysis set out in Section 2.3; values of the relevant derivatives, calculated from the formulae of Table 1 and Equations (2) (with $i_B = 0{\cdot}1$, $\mu_1 = 25$), are set out in Table 4.

Two additional response quantities—the increment of flight path angle $\hat{\gamma}$ and the incremental load factor Δn have also been calculated. The former is given simply by

$$\hat{\gamma} = \theta - \hat{w}. \tag{43}$$

To obtain an expression for Δn in terms of the applied control forces and the basic response quantities, we note that

$$\text{Incremental normal acceleration} = \Delta ng = U_s \frac{d\hat{\gamma}}{dt}$$

$$= \frac{U_s}{\hat{t}} \frac{d(\theta - \hat{w})}{d\tau}.$$

Hence, using the second of Equations (4), we have

$$\Delta n = -\frac{U_s}{g\hat{t}} (z_u \hat{u} + z_w \hat{w} + z_{\eta_T} \hat{\eta}_T + z_\vartheta \hat{\vartheta} + z_\lambda \hat{\lambda} + k'\theta)$$

$$= -\frac{\rho S U_s^2}{W} (z_u \hat{u} + z_w \hat{w} + z_{\eta_T} \hat{\eta}_T + z_\vartheta \hat{\vartheta} + z_\lambda \hat{\lambda} + k'\theta),$$

whence

$$\Delta n = -\frac{2 \cos \gamma_s}{C_{Ls}} (z_u \hat{u} + z_w \hat{w} + z_\vartheta \hat{\vartheta} + z_\lambda \hat{\lambda} + k'\theta) \tag{44}$$

if, as in the present analysis, we take $z_{\eta_T} = 0$. Substitution of appropriate values for the derivatives from Table 4 leads to the following expressions:

Basic design condition

$$\left.\begin{aligned}
\frac{\Delta n}{\hat{\eta}_{T\,0}} &= 0{\cdot}756\,\frac{\hat{u}}{\hat{\eta}_{T\,0}} + 1{\cdot}4736\,\frac{\hat{w}}{\hat{\eta}_{T\,0}} + 0{\cdot}2707\,\frac{\theta}{\hat{\eta}_{T\,0}}, \\
\frac{\Delta n}{\hat{\vartheta}_0} &= 0{\cdot}756\,\frac{\hat{u}}{\hat{\vartheta}_0} + 1{\cdot}4736\,\frac{\hat{w}}{\hat{\vartheta}_0} + 0{\cdot}2707\,\frac{\theta}{\hat{\vartheta}_0} + 0{\cdot}963, \\
\frac{\Delta n}{\hat{\lambda}_0} &= 0{\cdot}756\,\frac{\hat{u}}{\hat{\lambda}_0} + 1{\cdot}4736\,\frac{\hat{w}}{\hat{\lambda}_0} + 0{\cdot}2707\,\frac{\theta}{\hat{\lambda}_0} + 1{\cdot}952.
\end{aligned}\right\} \tag{45}$$

Cruising condition

$$\left.\begin{aligned}
\frac{\Delta n}{\hat{\eta}_{T\,0}} &= 1{\cdot}073\,\frac{\hat{u}}{\hat{\eta}_{T\,0}} + 25{\cdot}054\,\frac{\hat{w}}{\hat{\eta}_{T\,0}} - 0{\cdot}0731\,\frac{\theta}{\hat{\eta}_{T\,0}}, \\
\frac{\Delta n}{\hat{\vartheta}_0} &= 1{\cdot}073\,\frac{\hat{u}}{\hat{\vartheta}_0} + 25{\cdot}054\,\frac{\hat{w}}{\hat{\vartheta}_0} - 0{\cdot}0731\,\frac{\theta}{\hat{\vartheta}_0} + 3{\cdot}859, \\
\frac{\Delta n}{\hat{\lambda}_0} &= 1{\cdot}073\,\frac{\hat{u}}{\hat{\lambda}_0} + 25{\cdot}054\,\frac{\hat{w}}{\hat{\lambda}_0} - 0{\cdot}0731\,\frac{\theta}{\hat{\lambda}_0} + 1{\cdot}350,
\end{aligned}\right\} \tag{46}$$

Alternatively, solutions for Δn may be obtained by firstly deriving the operational solution $\Delta n(D)$ from the corresponding operational solutions $\theta(D)$, $\hat{w}(D)$ and then obtaining $\Delta n(\tau)$ as for the other response quantities. Thus

$$\frac{\Delta n(D)}{\hat{\eta}_{r\,0}} = \frac{U_s}{g\hat{t}}\,D\left\{\frac{\theta(D)}{\hat{\eta}_{r\,0}} - \frac{\hat{w}(D)}{\hat{\eta}_{r\,0}}\right\},$$

or

$$\frac{\Delta n(D)}{\hat{\eta}_{r\,0}} = \frac{U_s}{g\hat{t}}\,\frac{D\{F_\theta^{(r)}(D) - F_w^{(r)}(D)\}}{F(D)}, \tag{47}$$

from Equations (13), with $F_\theta^{(r)}(D)$, $F_w^{(r)}(D)$ given by (14). From Equation (47) the corresponding solution $\Delta n(\tau)/\hat{\eta}_{r\,0}$ may be obtained from Table 3 (Item 126) of Ref. 4.

3.5.2. *Results of calculations.* Tables 5 and 6 give the solutions of the response equations for the basic design and cruising conditions respectively. The four response quantities that are physically most interesting, $\hat{u}$, $\hat{w}$, $\hat{\gamma}$ and Δn have been plotted in Figs. 7 to 9 for the basic design condition and in Figs. 10 to 12 for the cruising condition. Also indicated on these figures are the values of $\hat{w}$, $\hat{\gamma}$ and Δn derived on the basis of quasi-steady manoeuvrability theory ($\hat{u}$ is, of course, zero according to this theory). The derivation of the simplified formulae for this case is given in Appendix II.

3.5.3. *Discussion of the results.* The modes of response to the individual controls in the basic design condition (Figs. 7 to 9) are dominated by the facts that the long period oscillation is divergent and that its period is only about three times that of the short period oscillation (*see* Fig. 6). Thus speed changes become pronounced quite early in the motion and conditions appropriate to the quasi-steady maneouvrability theory are never established. Accordingly, apart from giving crude

approximations to the first turning values of $\hat{w}(t)$ and $\Delta n(t)$ and to the change of flight path angle $\hat{\gamma}(t)$ achieved in the corresponding time, the above-mentioned theory is not really applicable under the basic design conditions of very high lift coefficient and low speed. The results given in Fig. 17 of Part I for 'Control actions per g in constant speed manoeuvres initiated from the basic design condition' should be reviewed in the light of the above remarks.

In the case of cruising conditions, Figs. 10 to 12 show that the quasi-steady manoeuvrability theory gives very good approximations to the conditions obtaining when the short-period oscillation has been damped out at $1\frac{1}{2}$ to 2 seconds after the initiation of the motion. Subsequently, as the speed begins to change under the influence of the long period oscillation, the response quantities $\hat{w}$, Δn and $\hat{\gamma}$ tend to drift away from the quasi-steady values.

A cursory examination of Figs. 7 to 12 indicates that there are important differences in the characteristics of the initial responses of a jet-flapped aircraft to the three controls. To enable these differences to be examined more closely, Figs. 13 and 14 have been prepared. In examining these figures it may be borne in mind that the curves for η_T-control give a qualitative indication of the response characteristics for a conventional aircraft with tail control. At the same time it must be remembered that Fig. 13 relates to a lift coefficient much higher than the $C_{L\,\max}$ of a conventional aircraft so that, as remarked in Section 3.4.2, the relevant stability characteristics differ considerably (in degree, if not in kind), from those usually exhibited in the high-lift condition. Furthermore, as an examination of Tables 1 and 2 readily shows, for a given C_L, the values of several aerodynamic derivatives are considerably influenced by the presence of the jet (particularly at the higher values of C_L and C_J). Thus m_u and $m_{\dot{w}}$, which would be taken as zero for the conventional aircraft, assume non-zero values for the jet-flap aircraft, while z_u, z_w and m_w are all significantly affected by the dependence of the lift on C_J. With the simplifying assumptions of the present work, x_u and x_w appear unaffected but if three-dimensional effects are taken into account, these two derivatives are also influenced by the jet through the induced drag terms. (*See* Appendix III.) It has, unfortunately, not been possible, with the limited computing effort available, to examine systematically the effects on stability and response of variations in values of individual derivatives.

Fig. 13 relates to the basic design (high lift) condition and compares the aircraft responses during the first six seconds following the control applications $\hat{\eta}_{T\,0} = -1$ deg, $\hat{\vartheta}_0 = 5$ deg and $\hat{\lambda}_0 = 0{\cdot}02$ respectively. These control amounts are largely arbitrary but may be thought of as representing something like one-fifth of the available deflection in each case*.

If the primary purpose of control application is to change the flight path angle, then it may be concluded from Fig. 13c that, in the basic design condition, the jet controls are initially more effective than the tail control. This is because (with the assumptions made in this Report) application of either jet control is considered to result in an instantaneous increase of lift (and hence of normal acceleration, *see* Fig. 13d), whereas with the application of tail control, the incremental lift (and hence normal acceleration) develops only gradually as the angle of attack of the aircraft is changed. However, as the motion following the application of ϑ- or λ-control develops, the aircraft acquires a negative angle of attack and since the corresponding (negative) lift increment opposes the direct (positive) increment produced by the control increment, the normal acceleration and also the rate of increase of flight path angle fall. Thus, after about two seconds, the incremental normal acceleration produced

* Relatively small deflections are considered so that the calculated perturbations are small enough for the linearized theory to be valid.

by the tail control exceeds that produced by either jet control. At the same time the change of flight path angle produced by $\hat{\eta}_{T0} = -1$ deg exceeds that produced by $\hat{\lambda}_0 = 0{\cdot}02$; however, while the *rate* of change of path angle due to the former is now greater than that due to $\hat{\vartheta}_0 = 5$ deg, the total change of path angle due to the tail control does not equal that due to jet deflection control until about six seconds have elapsed, by which time, both flight path angles have begun to decrease under the influence of the long period oscillation.

The aircraft speed decreases continuously under the influence of the tail or jet deflection control throughout the six-second interval considered, the decrease being rather more rapid for $\hat{\vartheta}_0 = 5$ deg than for $\hat{\eta}_{T0} = -1$ deg. Application of the thrust control $\hat{\lambda}_0 = 0{\cdot}02$ results in an initial slight increase in speed followed by a decrease. The considerable difference in the speed variation as between ϑ- and λ-controls may, at first sight, be a little surprising, but it may be accounted for by that fact that while the ϑ-control provides no increment of thrust, ($x_\vartheta = 0$) the λ-control provides a large increment ($x_\lambda = 2{\cdot}65$). Thus, if we consider the equations for longitudinal acceleration:

$$\vartheta\text{-control:} \qquad \frac{d\hat{u}}{d\tau} = x_u\hat{u} + x_w\hat{w} - k_L\theta + x_\vartheta\hat{\vartheta},$$

$$\lambda\text{-control:} \qquad \frac{d\hat{u}}{d\tau} = x_u\hat{u} + x_w\hat{w} - k_L\theta + x_\lambda\hat{\lambda}$$

and note that $k_L = x_w = 2{\cdot}65$, $x_u \approx 0$;
then putting $\theta - \hat{w} = \hat{\gamma}$, we have

$$\vartheta\text{-control:} \qquad \frac{d\hat{u}}{d\tau} \approx -2{\cdot}65\hat{\gamma},$$

$$\lambda\text{-control:} \qquad \frac{d\hat{u}}{d\tau} \approx 2{\cdot}65\hat{\lambda} - 2{\cdot}65\hat{\gamma}.$$

$\hat{\gamma}$ is initially zero in both cases but $\hat{\lambda} = \text{constant} = 0{\cdot}02$ throughout the motion. Thus with ϑ-control, $d\hat{u}/d\tau$ is initially zero but assumes increasing negative values as the aircraft begins to climb; with λ-control on the other hand $d\hat{u}/d\tau$ is initially positive so that the speed initially increases but then decreases as the aircraft begins to climb.

The general conclusion from the foregoing discussion would seem to be that when, with the aircraft in a high-lift condition, a sudden change in flight path angle is required (for instance, to avoid an unexpected obstacle), application of jet deflection or jet thrust control (in that order) should be more effective than application of tail control, although eventually the tail control might produce a larger change of flight path angle and a larger increment of normal acceleration than either jet control.

Fig. 14 compares the responses of the aircraft to the three controls in the cruising condition. The deflections assumed for the tail and jet-flap deflection controls are, as in the basic design condition, $\hat{\eta}_{T0} = -1$ deg, $\hat{\vartheta}_0 = 5$ deg but as the responses to jet thrust control are relatively small they are shown for $\hat{\lambda}_0 = 0{\cdot}1$ in this case.

Fig. 14b shows that when tail control is applied in the cruising condition, a change of angle of attack (and hence of lift) is very rapidly established so that although the jet controls provide instantaneous increments of normal acceleration, these are exceeded within one-fifth of a second of the application of tail control. Correspondingly, the change of flight path angle produced by the tail control exceeds that produced by either jet control within two-fifths of a second of application.

The changes of angle of attack which occur when the jet controls are applied are very small and initially in the sense which gives a negative lift increment, opposing the direct (positive) increment provided by the control action. Both the η_T-control and the ϑ-control (when applied to increase the flight path angle) tend to decrease the speed but the λ-control initially causes an increase in speed.

The general conclusion from Fig. 14 is that in the cruising condition, tail control is more effective than either jet deflection or jet thrust control; the latter, in particular, is very ineffective.

A further illustration of the differences in initial modes of response is given by Fig. 15 which shows the modes of Δn and $\hat{\gamma}$ for the cruising condition, arbitrarily normalized with respect to the values of these quantities at $t = 2$ seconds (at which time the short-period oscillation has been virtually damped out, while the long period oscillation has scarcely begun to affect the motion).

4. *General Summary, Discussion and Conclusions.* 4.1. *Scope and Validity of Investigation.* The generalised investigation of the longitudinal stability and control problems of jet-flapped aircraft, which was begun in Ref. 1 and Part I of the present Report with considerations of trim, static stability and quasi-steady manoeuvrability criteria, has been taken a stage further by the present study of dynamic stability and response characteristics. As in the earlier work, the analysis has been based on Spence's two-dimensional theoretical data and so again, the results should not be expected to apply to jet-flapped aircraft with low aspect ratio wings; for layouts of moderately high or high aspect ratio, the conclusions should be at least qualitatively valid.

One way in which the use of two-dimensional data might be suspected of invalidating the conclusions is through the neglect of induced drag. To obtain some idea of the importance of this factor, an assessment has been made of the effect on stability characteristics in the basic design condition, of including an induced drag term (in coefficient form: $C_{Di} = k_i C_L^2$) in the longitudinal force equation. The details are given in Appendix III, where it is concluded that for wings with aspect ratio of order 10, the effects are not sufficiently large to invalidate the conclusions qualitatively.

4.2. *Revised Trim and Static Stability Analysis.* The trim and stability analysis of Part I has been modified to the extent that the pitching moments due to thrust and drag forces, which were previously neglected, have now been taken into account and it has been seen (Fig. 2) that there is an appreciable effect on the tail volume and c.g. position required to satisfy specified design conditions.

4.3. *Dynamic Stability Characteristics.* The values of the stability derivatives (Table 2) and the characteristics of disturbed longitudinal motion (Table 3) in the 'basic design' (high lift) condition have been shown to be not very sensitive to the value assumed for the induced thrust factor k_T, defined by Equation (25b), and the bulk of the numerical work has been based on the assumption of full thrust recovery ($k_T = 1$).

The disturbed longitudinal motion about the basic design condition has been investigated for a range of values of the restoring margin $\overline{K}_{r\alpha}$ and it has been seen (Figs. 3a, b, c) that the period of the quicker oscillation, which is always well damped, increases as $\overline{K}_{r\alpha}$ is reduced, whereas, that of the slower (phugoid) oscillation, which is divergent*, decreases with diminishing $\overline{K}_{r\alpha}$. For $\overline{K}_{r\alpha} = 0{\cdot}1$, the longer period would be not much more than twice the shorter period so that the phugoid can begin to exert an appreciable influence on the resultant motion before the short-period oscillation has been damped out.

* It will be recalled from Section 3.4.2 and Fig. 6c that the phugoid, whose damping progressively deteriorates with increasing lift coefficient C_{Ls}, is, in fact, divergent for all C_{Ls} greater than about 1·0.

The trim and manoeuvrability considerations of Part I had suggested that if jet controls were to be used effectively, a value of at least 0·2 should be provided for $\bar{K}_{r\alpha}$, although a value as small as 0·1 might suffice in the case of tail controls. In considering the remainder of the stability and response results, which have been calculated for $\bar{K}_{r\alpha} = 0{\cdot}2$, it should therefore be remembered that the performance of the tail control in relation to that of either jet control could probably be improved by designing for a smaller restoring margin which, incidentally (*see* Fig. 2), would require a smaller tail volume.

The variations of longitudinal characteristics with trimmed lift coefficient have been studied for a fixed value of the design restoring margin $\bar{K}_{r\alpha} = 0{\cdot}2$. The salient points that emerge from the results (Figs. 6a, b, c) are:

(1) As the lift coefficient is increased, the period of the phugoid decreases, while that of the rapid oscillation increases. This feature is not peculiar to a jet-flapped aircraft but the fact that the jet-flap enables much higher C_L's to be achieved, means that the periods of the two modes may be brought into much closer proximity than in the case of conventional aircraft. Thus, at the highest lift coefficient considered ($C_{Ls} = 5{\cdot}3$), the ratio between the periods of the modes is not much more than 3, compared with values of about 9 at $C_{Ls} = 2{\cdot}0$ and approximately 80 at $C_{Ls} = 0{\cdot}25$. This would indicate a greater likelihood of the two modes interacting at high lift coefficients than at low, although some calculations (not reported in detail here) have indicated that even at the highest C_L, the approximation to the short-period mode, obtained by neglecting variations of forward speed, is quite good.

(2) The damping of the short-period mode is good at all C_L's and (in terms of cycles to halve amplitude), increases slightly with increasing C_L. The phugoid is positively damped at cruising C_L's but becomes unstable for C_L's greater than about 1·0; at the highest C_L the oscillation doubles its amplitude in about one cycle.

4.4. *Response to Control Application.* The responses of the jet-flapped aircraft to step-function inputs of tailplane, jet deflection and jet thrust controls have been calculated and the results, presented in Figs. 7 to 9 (high-lift condition) and Figs. 10 to 12 (cruising condition) have enabled us to assess the validity of the quasi-steady manoeuvrability criteria, used in Part I as a basis for comparing the effectiveness of the three controls.

The results indicate that in the high-lift case, nothing approaching a 'quasi-steady' condition is ever established; this is a consequence of the fact that the phugoid period is of the same order as the short period, the situation being aggravated by the additional fact of the phugoid being divergent. In the circumstances, the quasi-steady theory gives no more than a crude approximation to the first turning values of the response quantities $\hat{w}(t)$ and $\Delta n(t)$ and Fig. 17 of Part I should be re-interpreted accordingly.

In the cruising condition, the short-period oscillation rapidly dies out and, for a few seconds at least, before the phugoid makes its presence felt, a quasi-steady condition, agreeing well with the predictions of manoeuvrability theory, exists. A figure such as Fig. 18 of Part I is thus essentially valid although, if interest centres on comparative response in a very short interval following control application, the actual response curves must be considered.

Figs. 13 to 15 have revealed significant differences in the responses to jet controls on the one hand and tail control on the other. With the assumptions made in this investigation, the jet controls provide

instantaneous lift increments, whereas the lift increment due to tail control is built up only gradually as the result of changes in the angle of attack, occurring through the medium of the short-period oscillation. Since, in the basic design (high lift) condition, the 'short' period is relatively large, the response to tail control is initially much slower than the response to either jet control. Thus tail control no longer emerges as the most effective control in the high-lift condition, as it did in Part I, on the basis of the quasi-steady manoeuvrability criterion. Jet deflection control now appears as the most effective. It is to be noted, however, that while the rate of response to tail control builds up with increasing angle of attack, the initially high rates of response due to the direct lift increments applied by jet controls, are subsequently reduced by unfavourable changes in angle of attack.

In the cruising condition, because of the considerably shorter period of the rapid oscillation, the response to tail control is built up much more rapidly than in the high-lift case and the conclusion, arrived at in Part I on the basis of the quasi-steady manoeuvrability criterion, that for the cruise, tail control is more effective than jet control, is broadly substantiated.

It should be emphasized that the control effectivenesses have been compared purely on the basis of hypothetical step-function inputs, assuming that the corresponding *direct* aerodynamic control actions (pitching-moment increment in the case of tail control, lift increments in the case of jet controls) are developed instantaneously (*i.e.*, Wagner effects have been neglected). Should it transpire that the modes of control application and of development of corresponding control actions, which can be achieved in practice, differ considerably as between the three types of control, then the foregoing conclusions might need modification. In the basic design condition, the picture could be further changed as the result of measures that might be taken to suppress the 'speed instability'.

5. *Future Developments.* The investigation covered by the two Parts of this Report has not been as comprehensive as one might have wished. With so many parameters entering the problem, the field of possible exploration is almost unbounded. We have not, for instance, been able to examine very closely the influence of our admittedly crude downwash assumptions on the problems considered. Again, in the present Part, when considering response to controls, we have considered only the simplest (and hypothetical) case of step-function inputs and a study of more realistic modes of input (if these could be specified) would be instructive. In view of the 'speed instability' which, it has been shown, will exist at high lift coefficients, it would be interesting to consider the possible use of the controls to suppress speed variations and then to examine the 'stability under constraint' of the aircraft in the manner suggested by Neumark in Ref. 8.

However, with the pressing need to determine more precisely the stability and response characteristics of practicable jet-flap aircraft configurations, it is desirable that future efforts should be directed in the first instance to an investigation of the influence of finite aspect ratio on the stability and control derivatives.

A sound foundation for such an investigation has been provided by Maskell and Spence[6], and Ross[9]. It should be noted, however, that the fundamental theory of the jet-flap in three-dimensions has not yet been formally developed to the stage where it provides the flight dynamicist with all the aerodynamic information he needs, in immediately assimilable form. For instance, the results of Ref. 6 are confined to lift and drag (with no mention of pitching moment) and are appropriate only to the case of uniform angle of attack, while the downwash theory of Ref. 9 has not yet been fully substantiated by experiment.

As regards pitching moments, Küchemann[10] has suggested a simple method (using Spence's two-dimensional results[7] for chordwise loading on a thin, flat jet-flapped wing, in conjunction with Ref. 6) for calculating the chordwise loading on jet-flapped wings of finite aspect ratio, including effects of section thickness and camber.

Nevertheless, while there remains no insuperable obstacle in his way, the flight dynamicist is still confronted with a large amount of purely aerodynamic spade work to perform before he can calculate the complete range of derivatives involved in a comprehensive stability and response analysis for a jet-flapped aircraft.

LIST OF SYMBOLS

$A = \partial C_L/\partial\alpha$
$B = \partial C_L/\partial\vartheta$
, functions of C_J only for two-dimensional jet-flapped aerofoil

$B_1,\ C_1,\ D_1,\ E_1$ — Coefficients of stability quartic (*see* Equation (6))

$B_u^{(r)},\ C_u^{(r)},\ D_u^{(r)},\ E_u^{(r)}$
$B_w^{(r)},\ C_w^{(r)},\ D_w^{(r)},\ E_w^{(r)}$
$C_\theta^{(r)},\ D_\theta^{(r)},\ E_\theta^{(r)}$
— Coefficients of numerator polynomials $F_u^{(r)}$, $F_w^{(r)}$, $F_\theta^{(r)}$ in operational solutions for response to controls (*see* Equations (13) and (14))

C_{Di} — Induced drag coefficient for three-dimensional wing

C_{D0} — Skin-friction drag coefficient

C_F — Coefficient of resultant force in direction of motion

C_J — Jet coefficient $= J/\frac{1}{2}\rho U^2 c$

C_L — Total wing lift coefficient

$C_{L(\alpha)},\ C_{L(\vartheta)}$ — Component lift coefficients (Equation (22)), proportional to α and ϑ respectively for a given C_J

C_m — Pitching-moment coefficient of complete aircraft referred to c.g.

C_T — Total thrust coefficient $(= C_{TI} + C_{Tc})$

C_{Tc} — External (induced) thrust coefficient

C_{TI} — Internal (direct) thrust coefficient

D — Differential operator

E — Downwash constant (Equation (46))

$F(D)$ — Polynomial in D: L.H.S. of stability quartic (Equation (6))

$F_u^{(r)}(D),\ F_w^{(r)}(D),\ F_\theta^{(r)}(D)$ — Numerator polynomials in operational solutions for response to controls (*see* Equations (13) and (14))

J — Gross jet thrust per unit length

$K_{r\alpha} = -\partial C_m/\partial C_{L(\alpha)}$: aircraft restoring margin with respect to change of incidence

$K_{r\vartheta} = -\partial C_m/\partial C_{L(\vartheta)}$: aircraft restoring margin with respect to change of jet deflection

M — Pitching moment about aircraft c.g.

N_1, P_1, Q_1 R_1, S_1, T_1	Shorthand constants defined by Equations (8)
N_2, N_3, P_2, P_3	Shorthand constants defined by Equations (20)
P, Q	Coefficients of linear approximation (*see* Equations (33)) for trimmed lift coefficient C_{Ls}: functions of λ and ϑ
Q_2, Q_3	Shorthand constants defined by Equations (18)
S_2, S_3	Shorthand constants defined by Equations (16)
S, S_T	Wing and tailplane areas respectively
T	Total thrust on jet-flapped aerofoil
U	Component of velocity along x-axis in disturbed flight ($= U_s+u$)
U_s	Undisturbed flight speed
$\bar{V}$	Tail volume ratio
W	Weight of aircraft
X	Aerodynamic force along the x-axis
Z	Aerodynamic force along the z-axis
a_1	Tailplane lift slope $\partial C_{LT}/\partial \alpha_T$
c	Wing chord
g	Gravitational constant
h	Distance of c.g. from leading edge of chord as fraction of chord
i_B	Pitching inertia coefficient
k_L	$= \frac{1}{2}C_L$: coefficient in equations of motion (1)
k'	$= -k_L \tan \gamma_s$: coefficient in equations of motion (1)
k_i	Constant in assumed formula for induced drag coefficient (Equation (86), Appendix III)
k_T	Thrust recovery factor (*see* Equation (25b))
l_T	Tail arm
m	Aircraft mass

$m_u, m_{\dot{u}}, m_w, m_{\dot{w}}$ $m_q, m_{\eta_T}, m_\vartheta, m_\lambda$		Dimensionless pitching-moment derivatives due to parameters indicated by respective suffices, consistent with definitions of Ref. 2. (Except that $m_{\dot{u}}$, $m_{\dot{w}}$ are written for $\overline{m}_{\dot{u}}$, $\overline{m}_{\dot{w}}$)
Δng		Additional normal acceleration (relative to steady rectilinear flight)
$p_1 \cdots p_4$ $q_1 \cdots q_4$		Coefficients in linear approximations for A_s, B_s $(\xi_\alpha)_s$, $(\xi_\vartheta)_s$; functions of λ and ϑ only
q		Angular velocity in pitch
$\hat{t}$	$= \dfrac{W}{g\rho S U_s}$	Unit of aerodynamic time in seconds
u		Increment of velocity along x-axis in disturbed flight
$\hat{u}$	$= u/U_s$;	dimensionless increment of velocity along x-axis in disturbed flight
w		Increment of velocity along z-axis in disturbed flight
$\hat{w}$	$= w/U_s$;	dimensionless increment of velocity along z-axis in disturbed flight
$x_u, x_w, x_q,$ $x_{\eta_T}, x_\vartheta, x_\lambda$		Dimensionless longitudinal force derivatives due to parameters indicated by respective suffices, consistent with definitions of Ref. 2
$z_u, z_w, z_q,$ $z_{\eta_T}, z_\vartheta, z_\lambda$		Dimensionless normal force derivatives due to parameters indicated by respective suffices, consistent with definitions of Ref. 2
α		Wing incidence
γ		Angle of inclination of flight path to horizontal
$\hat{\gamma}$		Increment of flight path angle in disturbed flight
$\delta_{\eta_T}, \delta_\vartheta, \delta_\lambda$		Concise pitching-moment derivatives appropriate to control deflections indicated by respective suffices (*see* Equations (2))
ϵ		Angle of downwash at tail
$\hat{\eta}_r (r = 1, 2, 3)$		Increments of control settings (*see* Equation (9))
$\hat{\eta}_{r\,0} (r = 1, 2, 3)$		Constant values of $\hat{\eta}_r$ for step-inputs
η_T		Tailplane setting relative to wing

$\hat{\eta}_T$	Increment of tailplane setting applied as control
$\hat{\eta}_{T\,0}$	Constant value of $\hat{\eta}_T$ for step-input
θ	Angular displacement in pitch from equilibrium position
ϑ	Angle between jet and wing chord at jet exit
$\hat{\vartheta}$	Increment of ϑ, applied as a control
$\hat{\vartheta}_0$	Constant value of $\hat{\vartheta}$ for step-input
κ	Concise pitching-moment derivative due to u (*see* Equations (2))
$\lambda = \frac{J}{W}$	; jet thrust/weight ratio
$\hat{\lambda}$	Increment of λ applied as a control
$\hat{\lambda}_0$	Constant value of $\hat{\lambda}$ for step-input
$\mu_1 = \frac{m}{\rho S l_T}$	; aircraft relative density
ν	Concise pitching-moment derivative due to q (*see* Equations (2))
ξ_α, ξ_ϑ	Distances aft of wing leading edge at which component lift coefficients $C_{L(\alpha)}$, $C_{L(\vartheta)}$ respectively act (as fractions of chord)
ρ	Air density
σ	Relative air density
τ	Dimensionless aerodynamic time
γ	Concise pitching-moment derivative due to $\dot{u}$ (*see* Equations (2))
χ	Concise pitching-moment derivative due to $\dot{w}$ (*see* Equations (2))
ω	Concise pitching-moment derivative due to w (*see* Equations (2))

Suffix

s	Referring to steady rectilinear flight

A bar over a symbol (*e.g.*, $\bar{\vartheta}$) is used to denote the value appropriate to the basic design condition (except in $\bar{V} \equiv$ tail volume ratio).

REFERENCES

No.	*Author*	*Title, etc.*
1	A. S. Taylor	A preliminary examination of the stability and control problems associated with the design of a jet-flap aircraft with conventional tailplane and elevator. A.R.C. 18,208. June, 1955.
2	—	Royal Aeronautical Society Data Sheets. Aerodynamics. Number Aircraft. 00.00.02.
3	S. Neumark	The disturbed longitudinal motion of an uncontrolled aircraft and of an aircraft with automatic control. A.R.C. R. & M. 2078. January, 1943.
4	S. Neumark	Operational formulae for response calculations. A.R.C. R. & M. 3075. June, 1956.
5	D. A. Spence	Some simple results for two-dimensional jet-flap aerofoils. *Aeronautical Quarterly*. Vol. IX. pp. 395 to 406. November, 1958.
6	E. C. Maskell and D. A. Spence	A theory of the jet flap in three dimensions. *Proc. Roy. Soc.* A. Vol. 251, pp. 407 to 425. 1959.
7	D. A. Spence	The lift coefficient of a thin jet-flapped wing. *Proc. Roy. Soc.* A. Vol. 238. pp. 46 to 68. 1956.
8	S. Neumark	Problems of longitudinal stability below minimum drag speed, and theory of stability under constraint. A.R.C. R. & M. 2983. July, 1953.
9	A. J. Ross	The theoretical evaluation of the downwash behind jet-flapped wings. A.R.C. R. & M. 3119. January, 1958.
10	D. Küchemann	A method for calculating the pressure distribution over jet-flapped wings. A.R.C. R. & M. 3036. May, 1956.

APPENDIX I

Derivation of Formulae for Aerodynamic Derivatives

We consider an initial steady condition of flight with speed U_s at inclination γ_s to the horizontal, with control settings η_{Ts}, λ_s, ϑ_s, incidence α_s and jet and lift coefficients C_{Js}, C_{Ls} respectively. Then

$$C_{Js} = \lambda_s C_{Ls}. \tag{48}$$

In the disturbed flight condition (small perturbations), we write

$$\left.\begin{aligned} U &= U_s + u = U_s(1+\hat{u}), \\ \alpha &= \alpha_s + \hat{\alpha} = \alpha_s + \hat{w}, \\ \eta_T &= \eta_{Ts} + \hat{\eta}_T, \\ \vartheta &= \vartheta_s + \hat{\vartheta}, \\ \lambda &= \lambda_s + \hat{\lambda}. \end{aligned}\right\} \tag{49}$$

We also have

$$C_J = \frac{\lambda}{\lambda_s}\left(\frac{U_s}{U}\right)^2 C_{Js},$$

or

$$C_J \approx \left(1 + \frac{\hat{\lambda}}{\lambda_s}\right)(1-2\hat{u})C_{Js}. \tag{50}$$

FORMULAE FOR THE LONGITUDINAL FORCE DERIVATIVES

If we neglect tail drag, the longitudinal force X in the disturbed motion is given by

$$\frac{X}{\frac{1}{2}\rho(U_s+u)^2 S} \approx -C_{D0} + C_T + C_L\hat{w},$$

whence

$$\frac{X}{\rho U_s^2 S} = (-C_{D0} + C_T + C_L\hat{w})(\tfrac{1}{2}+\hat{u}). \tag{51}$$

Then

$$\begin{aligned} x_u &= -C_{D0} + C_{Ts} + \tfrac{1}{2}\left(\frac{\partial C_T}{\partial \hat{u}}\right)_s \\ &= -C_{D0} + C_{Ts} + \tfrac{1}{2}\left[\frac{\partial}{\partial \hat{u}}\left\{\frac{C_{Ts}}{C_{Js}}C_J\right\}\right]_s \\ &= -C_{D0} + C_{Ts} - C_{Ts}, \qquad \text{by use of (50)}, \end{aligned}$$

or

$$x_u = -C_{D0}, \tag{52}$$

$$\begin{aligned} x_w &= \tfrac{1}{2}C_{Ls} + \tfrac{1}{2}\left(\frac{\partial C_T}{\partial \hat{w}}\right)_s \\ &= \tfrac{1}{2}[C_{Ls} - C_{Js}(1-k_T)\sin(\alpha_s+\vartheta_s)], \qquad \text{from (26b)}, \end{aligned}$$

or

$$x_w = \tfrac{1}{2}C_{Ls}[1 - \lambda_s(1-k_T)\sin(\alpha_s + \vartheta_s)], \tag{53}$$

$$x_\vartheta = \tfrac{1}{2}\left(\frac{\partial C_T}{\partial \vartheta}\right)_s$$

$$= -\tfrac{1}{2}C_{Js}(1-k_T)\sin(\alpha_s+\vartheta_s), \tag{54}$$

$$x_\lambda = \tfrac{1}{2}\left(\frac{\partial C_T}{\partial \hat{\lambda}}\right)_s,$$

$$= \tfrac{1}{2}\frac{C_{Ts}}{C_{Js}}\left(\frac{\partial C_J}{\partial \hat{\lambda}}\right)_s = \tfrac{1}{2}\frac{C_{Ts}}{\lambda_s}, \qquad \text{from (50)}.$$

Hence

$$x_\lambda = \tfrac{1}{2}C_{Ls}[(1-k_T)\cos(\alpha_s+\vartheta_s) + k_T]. \tag{55}$$

Also

$$x_q = x_{\eta_T} = 0. \tag{56}$$

FORMULAE FOR THE VERTICAL FORCE DERIVATIVES

If we neglect tail lift forces, the force along the z-axis is given by

$$\frac{Z}{\frac{1}{2}\rho(U_s+u)^2 S} = -C_L + (C_T - C_{D0})\hat{w},$$

or

$$\frac{Z}{\rho U_s^2 S} = \{-C_L + (C_T - C_{D0})\hat{w}\}(\tfrac{1}{2}+\hat{u}). \tag{57}$$

Then

$$z_u = -C_{Ls} - \tfrac{1}{2}\left(\frac{\partial C_L}{\partial \hat{u}}\right)_s$$

$$= -C_{Ls} - \tfrac{1}{2}\left\{\left(\frac{\partial A}{\partial C_J}\right)_s \alpha_s + \left(\frac{\partial B}{\partial C_J}\right)_s \vartheta_s\right\}\left(\frac{\partial C_J}{\partial \hat{u}}\right)_s$$

$$= -C_{Ls} + C_{Js}\left\{\left(\frac{\partial A}{\partial C_J}\right)_s \alpha_s + \left(\frac{\partial B}{\partial C_J}\right)_s \vartheta_s\right\}, \qquad \text{from (50)}.$$

Hence

$$z_u = -\left\{A_s - C_{Js}\left(\frac{\partial A}{\partial C_J}\right)_s\right\}\alpha_s - \left\{B_s - C_{Js}\left(\frac{\partial B}{\partial C_J}\right)_s\right\}\vartheta_s, \tag{58}$$

$$z_w = \tfrac{1}{2}(C_{Ts} - C_{D0}) - \tfrac{1}{2}\left(\frac{\partial C_L}{\partial \hat{w}}\right)_s$$

$$= \tfrac{1}{2}(C_{Ts} - C_{D0} - A_s),$$

i.e.,

$$z_w = \tfrac{1}{2}[C_{Js}\{(1-k_T)\cos(\alpha_s+\vartheta_s) + k_T\} - C_{D0} - A_s], \tag{59}$$

$$z_\vartheta = -\tfrac{1}{2}\left(\frac{\partial C_L}{\partial \vartheta}\right)_s = -\tfrac{1}{2}B_s, \tag{60}$$

$$z_\lambda = -\tfrac{1}{2}\left(\frac{\partial C_L}{\partial \lambda}\right)_s$$

$$= -\tfrac{1}{2}\left\{\left(\frac{\partial A}{\partial C_J}\right)_s \alpha_s + \left(\frac{\partial B}{\partial C_J}\right)_s \vartheta_s\right\}\left(\frac{\partial C_J}{\partial \hat{\lambda}}\right)_s$$

$$= -\tfrac{1}{2}\left\{\left(\frac{\partial A}{\partial C_J}\right)_s \alpha_s + \left(\frac{\partial B}{\partial C_J}\right)_s \vartheta_s\right\}\frac{C_{Js}}{\lambda_s}, \quad \text{from (50)}.$$

Hence

$$z_\lambda = -\tfrac{1}{2} C_{Ls} \left\{ \left(\frac{\partial A}{\partial C_J} \right)_s \alpha_s + \left(\frac{\partial B}{\partial C_J} \right)_s \vartheta_s \right\}. \tag{61}$$

Also

$$z_q = z_{\eta_T} = 0. \tag{62}$$

FORMULAE FOR THE PITCHING-MOMENT DERIVATIVES

The pitching moment about the c.g. is given by

$$\frac{M}{\rho(U_s+u)^2 S l_T} = \frac{c}{2l_T} C_m,$$

or

$$\frac{M}{\rho U_s^2 S l_T} = \frac{c}{2l_T} (1+2\hat{u}) C_m, \tag{63}$$

where C_m is given by Equation (27), reproduced here from the main text

$$C_m = C_{L(\alpha)}(h-\xi_\alpha) + C_{L(\vartheta)}(h-\xi_\vartheta) + C_{D0}\{h-\xi_\alpha(0)\}\alpha - C_T h\alpha - \\ - a_1 \overline{V} \left\{ \alpha - \epsilon(t) + \eta_T + \frac{q l_T}{U} \right\}. \tag{27}$$

Then

$$m_u = \frac{c}{l_T}(C_m)_s + \frac{c}{2l_T}\left(\frac{\partial C_m}{\partial \hat{u}}\right)_s = \frac{c}{2l_T}\left(\frac{\partial C_m}{\partial \hat{u}}\right)_s$$

$$= \frac{c}{2l_T}\left[\left\{ (h-\xi_{\alpha s})\alpha_s \left(\frac{\partial A}{\partial C_J}\right)_s - A_s \alpha_s \left(\frac{\partial \xi_\alpha}{\partial C_J}\right)_s + (h-\xi_{\vartheta s})\vartheta_s \left(\frac{\partial B}{\partial C_J}\right)_s - \right.\right.$$

$$\left.\left. - B_s \vartheta_s \left(\frac{\partial \xi_\vartheta}{\partial C_J}\right)_s - h\alpha_s \left(\frac{\partial C_T}{\partial C_J}\right)_s \right\} \left(\frac{\partial C_J}{\partial \hat{u}}\right)_s + a_1 \overline{V} \left(\frac{\partial B}{\partial \hat{u}}\right)_s \right],$$

or, if we make use of (50) and (26b),

$$m_u = -\frac{c}{l_T} C_{Js} \left[\left\{ (h-\xi_{\alpha s}) \left(\frac{\partial A}{\partial C_J}\right)_s - A_s \left(\frac{\partial \xi_\alpha}{\partial C_J}\right)_s - h\left[(1-k_T)\cos(\alpha_s+\vartheta_s) + k_T\right] \right\} \alpha_s + \right.$$

$$\left. + \left\{ (h-\xi_{\vartheta s}) \left(\frac{\partial B}{\partial C_J}\right)_s - B_s \left(\frac{\partial \xi_\vartheta}{\partial C_J}\right)_s \right\} \vartheta_s \right] + \tfrac{1}{2} a_1 \frac{S_T}{S} \left(\frac{\partial \epsilon}{\partial \hat{u}}\right)_s, \tag{64}$$

$$m_w = \frac{c}{2l_T}\left(\frac{\partial C_m}{\partial \hat{w}}\right)_s = \frac{c}{2l_T}\left(\frac{\partial C_m}{\partial \alpha}\right)_s = -\frac{c}{2l_T} A_s (K_{r\alpha})_s, \tag{65a}$$

where $K_{r\alpha}$ is the α-restoring margin given by Equation (28). If we use the latter equation with the downwash assumption of Equation (36), we obtain

$$m_w = \frac{c}{2l_T}\left[(h-\xi_{\alpha s})A_s + C_{D0}(h-\xi_\alpha(0)) - C_{Ts} h - \right.$$

$$\left. - a_1 \overline{V}(1-EA_s) + C_{Js} h \alpha_s (1-k_T)\sin(\alpha_s+\vartheta_s)\right], \tag{65b}$$

$$m_q = \frac{c}{2l_T}\frac{\partial C_m}{\partial (q l_T/U)} = -\frac{c}{2l_T} a_1 \overline{V} = -\tfrac{1}{2}\frac{S_T}{S} a_1, \tag{66}$$

$$m_{\eta_T} = \frac{c}{2l_T}\frac{\partial C_m}{\partial \eta_T} = -\frac{c}{2l_T} a_1 \overline{V} = -\tfrac{1}{2}\frac{S_T}{S} a_1, \tag{67}$$

$$m_\vartheta = \frac{c}{2l_T}\left(\frac{\partial C_m}{\partial \vartheta}\right)_s = -\frac{c}{2l_T} B_s (K_{r\vartheta})_s, \tag{68a}$$

where $K_{r\vartheta}$ is the ϑ-restoring margin given by Equation (29), so that

$$m_\vartheta = \frac{c}{2l_T}\left[(h-\xi_{\vartheta s}+a_1\bar{V}E)B_s + \alpha_s C_{Js}h(1-k_T)\sin(\alpha_s+\vartheta_s)\right], \tag{68b}$$

$$m_\lambda = \frac{c}{2l_T}\left(\frac{\partial C_m}{\partial\lambda}\right)_s = \frac{c}{2l_T}\left(\frac{\partial C_m}{\partial C_J}\right)_s\left(\frac{\partial C_J}{\partial\hat{\lambda}}\right)_s$$

$$= \frac{c}{2l_T}\left[\left\{(h-\xi_{\alpha s})\alpha_s\left(\frac{\partial A}{\partial C_J}\right)_s - A_s\alpha_s\left(\frac{\partial\xi_\alpha}{\partial C_J}\right)_s + (h-\xi_{\vartheta s})\vartheta_s\left(\frac{\partial B}{\partial C_J}\right)_s -\right.\right.$$

$$\left.\left. - B_s\vartheta_s\left(\frac{\partial\xi_\vartheta}{\partial C_J}\right)_s - h\alpha_s\left(\frac{\partial C_T}{\partial C_J}\right)_s\right\}\frac{C_{Js}}{\lambda_s} + a_1\bar{V}\left(\frac{\partial\epsilon}{\partial\hat{\lambda}}\right)_s\right],$$

or

$$m_\lambda = \frac{c}{2l_T}C_{Ls}\left[\left\{(h-\xi_{\alpha s})\left(\frac{\partial A}{\partial C_J}\right)_s - A_s\left(\frac{\partial\xi_\alpha}{\partial C_J}\right)_s - h[(1-k_T)\cos(\alpha_s+\vartheta_s)+k_T]\right\}\alpha_s +\right.$$

$$\left. + \left\{(h-\xi_{\vartheta s})\left(\frac{\partial B}{\partial C_J}\right)_s - B_s\left(\frac{\partial\xi_\vartheta}{\partial C_J}\right)_s\right\}\vartheta_s\right] + \tfrac{1}{2}a_1\frac{S_T}{S}\left(\frac{\partial\epsilon}{\partial\hat{\lambda}}\right)_s, \tag{69}$$

$$m_{\dot{u}} = \frac{c}{2l_T}\left[\frac{\partial C_m}{\partial(\dot{u}l_T/U^2)}\right]_s = \frac{c}{2l_T}a_1\bar{V}\left[\frac{\partial\epsilon}{\partial(\dot{u}l_T/U^2)}\right]_s,$$

or

$$m_{\dot{u}} = \tfrac{1}{2}\frac{S_T}{S}a_1\left[\frac{\partial\epsilon}{\partial(\dot{\hat{u}}l_T/U)}\right]_s. \tag{70}$$

Similarly,

$$m_{\dot{w}} = \tfrac{1}{2}\frac{S_T}{S}a_1\left[\frac{\partial\epsilon}{\partial(\dot{\hat{w}}l_T/U)}\right]_s. \tag{71}$$

THE DOWNWASH DERIVATIVES

Employing the concept of downwash delay, we may express the downwash at the tail, at time t after the initiation of a disturbance, in the form

$$\epsilon(t) = EC_L(t-l_T/U_s),$$

where

$$C_L(t) = A\{C_J(t)\}\{\alpha_s+\hat{w}(t)\} + B\{C_J(t)\}\{\vartheta_s+\hat{\vartheta}(t)\}$$

and

$$C_J(t) = \left(1+\frac{\hat{\lambda}(t)}{\lambda_s}\right)\{1-2\hat{u}(t)\}C_{Js} \qquad (\textit{see}\ \text{Equation (50)}$$

$$\approx \left\{1+\frac{\hat{\lambda}(t)}{\lambda_s}-2\hat{u}(t)\right\}C_{Js}$$

$$= C_{Js}+\Delta C_J,$$

with

$$\Delta C_J = \left\{\frac{\hat{\lambda}(t)}{\lambda_s}-2\hat{u}(t)\right\}C_{Js}.$$

Then

$$C_L(t) \approx \left\{A_s + \left(\frac{\partial A}{\partial C_J}\right)_s \Delta C_J\right\}\{\alpha_s + \hat{w}(t)\} + \\ + \left\{B_s + \left(\frac{\partial B}{\partial C_J}\right)_s \Delta C_J\right\}\{\vartheta_s + \hat{\vartheta}(t)\},$$

or

$$C_L(t) \approx C_{Ls} + A_s\hat{w}(t) + B_s\hat{\vartheta}(t) + \\ + \left\{\left(\frac{\partial A}{\partial C_J}\right)_s \alpha_s + \left(\frac{\partial B}{\partial C_J}\right)_s \vartheta_s\right\}\left\{\frac{\hat{\lambda}(t)}{\lambda_s} - 2\hat{u}(t)\right\} C_{Js}.$$

Now for $t < 0$

$$\hat{\lambda}(t) = \hat{\vartheta}(t) = \hat{w}(t) = \hat{u}(t) = 0$$

Thus, for $t < l_T/U_s$,

$$C_L\left(t - \frac{l_T}{U_s}\right) = C_{Ls}$$

and

$$\epsilon(t) = EC_{Ls},$$

so that

$$\frac{\partial \epsilon}{\partial \hat{u}} = \frac{\delta \epsilon}{\partial \hat{w}} = \frac{\partial \epsilon}{\partial \hat{\vartheta}} = \frac{\partial \epsilon}{\partial \hat{\lambda}} = \frac{\partial \epsilon}{\partial \dot{\hat{u}}} = \frac{\partial \epsilon}{\partial \dot{\hat{w}}} = 0, \tag{72}$$

while for $t \geqslant l_T/U_s$, if we assume $\hat{\vartheta}$ = constant,

$$C_L\left(t - \frac{l_T}{U_s}\right) \approx C_{Ls} + A_s\left\{\hat{w}(t) - \frac{l_T}{U_s}\dot{\hat{w}}\right\} + B_s\hat{\vartheta} + \\ + \left\{\left(\frac{\partial A}{\partial C_J}\right)_s \alpha_s + \left(\frac{\partial B}{\partial C_J}\right)_s \vartheta_s\right\}\left\{\frac{\hat{\lambda}}{\lambda_s} - 2\left[\hat{u}(t) - \frac{l_T}{U_s}\dot{\hat{u}}\right]\right\} C_{Js},$$

provided that l_T/U_s is small compared with the period of oscillation. Then

$$\epsilon(t) \approx E\left[C_{Ls} + A_s\{\hat{w} - \dot{\hat{w}}l_T/U_s\} + B_s\hat{\vartheta} + \right. \\ \left. + \left\{\left(\frac{\partial A}{\partial C_J}\right)_s \alpha_s + \left(\frac{\partial B}{\partial C_J}\right)_s \vartheta_s\right\}\left\{\frac{\hat{\lambda}}{\lambda_s} - 2[\hat{u} - \dot{\hat{u}}l_T/U_s]\right\} C_{Js}\right]. \tag{73}$$

Hence

$$\left.\begin{aligned} \left(\frac{\partial \epsilon}{\partial \hat{u}}\right)_s &= -2EC_{Js}\left\{\left(\frac{\partial A}{\partial C_J}\right)_s \alpha_s + \left(\frac{\partial B}{\partial C_J}\right)_s \vartheta_s\right\}; \\ \left(\frac{\partial \epsilon}{\partial \hat{w}}\right)_s &= EA_s; \\ \left(\frac{\partial \epsilon}{\partial \hat{\vartheta}}\right)_s &= EB_s; \quad \left(\frac{\partial \epsilon}{\partial \hat{\lambda}}\right)_s = EC_{Ls}\left\{\left(\frac{\partial A}{\partial C_J}\right)_s \alpha_s + \left(\frac{\partial B}{\partial C_J}\right)_s \vartheta_s\right\}; \\ [\partial \epsilon/\partial(\dot{\hat{u}}l_T/U_s)]_s &= 2EC_{Js}\left\{\left(\frac{\partial A}{\partial C_J}\right)_s \alpha_s + \left(\frac{\partial B}{\partial C_J}\right)_s \vartheta_s\right\}; \\ [\partial \epsilon/\partial(\dot{\hat{w}}l_T/U_s)]_s &= -EA_s. \end{aligned}\right\} \tag{74}$$

In strict accordance with the downwash delay theory we should, in analysing the disturbed motion, take all the downwash derivatives to be zero up to time $t = l_T/U_s$ (*see* Equations (72)) and to be given by Equations (74) thereafter. In practice, if l_T/U_s is small compared with the periods of oscillation, it is reasonable to calculate the downwash derivatives from Equations (74) for the whole of the disturbed motion. This assumption is implicit in the formulae for m_w and m_ϑ (Equations (65b) and (68b)).

APPENDIX II

Derivation of Response Formulae Appropriate to Quasi-Steady Manoeuvrability Theory

For steady manoeuvring flight in a vertical circle, we may put $\hat{u} = 0$ in Equations (4) and neglect the first equation. The remaining two reduce to

$$\begin{aligned} -z_w\hat{w} - \left(\frac{d}{d\tau} + k'\right)\theta &= z_{\eta_T}\hat{\eta}_T + z_\vartheta\hat{\vartheta} + z_\lambda\hat{\lambda}, \\ \omega\hat{w} + \nu\frac{d\theta}{d\tau} &= -\delta_{\eta_T}\hat{\eta}_T - \delta_\vartheta\hat{\vartheta} - \delta_\lambda\hat{\lambda}, \end{aligned}$$

of if we put $k' = 0$ (*i.e.*, assume $\gamma_s = 0$) and write

$$\left.\begin{aligned} \hat{q} &= \frac{d\theta}{d\tau}, \\ -z_w\hat{w} - \hat{q} &= z_{\eta_T}\hat{\eta}_T + z_\vartheta\hat{\vartheta} + z_\lambda\hat{\lambda}, \\ \omega\hat{w} + \nu\hat{q} &= -\delta_{\eta_T}\hat{\eta}_T - \delta_\vartheta\hat{\vartheta} - \delta_\lambda\hat{\lambda}. \end{aligned}\right\} \tag{75}$$

RESPONSE TO TAILPLANE CONTROL

The solutions of Equations (75), with $\hat{\vartheta} = \hat{\lambda} = 0$ and with the usual assumption $z_{\eta_T} \approx 0$, are

$$\frac{\hat{w}}{\hat{\eta}_T} = \frac{-\delta_{\eta_T}}{\omega - \nu z_w}; \quad \frac{\hat{q}}{\hat{\eta}_T} = \frac{z_w\delta_{\eta_T}}{\omega - \nu z_w}. \tag{76}$$

The incremental normal load factor Δn is given by

$$\frac{\Delta n}{\hat{\eta}_T} = \frac{U_s}{g\hat{t}}\frac{d(\hat{\gamma}/\hat{\eta}_T)}{d\tau} = \frac{U_s}{g\hat{t}}\frac{d}{d\tau}\left(\frac{\theta}{\hat{\eta}_T} - \frac{\hat{w}}{\hat{\eta}_T}\right) = \frac{U_s}{g\hat{t}}\frac{\hat{q}}{\hat{\eta}_T},$$

since $d\hat{w}/d\tau = 0$.

Hence

$$\frac{\Delta n}{\hat{\eta}_T} = \frac{2}{C_L}\frac{z_w\delta_{\eta_T}}{\omega - \nu z_w}, \tag{77}$$

since

$$\hat{t} = \frac{W}{g\rho S U_s} \text{ and } W = C_L\tfrac{1}{2}\rho U_s^2 S. \tag{78}$$

Also

$$\frac{d}{dt}\left(\frac{\hat{\gamma}}{\hat{\eta}_T}\right) = \frac{g}{U_s}\frac{\Delta n}{\hat{\eta}_T}. \tag{79}$$

RESPONSE TO JET-FLAP DEFLECTION CONTROL

The solutions of Equations (75) with $\hat{\eta}_T = \hat{\lambda} = 0$ are

$$\frac{\hat{w}}{\hat{\vartheta}} = \frac{\nu z_\vartheta - \delta_\vartheta}{\omega - \nu z_w}; \quad \frac{\hat{q}}{\hat{\vartheta}} = \frac{z_w\delta_\vartheta - z_\vartheta\omega}{\omega - \nu z_w}, \tag{80}$$

from which we may readily deduce

$$\frac{\Delta n}{\hat{\vartheta}} = \frac{2}{C_L}\frac{z_w\delta_\vartheta - z_\vartheta\omega}{\omega - \nu z_w}. \tag{81}$$

Also

$$\frac{d}{dt}\left(\frac{\hat{\gamma}}{\hat{\vartheta}}\right) = \frac{g}{U_s}\frac{\Delta n}{\hat{\vartheta}}. \tag{82}$$

RESPONSE TO JET THRUST CONTROL

The solutions of Equations (75) with $\hat{\eta}_T = \hat{\vartheta} = 0$ are

$$\frac{\hat{w}}{\hat{\lambda}} = \frac{\nu z_\lambda - \delta_\lambda}{\omega - \nu z_w}; \quad \frac{\hat{q}}{\hat{\lambda}} = \frac{z_w \delta_\vartheta - z_\lambda \omega}{\omega - \nu z_w}, \tag{83}$$

from which we deduce

$$\frac{\Delta n}{\hat{\lambda}} = \frac{2}{C_L} \frac{z_w \delta_\lambda - z_\lambda \omega}{\omega - \nu z_w} \tag{84}$$

and

$$\frac{d}{dt}\left(\frac{\hat{\gamma}}{\hat{\lambda}}\right) = \frac{g}{U_s} \frac{\Delta n}{\hat{\lambda}}. \tag{85}$$

Values of $\hat{w}$, Δn, $\hat{\gamma}$, deduced from Equations (76) to (77), (79) to (85), using appropriate values of the derivatives from Table 4, are shown on Figs. 7 to 12 for comparison with the results of the full response calculations.

APPENDIX III

An Approximate Assessment of the Effect of Induced Drag on Dynamic Stability

We assume that in flight at lift coefficient C_L there is induced drag corresponding to the coefficient

$$C_{Di} = k_i C_L^2, \tag{86}$$

where for our present purpose we assume k_i to be a constant.* We neglect the effect of the induced drag on the pitching moment.

Referring to Appendix I, Equations (51) and (57) we see that the equations for X- and Z-forces in disturbed motion will now be:

$$\frac{X}{\rho U_s^2 S} = (-C_{D0} - k_i C_L^2 + C_T + C_L\hat{w})(\tfrac{1}{2} + \hat{u}), \tag{87}$$

$$\frac{Z}{\rho U_s^2 S} = \{-C_L + (C_T - C_{D0} - k_i C_L^2)\hat{w}\}(\tfrac{1}{2} + \hat{u}), \tag{88}$$

from which the following formulae for the x- and z-derivatives may be readily deduced:

$$\left.\begin{aligned}
x_u &= -C_{D0} - k_i C_{Ls}^2\left[1 - 2\lambda_s\left\{\left(\frac{\partial A}{\partial C_J}\right)_s \alpha_s + \left(\frac{\partial B}{\partial C_J}\right)_s \vartheta_s\right\}\right],\\
x_w &= \tfrac{1}{2}C_{Ls}[1 - \lambda_s(1-k_T)\sin(\alpha_s+\vartheta_s) - 2k_i A_s],\\
x_\vartheta &= -\tfrac{1}{2}C_{Ls}\{\lambda_s(1-k_T)\sin(\alpha_s+\vartheta_s) + 2k_i B_s\},\\
x_\lambda &= \tfrac{1}{2}C_{Ls}\left[(1-k_T)\cos(\alpha_s+\vartheta_s) + k_T - 2k_i C_{Ls}\left\{\left(\frac{\partial A}{\partial C_J}\right)_s \alpha_s + \left(\frac{\partial B}{\partial C_J}\right)_s \vartheta_s\right\}\right],
\end{aligned}\right\} \tag{89}$$

$$\left.\begin{aligned}
z_u &= -\left\{A_s - C_{Js}\left(\frac{\partial A}{\partial C_J}\right)_s\right\}\alpha_s - \left\{B_s - C_{Js}\left(\frac{\partial B}{\partial C_J}\right)_s\right\}\vartheta_s,\\
z_w &= \tfrac{1}{2}[C_{Js}\{(1-k_T)\cos(\alpha_s+\vartheta_s) + k_T\} - C_{D0} - k_i C_{Ls}^2 - A_s,\\
z_\vartheta &= -\tfrac{1}{2}B_s,\\
z_\lambda &= -\tfrac{1}{2}C_{Ls}\left\{\left(\frac{\partial A}{\partial C_J}\right)_s \alpha_s + \left(\frac{\partial B}{\partial C_J}\right)_s \vartheta_s\right\}.
\end{aligned}\right\} \tag{90}$$

Comparison of formulae (89) and (90) with the formulae of Table 1 shows that all the x-derivatives are modified by the inclusion of induced drag while, of the z-derivatives, only z_w is changed.

Numerical Example. The force derivatives have been evaluated from formulae (89) and (90) for the basic design condition considered in the examples of the main text. The induced thrust coefficient k_T has been taken as 1·0 while a value of 0·03 has been assumed for the induced drag coefficient k_i. (If we consider the formula for C_{Di} given by Maskell and Spence in Ref. 6, *viz.*,

$$C_{Di} = C_L^2/(\pi A + 2C_J)$$

where A denotes aspect ratio then with $C_J = 1{\cdot}59$, as in the present example, we see that our assumption is appropriate to an aspect ratio of 9·58).

* It will be seen later in the numerical example, that according to three-dimensional theory, k_i would actually be a function of C_J for a wing of given aspect ratio.

The calculated derivatives are compared with the corresponding ones from Table 4 in Table 7. The results of comparative calculations of the periods and dampings are given in Table 8. (For these calculations, the moment derivatives have been assumed unaffected by induced drag.)

It will be seen from Table 8 that the induced drag has an almost negligible effect on the short period characteristics; the effect on the phugoid is somewhat greater but still insufficient to change the general character of the motion.

TABLE 1

Formulae for Aerodynamic Derivatives

(a) Longitudinal force derivatives

Derivative	Formula
x_u	$-C_{D0}$
x_w	$\frac{1}{2}C_L\{1-\lambda(1-k_T)\sin(\alpha+\vartheta)\}$
x_ϑ	$-\frac{1}{2}C_J(1-k_T)\sin(\alpha+\vartheta)$
x_λ	$\frac{1}{2}C_L\{(1-k_T)\cos(\alpha+\vartheta)+k_T\}$

(b) Vertical force derivatives

Derivative	Formula
z_u	$\left(C_J\frac{\partial A}{\partial C_J}-A\right)\alpha+\left(C_J\frac{\partial B}{\partial C_J}-B\right)\vartheta$
z_w	$\frac{1}{2}[C_J\{(1-k_T)\cos(\alpha+\vartheta)+k_T\}-C_{D0}-A]$
z_ϑ	$-\frac{1}{2}B$
z_λ	$-\frac{1}{2}C_L\left\{\frac{\partial A}{\partial C_J}\alpha+\frac{\partial B}{\partial C_J}\vartheta\right\}$

TABLE 1—*continued*

(c) Pitching-moment derivatives

Derivative	Formula
m_u	$-\frac{c}{l_T}C_J\left[\left\{(h-\xi_\alpha)\frac{\partial A}{\partial C_J}-A\frac{\partial \xi_\alpha}{\partial C_J}-h[(1-k_T)\cos(\alpha+\vartheta)+k_T]\right\}\alpha+\right.$ $\left.+\left\{(h-\xi_\vartheta)\frac{\partial B}{\partial C_J}-B\frac{\partial \xi_\vartheta}{\partial C_J}\right\}\vartheta\right]+\frac{1}{2}a_1\frac{S_T}{S}\left(\frac{\partial \epsilon}{\partial \hat{u}}\right)$
m_w	$\frac{c}{2l_T}[(h-\xi_\alpha)A+C_{D\,0}\{h-\xi_\alpha(0)\}-C_T h-a_1 V(1-EA)+$ $+C_J h\,\alpha(1-k_T)\sin(\alpha+\vartheta)]$
m_q	$-\frac{1}{2}\frac{S_T}{S}a_1$
m_{η_T}	$-\frac{1}{2}\frac{S_T}{S}a_1$
m_ϑ	$\frac{c}{2l_T}[(h-\xi_\vartheta+a_1\bar{V}E)B+C_J h\,\alpha(1-k_T)\sin(\alpha+\vartheta)]$
m_λ	$\frac{c}{2l_T}C_L\left[\left\{(h-\xi_\alpha)\frac{\partial A}{\partial C_J}-A\frac{\partial \xi_\alpha}{\partial C_J}-h[(1-k_T)\cos(\alpha+\vartheta)+k_T]\right\}\alpha+\right.$ $\left.+\left\{(h-\xi_\vartheta)\frac{\partial B}{\partial C_J}-B\frac{\partial \xi_\vartheta}{\partial C_J}\vartheta\right\}\right]+\frac{1}{2}a_1\frac{S_T}{S}\left(\frac{\partial \epsilon}{\partial \hat{\lambda}}\right)$
$m_{\dot{u}}$	$\frac{1}{2}\frac{S_T}{S}a_1\frac{\partial \epsilon}{\partial(\dot{u}l_T/U)}$
$m_{\dot{w}}$	$\frac{1}{2}\frac{S_T}{S}a_1\frac{\partial \epsilon}{\partial(\dot{w}l_T/U)}$

TABLE 1—*continued*

(d) Downwash derivatives

Derivative	Formula
$\partial\epsilon/\partial\hat{u}$	$-2EC_J\left\{\frac{\partial A}{\partial C_J}\alpha+\frac{\partial B}{\partial C_J}\vartheta\right\}$
$\partial\epsilon/\partial\hat{w}$	EA
$\partial\epsilon/\partial\hat{\vartheta}$	EB
$\partial\epsilon/\partial\hat{\lambda}$	$EC_L\left\{\frac{\partial A}{\partial C_J}\alpha+\frac{\partial B}{\partial C_J}\vartheta\right\}$
$\frac{\partial\epsilon}{\partial(\dot{\hat{u}}l_T/U)}$	$2EC_J\left\{\frac{\partial A}{\partial C_J}\alpha+\frac{\partial B}{\partial C_J}\vartheta\right\}$
$\frac{\partial\epsilon}{\partial(\dot{\hat{w}}l_T/U)}$	$-EA$

TABLE 2

Values of the Aerodynamic Derivatives in the Basic Design Condition

Derivative	$k_T = 1$	$k_T = 0$
x_u	−0·1	−0·1
x_w	+2·65	+1·983
z_u	−2·08	−2·08
z_w	−4·055	−4·42
m_u	+0·074	+0·074
m_w	−0·274	−0·274
m_q	−0·665	−0·61
$m_{\dot{w}}$	−0·16	−0·1465
$m_{\dot{u}}$	+0·107	+0·098
$k_L = \frac{1}{2} C_L$	+2·65	+2·65
$k' = -k_L \tan \gamma_s$	−0·745	−0·38

Concise moment derivative ($i_B = 0{\cdot}1$, $\mu_1 = 25$)	$k_T = 1$	$k_T = 0$
$\kappa = -\mu_1 m_u / i_B$	−18·5	−18·5
$\omega = -\mu_1 m_w / i_B$	+68·5	+68·5
$\nu = -\ m_q / i_B$	+ 6·65	+ 6·1
$\chi = -\ m_{\dot{w}} / i_B$	+ 1·6	+ 1·465
$\Upsilon = -\ m_{\dot{u}} / i_B$	− 1·07	− 0·98

Stability Quartics

$$\underline{k_T = 1}: \quad F(D) = D^4 + 12{\cdot}405\, D^3 + 101{\cdot}01\, D^2 + 17{\cdot}39\, D + 607{\cdot}9 = 0$$
$$= (D^2 + 12{\cdot}985\, D + 102{\cdot}62)\,(D^2 - 0{\cdot}580\, D + 5{\cdot}924)$$
$$\underline{k_T = 0}: \quad F(D) = D^4 + 12{\cdot}085\, D^3 + 101{\cdot}32\, D^2 + 41{\cdot}19\, D + 603{\cdot}7 = 0$$
$$= (D^2 + 12{\cdot}429\, D + 99{\cdot}525)\,(D^2 - 0{\cdot}3437\, D + 6{\cdot}066)\,.$$

TABLE 3

Characteristics of Motion

Mode	$k_T = 1$			$k_T = 0$		
	Period (sec)	Time to ½ amp	Time to 2 × amp	Period (sec)	Time to ½ amp	Time to 2 × amp
Short period oscillation	5·43	0·717 sec (0·132 period)	—	5·35	0·74 sec (0·138 period)	—
Long period oscillation	17·48	—	16·06 sec (0·918 period)	17·0	—	26·8 sec (1·574 period)

TABLE 4

Values of the Derivatives used in Response Calculations

Derivative	Basic design condition $\vartheta = 1$, $C_{L\,s} = 5{\cdot}3$ $\gamma_s = 15{\cdot}6$ deg	Cruising condition $\vartheta = 0{\cdot}2$, $C_{L\,s} = 0{\cdot}268$ $\gamma_s = -4{\cdot}2$ deg
x_u	$-0{\cdot}1$	$-0{\cdot}1$
x_w	$+2{\cdot}65$	$+0{\cdot}134$
x_{η_T}	0	0
x_ϑ	0	0
x_λ	$+2{\cdot}65$	$+0{\cdot}134$
z_u	$-2{\cdot}08$	$-0{\cdot}144$
z_w	$-4{\cdot}055$	$-3{\cdot}36$
z_{η_T}	0	0
z_ϑ	$-2{\cdot}65$	$-0{\cdot}518$
z_λ	$-5{\cdot}37$	$-0{\cdot}181$
m_u	$+0{\cdot}074$	$-0{\cdot}0017$
m_w	$-0{\cdot}274$	$-0{\cdot}337$
m_q	$-0{\cdot}665$	$-0{\cdot}665$
$m_{\dot{u}}$	$+0{\cdot}107$	$-0{\cdot}0036$
$m_{\dot{w}}$	$-0{\cdot}16$	$-0{\cdot}1114$
m_{η_T}	$-0{\cdot}665$	$-0{\cdot}665$
m_ϑ	0	$+0{\cdot}0109$
m_λ	$-0{\cdot}123$	$+0{\cdot}00283$
$k_L = \frac{1}{2} C_L$	$+2{\cdot}65$	$+0{\cdot}134$
$k' = -k_L \tan \gamma_s$	$-0{\cdot}745$	$+0{\cdot}0098$

Concise moment derivative ($i_B = 0{\cdot}1$, $\mu_1 = 25$)	Basic design condition	Cruising condition
$\kappa = -\mu_1 m_u / i_B$	$-$ 18·5	$+$ 0·425
$\omega = -\mu_1 m_w / i_B$	$+$ 68·5	$+$ 84·3
$\nu = -\ m_q / i_B$	$+$ 6·65	$+$ 6·65
$\Upsilon = -\ m_{\dot{u}} / i_B$	$-$ 1·07	$-$ 0·036
$\chi = -\ m_{\dot{w}} / i_B$	$+$ 1·60	$+$ 1·114
$\delta_{\eta_T} = -\mu_1 m_{\eta T} / i_B$	$+166{\cdot}2$	$+166{\cdot}2$
$\delta_\vartheta = -\mu_1 m_\vartheta / i_B$	0	$-$ 2·725
$\delta_\lambda = -\mu_1 m_\lambda / i_B$	$+$ 30·75	$-$ 0·7075

TABLE 5

Response to Controls in Basic Design Condition

Solutions for the various response quantities per unit increment of control parameter are all of the form

$$A + (L \cos 1{\cdot}1571\, t + M \sin 1{\cdot}1571\, t)\, e^{-0{\cdot}9669t} + \\ + (l \cos 0{\cdot}3599\, t + m \sin 0{\cdot}3599\, t)\, e^{0{\cdot}04318t}$$

with coefficients A, L, M, l, m as given in the following table.

Control	Response quantity	A	L	M	l	m
η_T	$\hat{u}/\hat{\eta}_{T\,0}$	+3·4775	−0·1461	+0·2074	−3·3313	−0·6596
	$\hat{w}/\hat{\eta}_{T\,0}$	−1·4871	+1·6271	+1·3601	−0·1400	+0·0150
	$\theta/\hat{\eta}_{T\,0}$	−1·6170	+0·6659	+1·4315	+0·9511	−2·9273
	$\hat{\gamma}/\hat{\eta}_{T\,0}$	−0·1299	−0·9612	+0·0714	+1·0911	−2·9423
	$\Delta n/\hat{\eta}_{T\,0}$	0	+2·4675	+2·5485	−2·4675	−1·2690
ϑ	$\hat{u}/\hat{\vartheta}_0$	−0·7920	+0·0238	+0·0202	+0·7682	−0·0931
	$\hat{w}/\hat{\vartheta}_0$	−0·2137	+0·1846	−0·1838	+0·0291	−0·0134
	$\theta/\hat{\vartheta}_0$	−0·1836	+0·1823	−0·0655	+0·0013	+0·7001
	$\hat{\gamma}/\hat{\vartheta}_0$	+0·0301	−0·0023	+0·1183	−0·0278	+0·7135
	$\Delta n/\hat{\vartheta}_0$	0	+0·3390	−0·2733	+0·6240	+0·0994
λ	$\hat{u}/\hat{\lambda}_0$	−1·1833	+0·0192	+0·0840	+1·1640	+0·7384
	$\hat{w}/\hat{\lambda}_0$	−0·7681	+0·7126	−0·1022	+0·0554	+0·0145
	$\theta/\hat{\lambda}_0$	+0·2759	+0·5126	+0·1569	−0·7885	+0·9674
	$\hat{\gamma}/\hat{\lambda}_0$	+1·0440	−0·2000	+0·2591	−0·8439	+0·9529
	$\Delta n/\hat{\lambda}_0$	0	+1·2034	−0·0446	+0·7482	+0·8415

TABLE 6

Response to Controls in Cruising Condition

Solutions for the various response quantities per unit increment of control parameter are all of the form

$$A + (L \cos 5{\cdot}8582\, t + M \sin 5{\cdot}8582\, t)\, e^{-3{\cdot}743t}$$
$$+ (l \cos 0{\cdot}07183\, t + m \sin 0{\cdot}07183\, t)\, e^{-0{\cdot}0364t}$$

with coefficients A, L, M, l, m as given in the following table.

Control	Response quantity	A	L	M	l	m
η_T	$\hat{u}/\hat{\eta}_{T\,0}$	+48·9668	− 0·0010	+ 0·0078	−48·9660	−25·4947
	$\hat{w}/\hat{\eta}_{T\,0}$	− 2·2140	+ 1·5592	+ 0·9964	+ 0·6547	+ 0·3128
	$\theta/\hat{\eta}_{T\,0}$	−38·7153	+ 1·0142	+ 1·2492	+37·7013	−29·9309
	$\hat{\gamma}/\hat{\eta}_{T\,0}$	−36·5013	− 0·5450	+ 0·2528	+37·0466	−30·2437
	$\Delta n/\hat{\eta}_{T\,0}$	0	+39·0378	+24·9106	−39·0378	−17·2968
ϑ	$\hat{u}/\hat{\vartheta}_0$	− 4·6390	+ 0·0002	− 0·0007	+ 4·6388	+ 2·3682
	$\hat{w}/\hat{\vartheta}_0$	+ 0·0556	+ 0·0067	− 0·0552	− 0·0624	− 0·0291
	$\theta/\hat{\vartheta}_0$	+ 3·5167	+ 0·0207	− 0·0437	− 3·5374	+ 2·8515
	$\hat{\gamma}/\hat{\vartheta}_0$	+ 3·4611	+ 0·0140	+ 0·0115	− 3·4750	+ 2·8806
	$\Delta n/\hat{\vartheta}_0$	0	+ 0·1676	− 1·3872	+ 3·6964	+ 1·6051
λ	$\hat{u}/\hat{\lambda}_0$	− 1·4774	+ 0·00008	− 0·00002	+ 1·4773	+ 2·0100
	$\hat{w}/\hat{\lambda}_0$	+ 0·0158	+ 0·0046	− 0·0177	− 0·0204	− 0·0258
	$\theta/\hat{\lambda}_0$	+ 2·1137	+ 0·0086	− 0·0133	− 2·1223	+ 0·4615
	$\hat{\gamma}/\hat{\lambda}_0$	+ 2·0979	+ 0·0040	+ 0·0044	− 2·1019	+ 0·4873
	$\Delta n/\hat{\lambda}_0$	0	+ 0·1151	− 0·4423	+ 1·2363	+ 1·4773

TABLE 7

Effect of Induced Drag on Force Derivatives

Basic design condition: $C_{L\,s} = 5{\cdot}3$; $C_{J\,s} = 1{\cdot}59$; $k_T = 1$.

$$C_{D\,i} = k_i\,C_L^2$$

Derivative	$k_i = 0$ $U_s = 78{\cdot}9$ ft/sec $\gamma_s = 15{\cdot}6$ deg	$k_i = 0{\cdot}03$ $U_s = 80$ ft/sec $\gamma_s = 7$ deg
x_u	$-0{\cdot}1$	$+0{\cdot}081$
x_w	$+2{\cdot}65$	$+1{\cdot}126$
x_ϑ	0	$-0{\cdot}843$
x_λ	$+2{\cdot}65$	$+0{\cdot}941$
z_u	$-2{\cdot}08$	$-2{\cdot}08$
z_w	$-4{\cdot}055$	$-4{\cdot}476$
z_ϑ	$-2{\cdot}65$	$-2{\cdot}65$
z_λ	$-5{\cdot}37$	$-5{\cdot}37$

TABLE 8

Effect of Induced Drag on Stability Characteristics

Mode	$k_T = 1$, $k_i = 0$			$k_T = 1$, $k_i = 0{\cdot}03$		
	Period	Time to ½ amp	Time to 2 × amp	Period	Time to ½ amp	Time to 2 × amp
Short period oscillation	5·43 sec	0·717 sec (0·132 period)	—	5·47 sec	0·703 sec (0·1285 period)	—
Long period oscillation	17·48 sec	—	16·06 sec (0·918 period)	17·05 sec	—	21·63 sec (1·268 period)

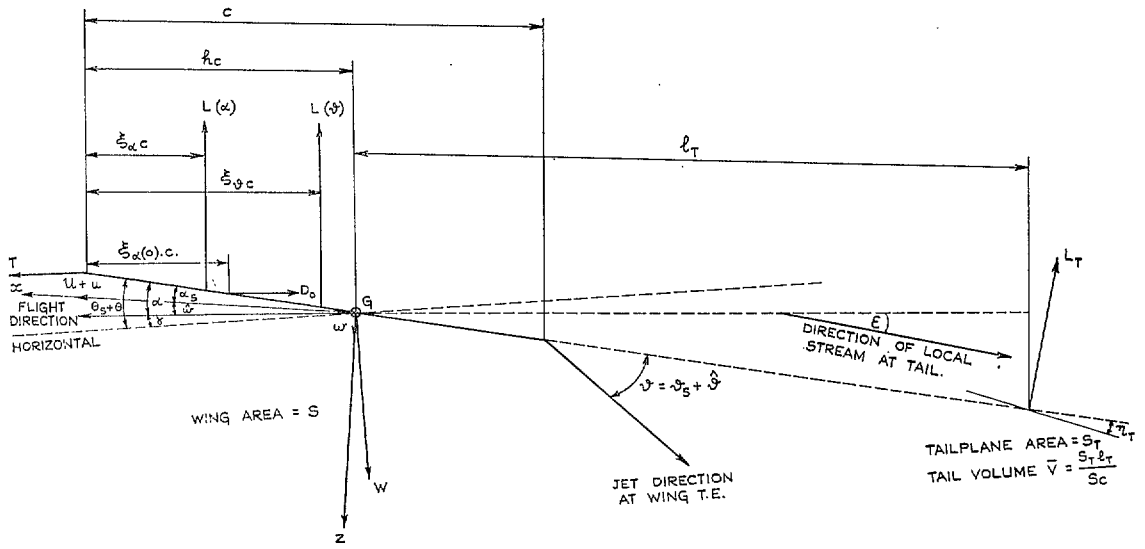

FIG. 1. Configuration of aircraft showing forces acting on it in disturbed flight.

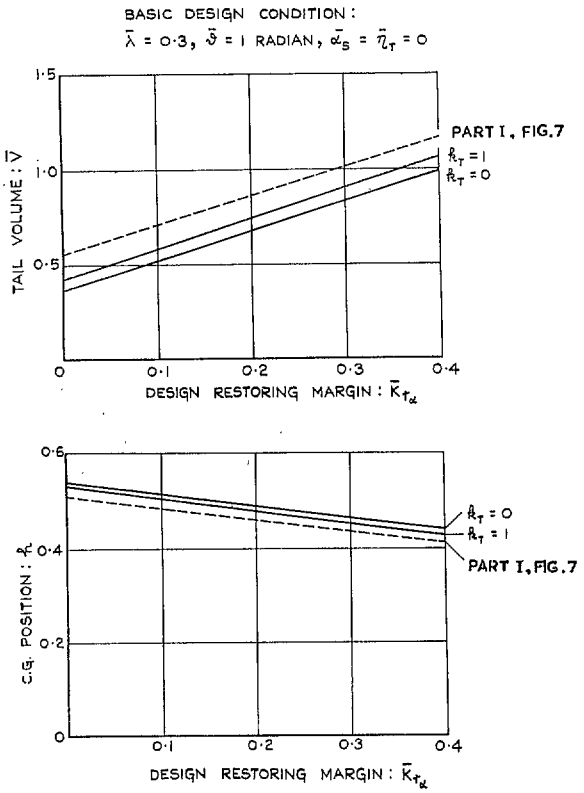

FIG. 2. Tail volume and c.g. position as determined by basic design conditions.

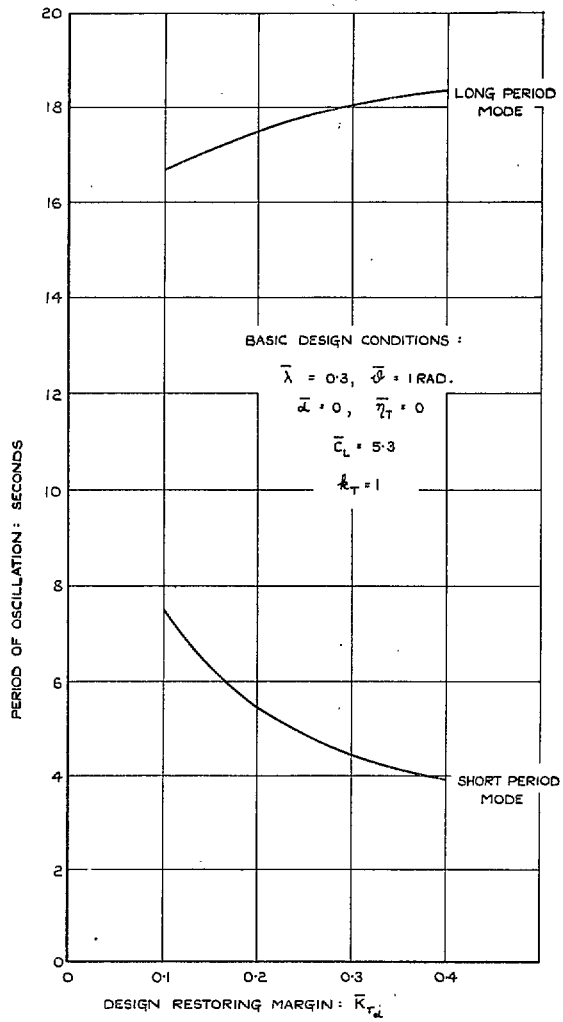

(a) PERIODS OF OSCILLATION.

FIG. 3. Characteristics of the longitudinal motion in the basic design condition.

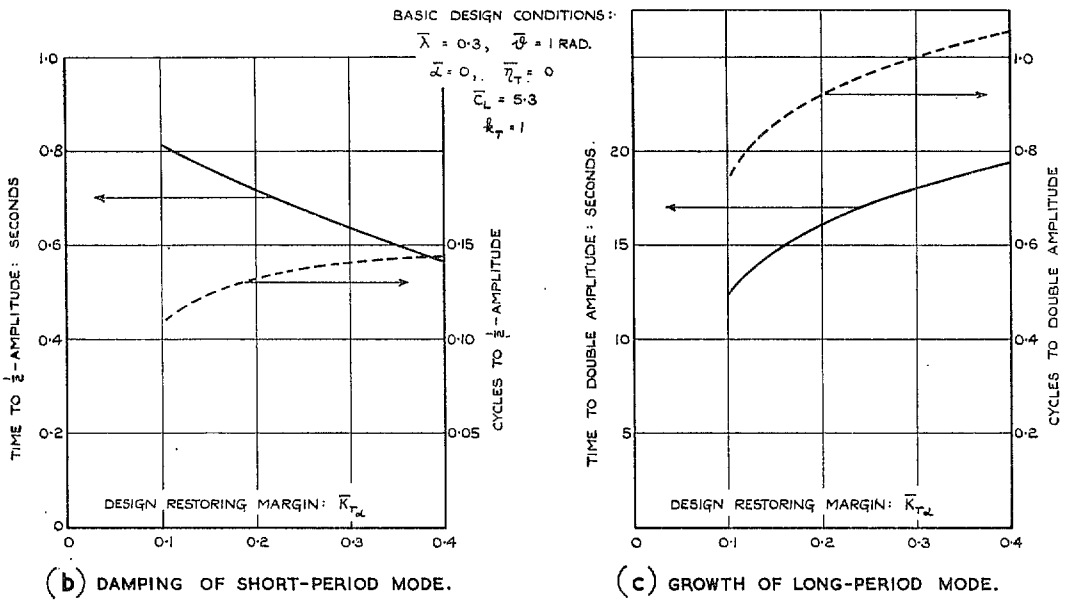

(b) DAMPING OF SHORT-PERIOD MODE. (c) GROWTH OF LONG-PERIOD MODE.

FIG. 3 (*contd.*). Characteristics of the longitudinal motion in the basic design condition.

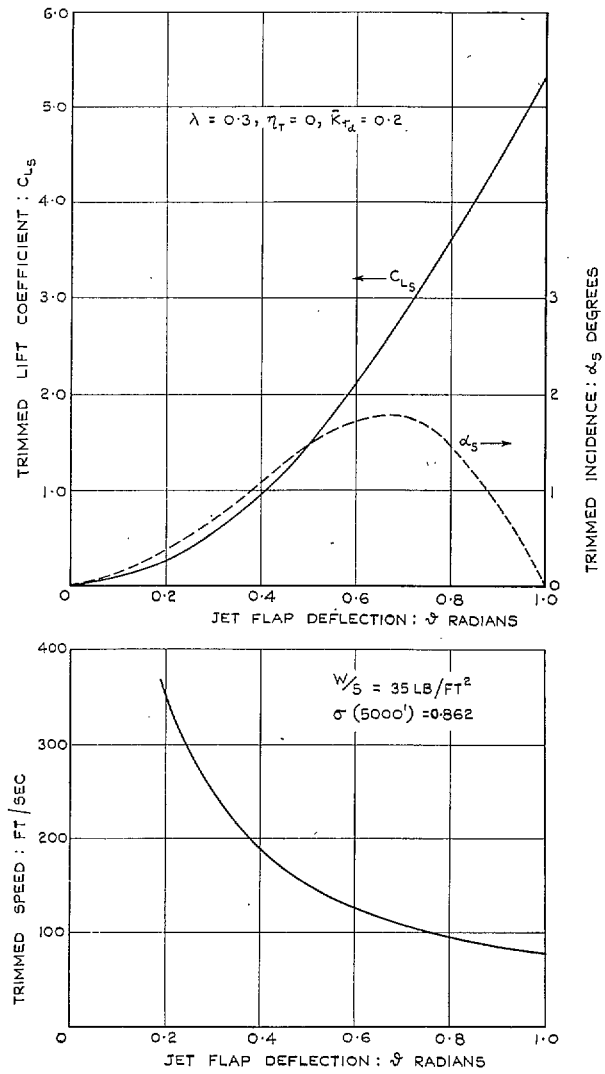

FIG. 4. Variation of trim conditions with jet-flap deflection.

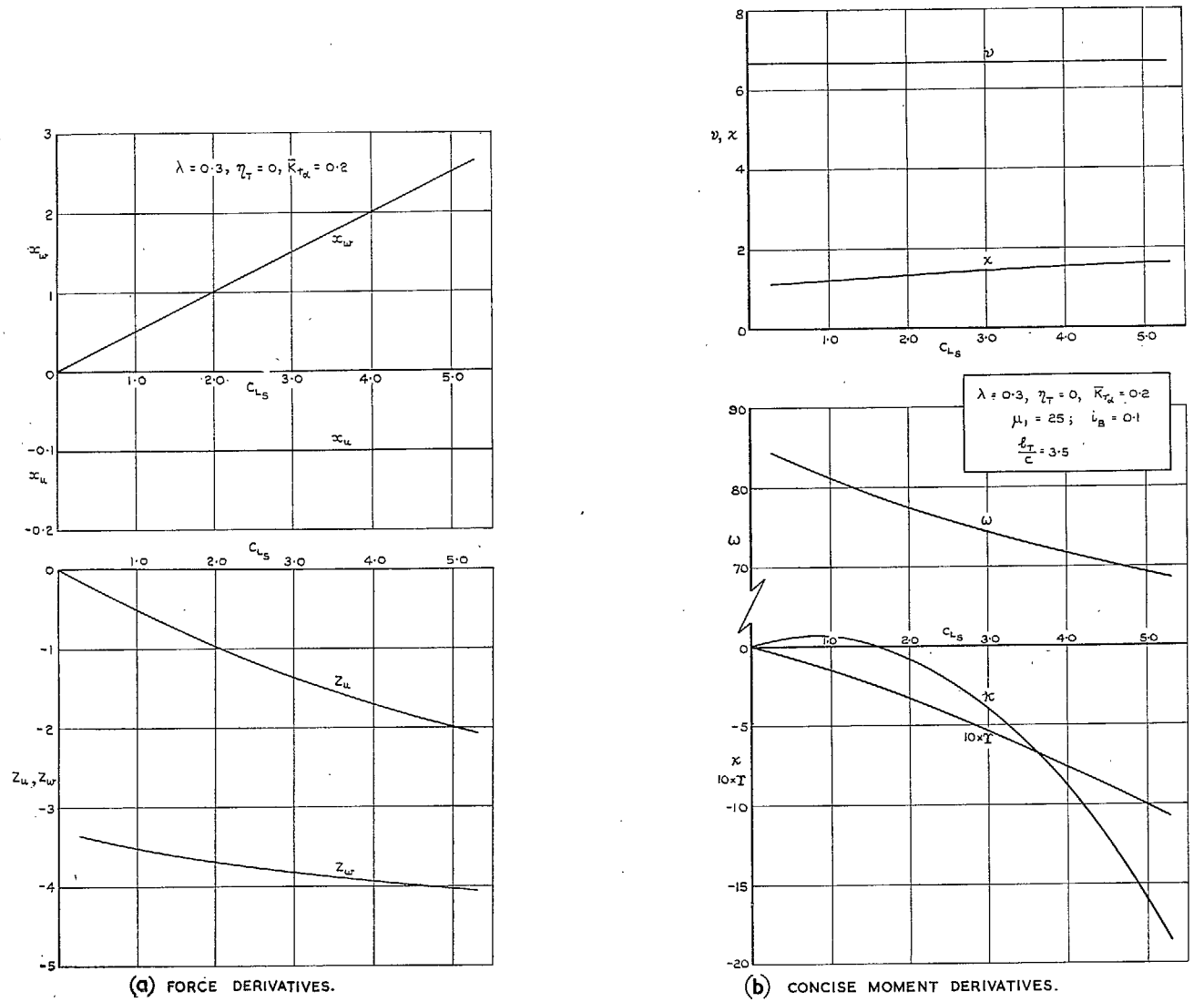

FIG. 5. Variation of longitudinal stability derivatives with lift coefficient (variable jet-flap deflection).

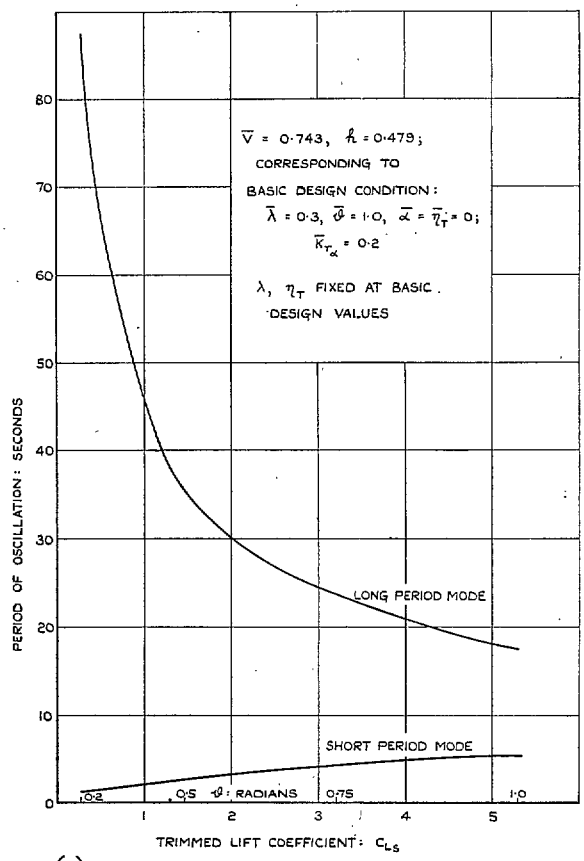

(a) PERIODS OF OSCILLATION.

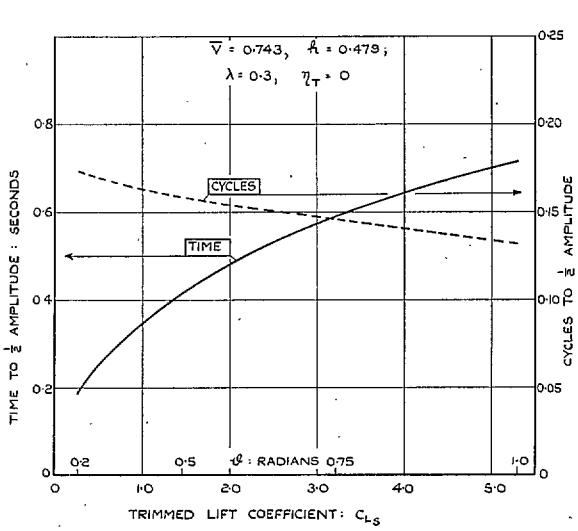

(b) DAMPING OF SHORT-PERIOD MODE.

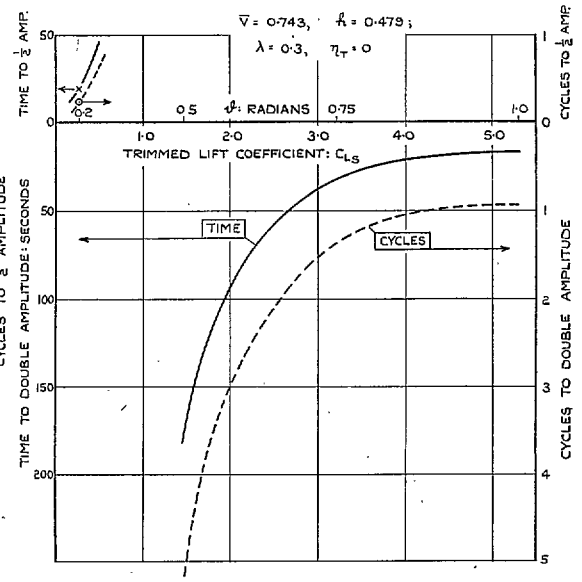

(c) DAMPING OR GROWTH OF LONG-PERIOD MODE.

FIG. 6. Variation of longitudinal characteristics with lift coefficient (variable jet-flap deflection).

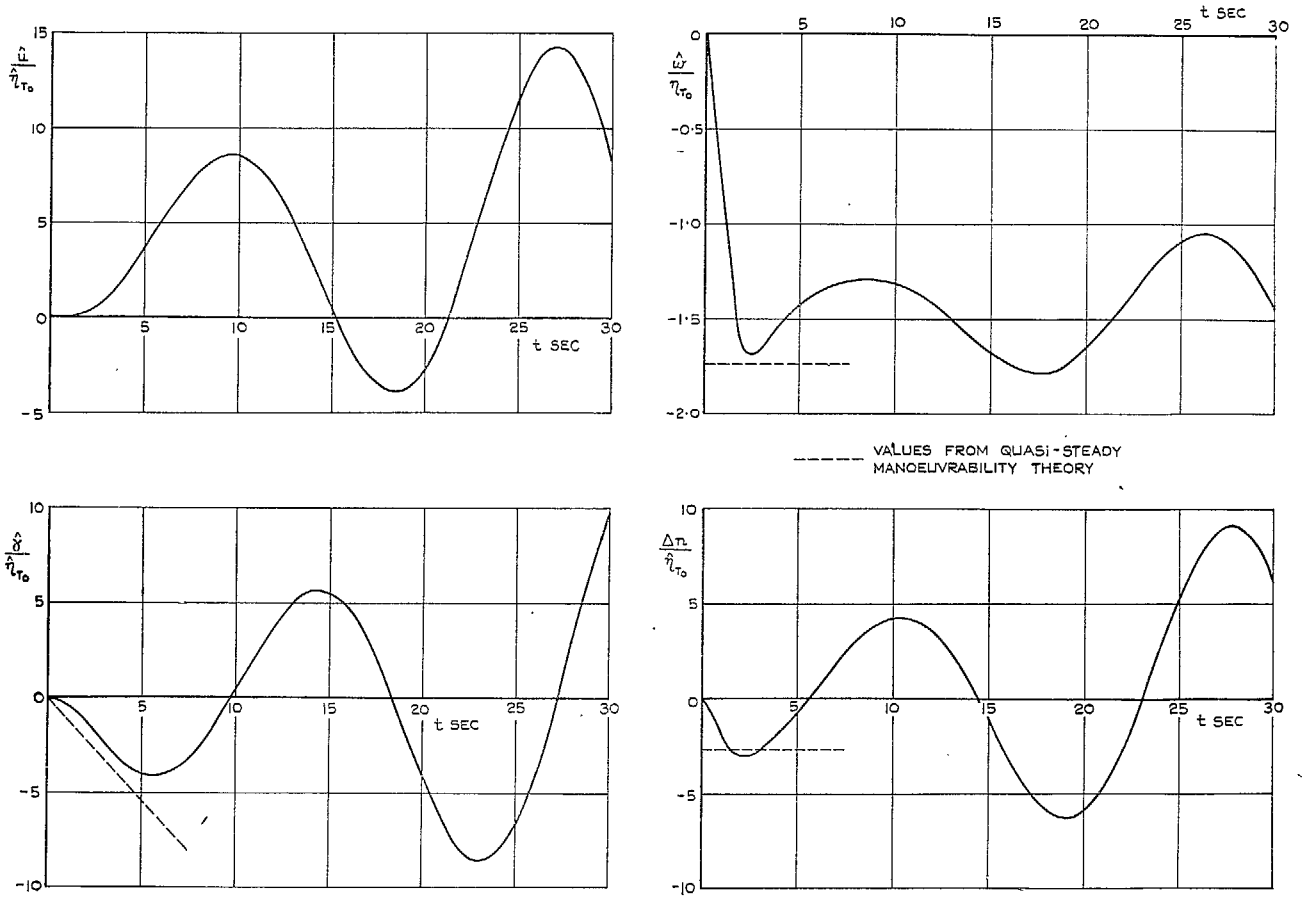

FIG. 7. Response to step function input of tailplane control—Basic design condition: $C_{Ls} = 5{\cdot}3$.

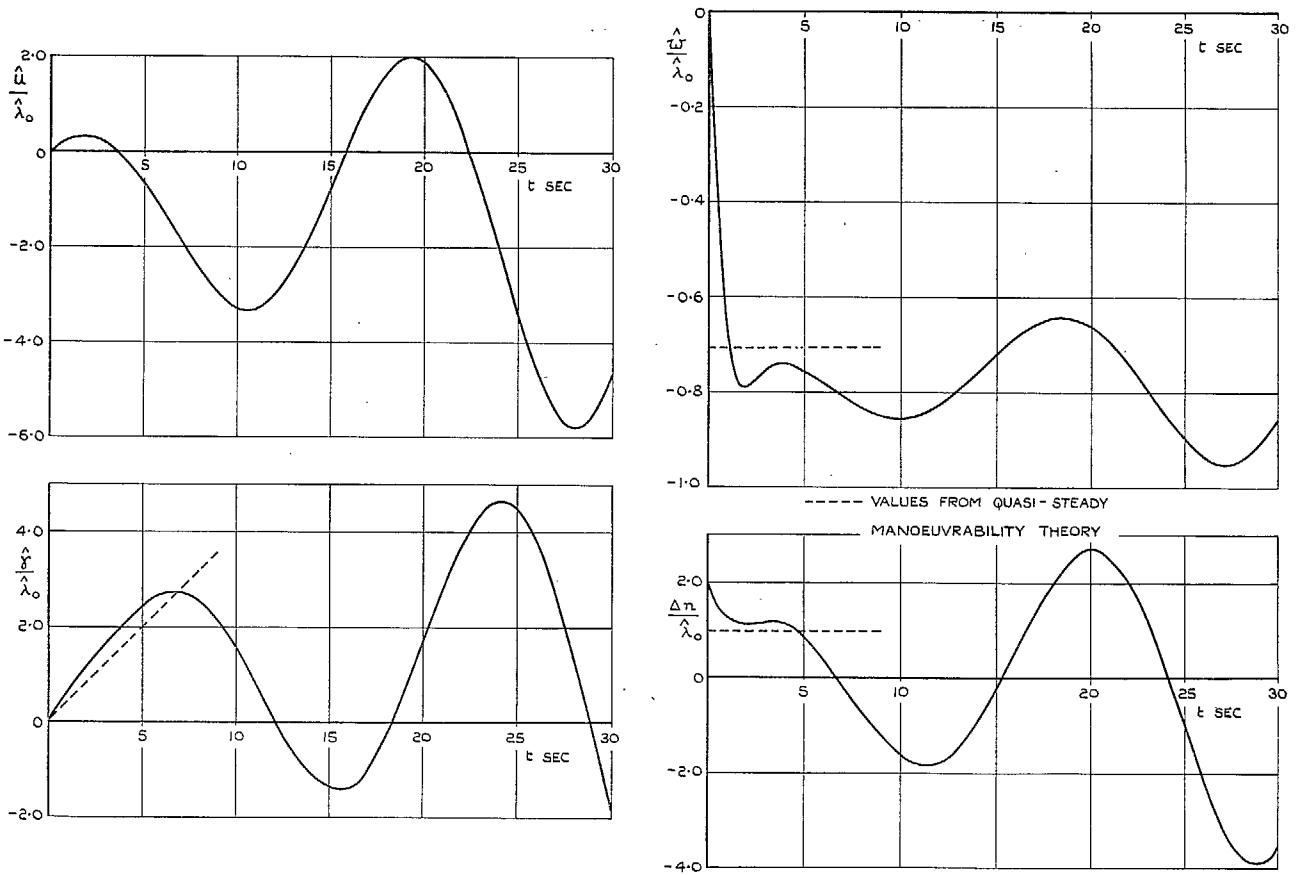

FIG. 8. Response to step function input of jet thrust control—Basic design condition: $C_{L\,\delta} = 5{\cdot}3$.

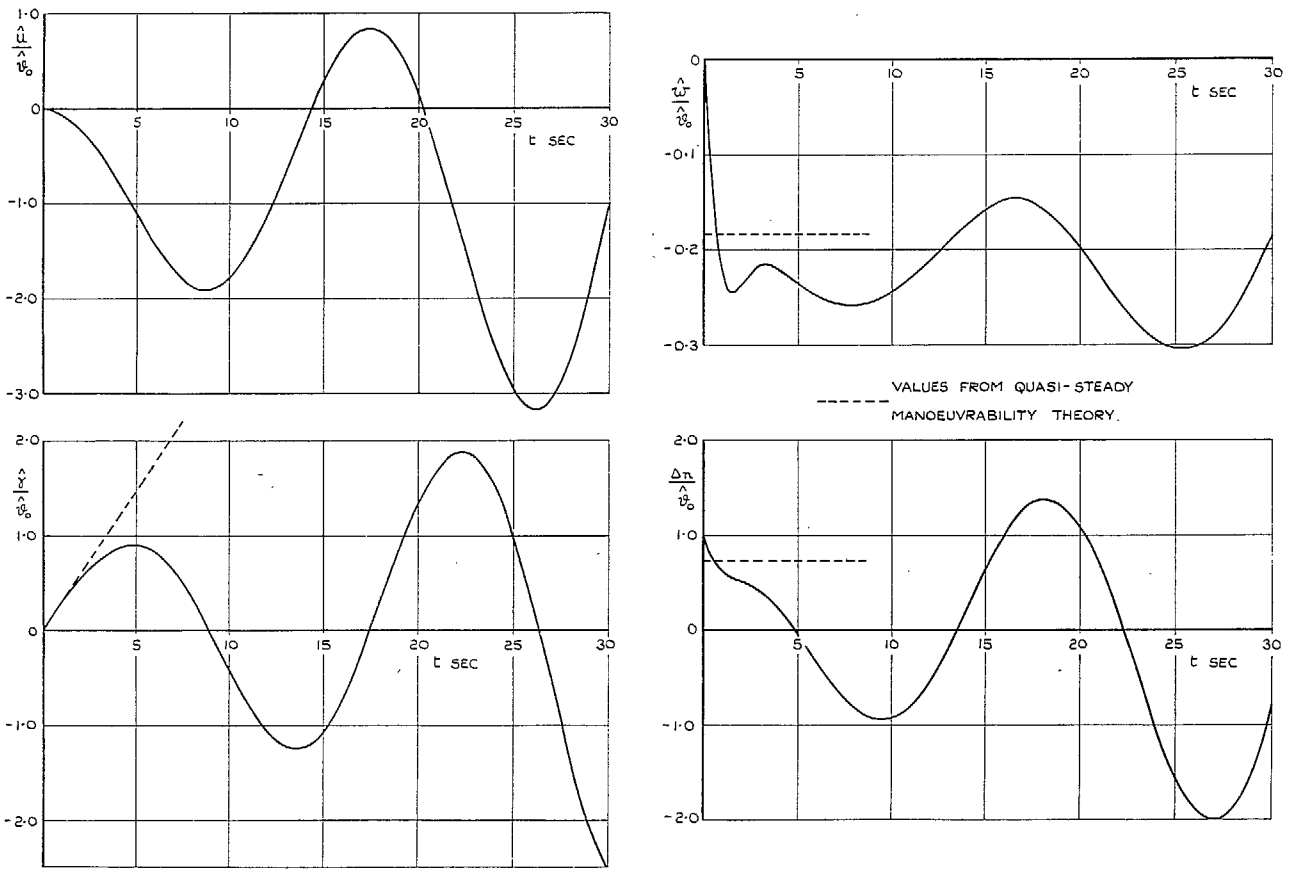

FIG. 9. Response to step function input of jet-flap deflection—Basic design condition: $C_{Ls} = 5 \cdot 3$.

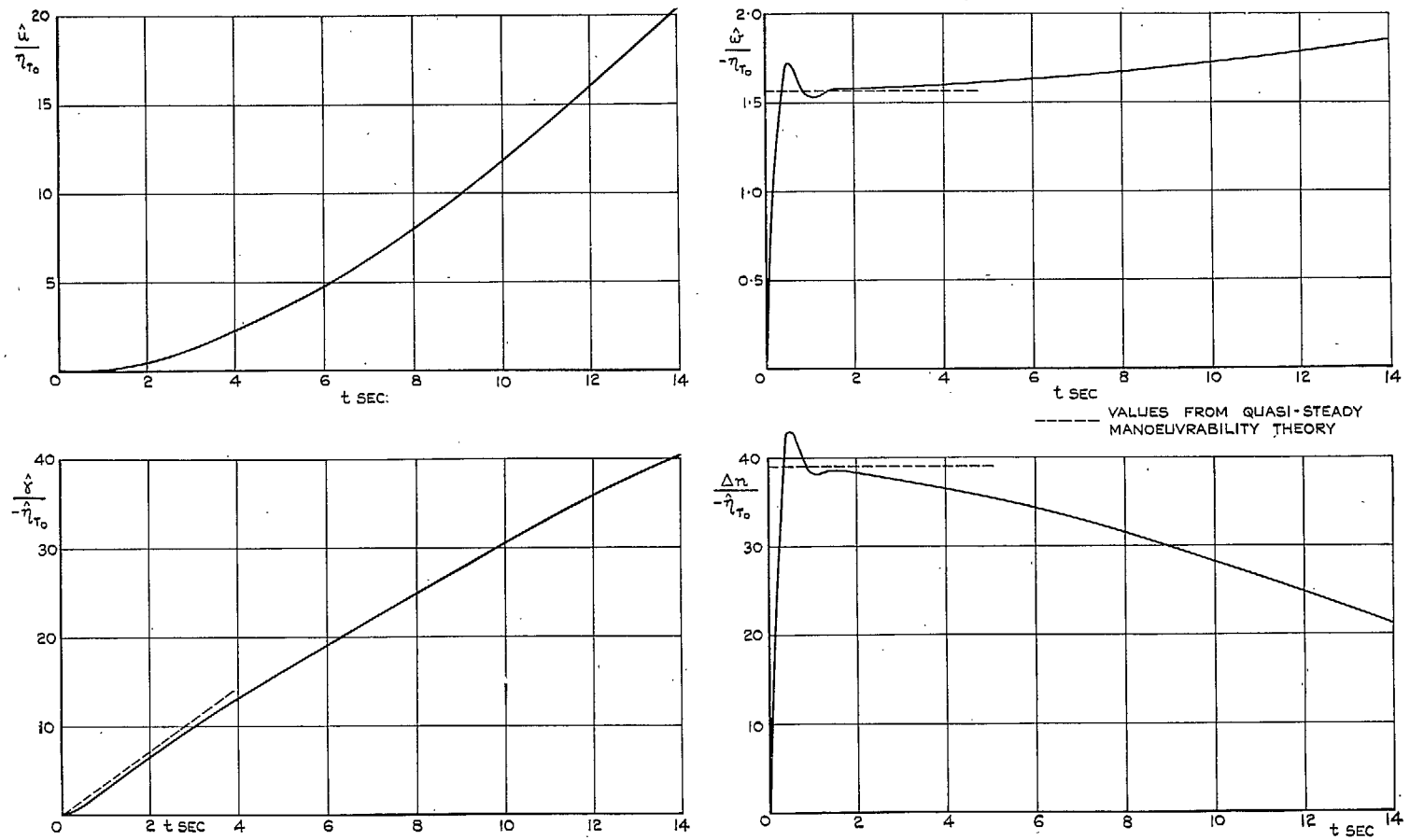

FIG. 10. Response to step function input of tailplane control—Cruising condition: $C_{Ls} = 0{\cdot}268$.

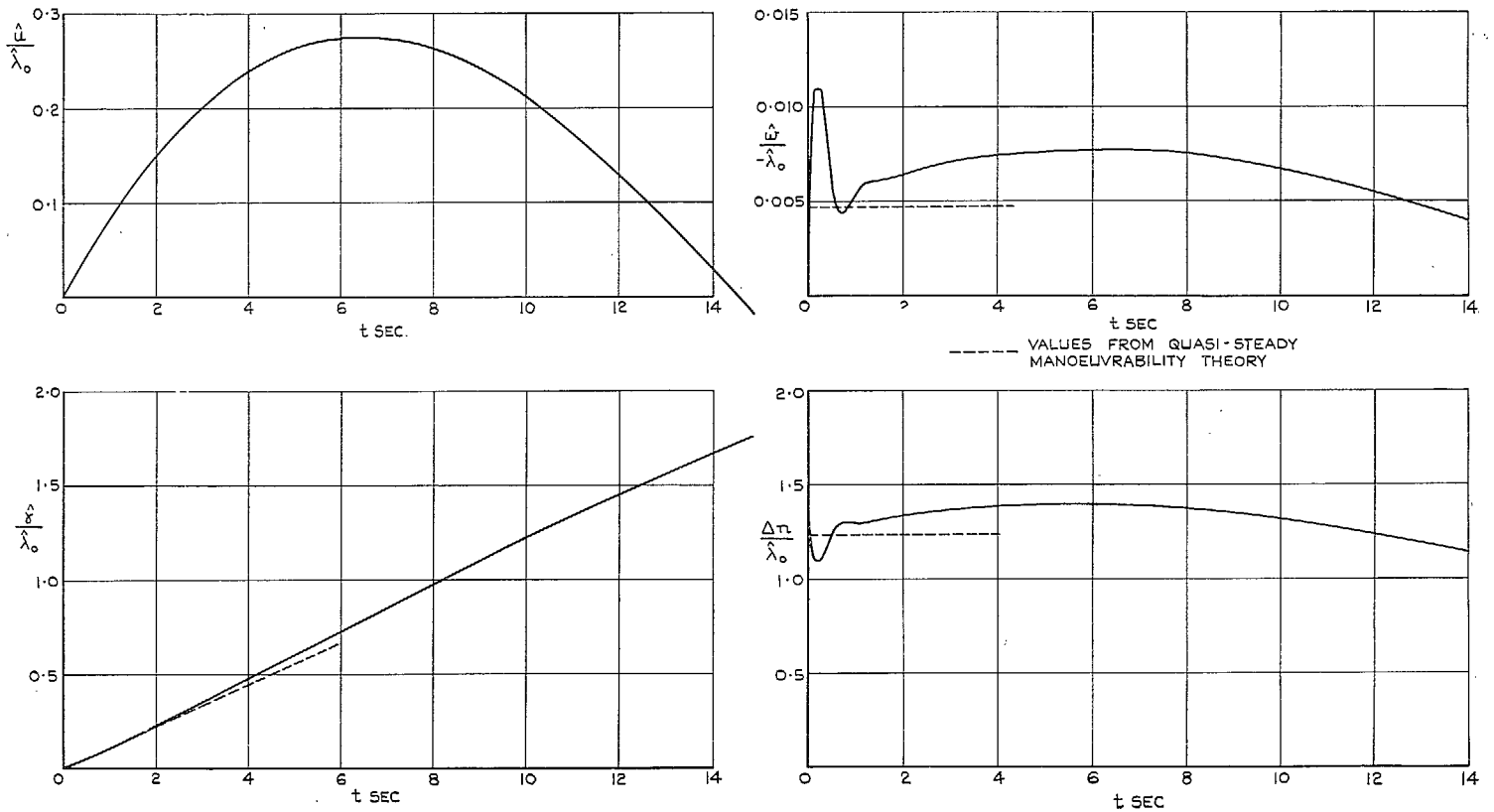

FIG. 11. Response to step function input of jet thrust control—Cruising condition: $C_{Ls} = 0{\cdot}268$.

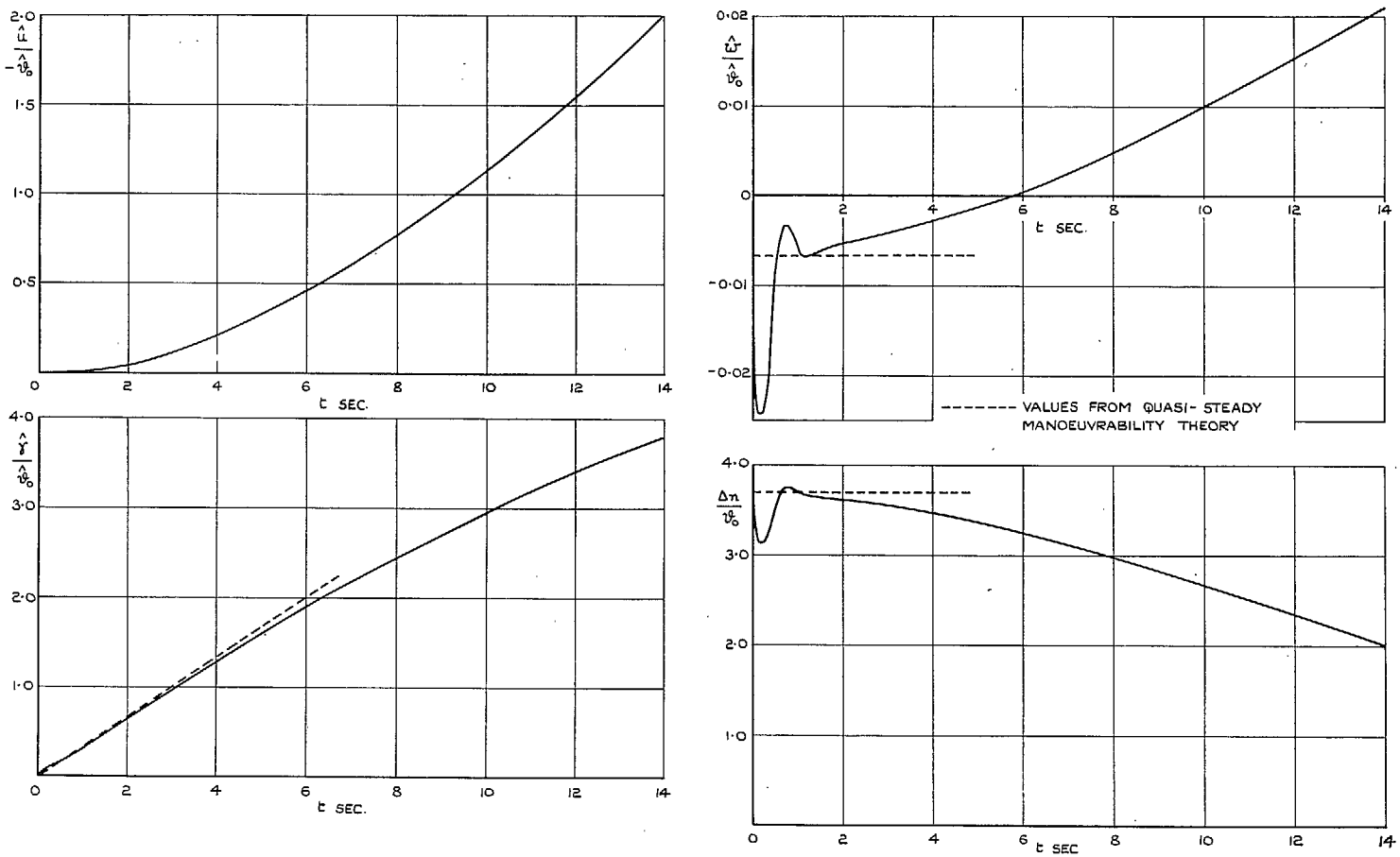

FIG. 12. Response to step function input of jet-flap deflection—Cruising condition: $C_{Ls} = 0{\cdot}268$.

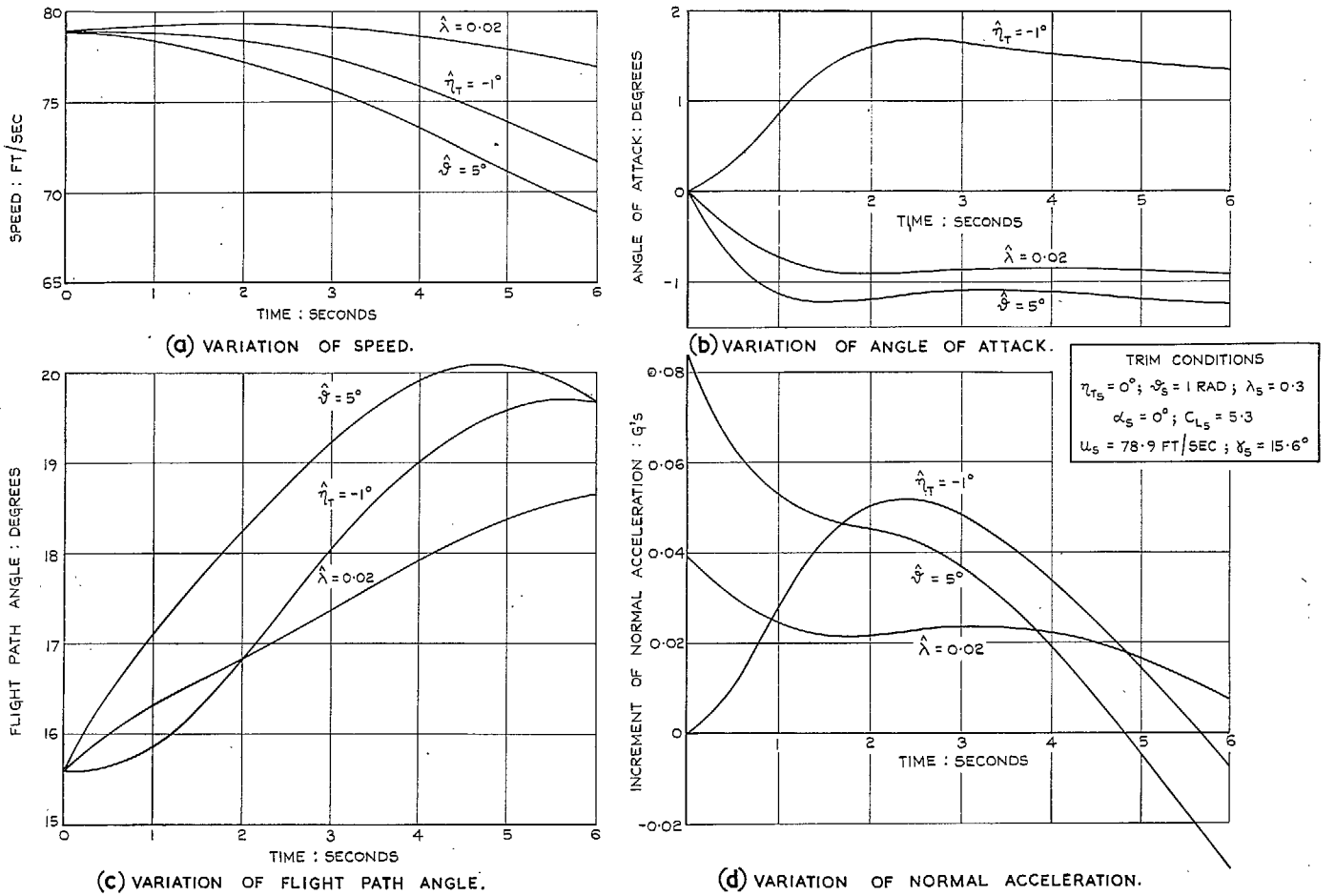

FIG. 13. Comparative response to three controls: Basic design condition.

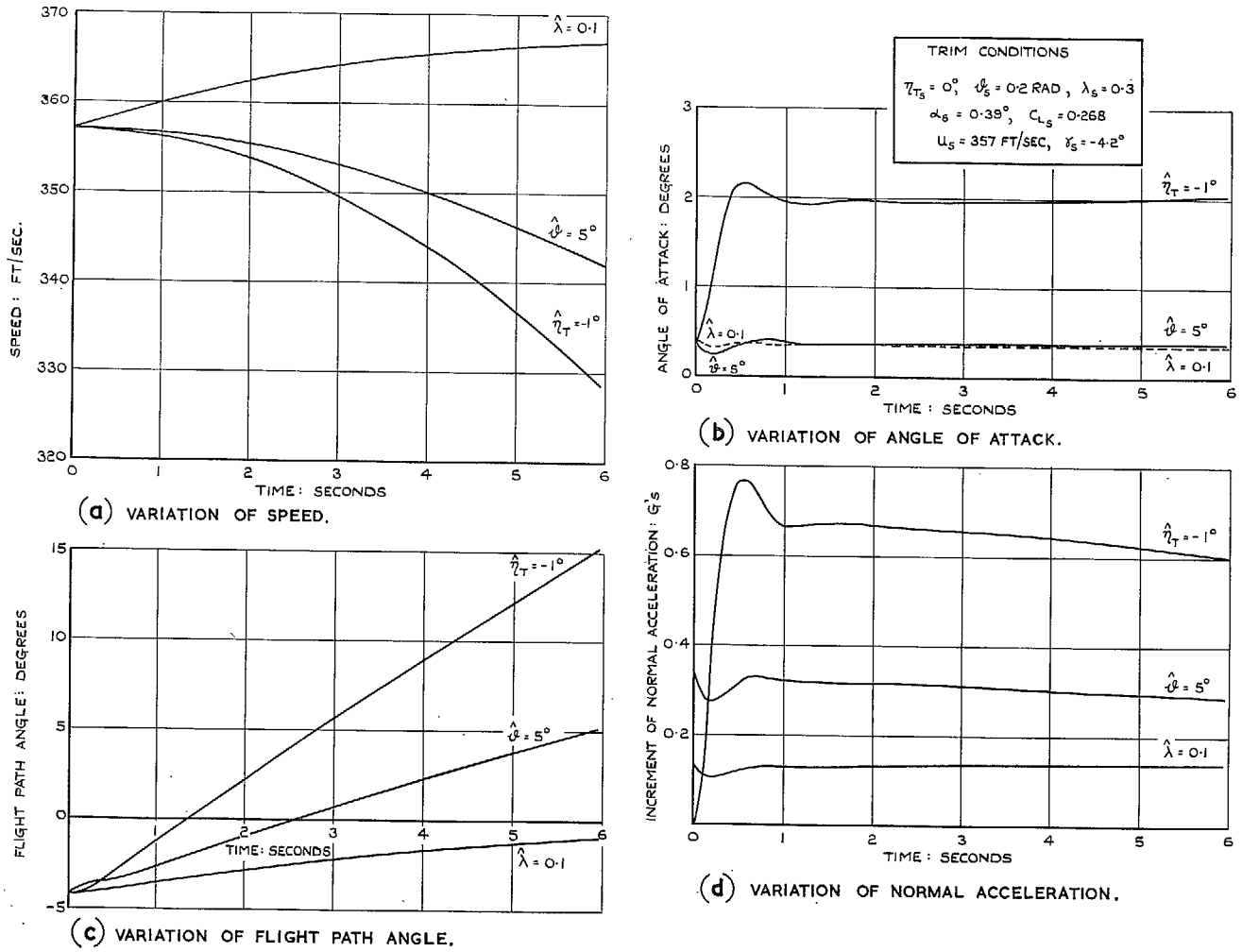

FIG. 14. Comparative response to three controls: Cruising condition.

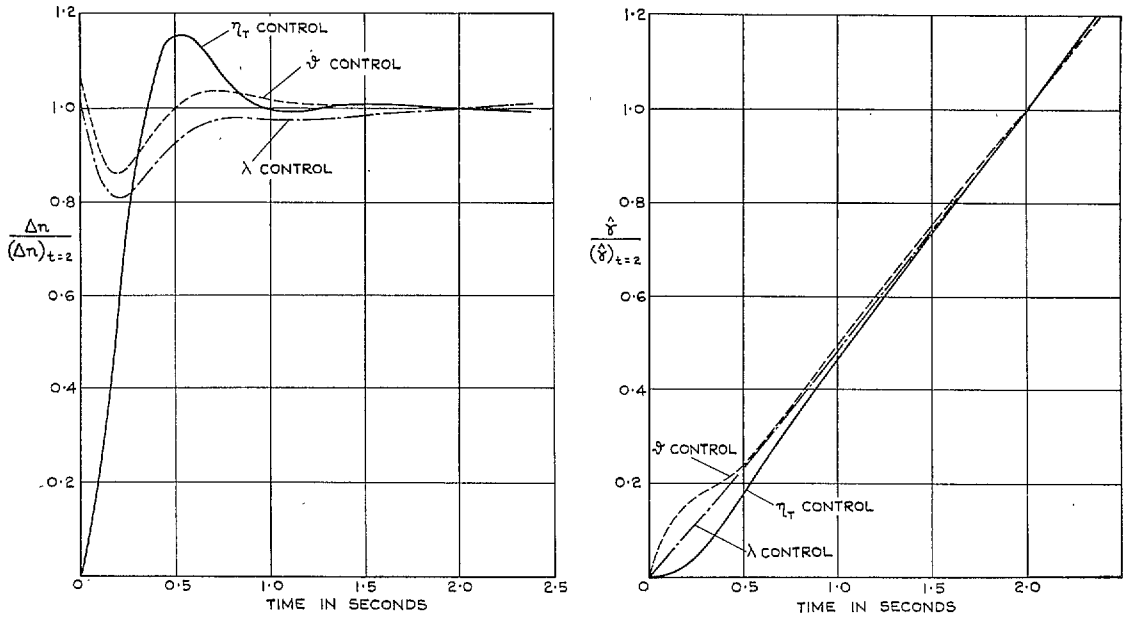

FIG. 15. Comparison of normalized modes of response to three controls: Cruising condition.

(84109) Wt. 67/1876 K.5 7/62 Hw.

Publications of the Aeronautical Research Council

ANNUAL TECHNICAL REPORTS OF THE AERONAUTICAL RESEARCH COUNCIL (BOUND VOLUMES)

1942 Vol. I. Aero and Hydrodynamics, Aerofoils, Airscrews, Engines. 75*s.* (post 2*s.* 9*d.*)
Vol. II. Noise, Parachutes, Stability and Control, Structures, Vibration, Wind Tunnels. 47*s.* 6*d.* (post 2*s.* 3*d.*)

1943 Vol. I. Aerodynamics, Aerofoils, Airscrews. 80*s.* (post 2*s.* 6*d.*)
Vol. II. Engines, Flutter, Materials, Parachutes, Performance, Stability and Control, Structures. 90*s.* (post 2*s.* 9*d.*)

1944 Vol. I. Aero and Hydrodynamics, Aerofoils, Aircraft, Airscrews, Controls. 84*s.* (post 3*s.*)
Vol. II. Flutter and Vibration, Materials, Miscellaneous, Navigation, Parachutes, Performance, Plates and Panels, Stability, Structures, Test Equipment, Wind Tunnels. 84*s.* (post 3*s.*)

1945 Vol. I. Aero and Hydrodynamics, Aerofoils. 130*s.* (post 3*s.* 6*d.*)
Vol. II. Aircraft, Airscrews, Controls. 130*s.* (post 3*s.* 6*d.*)
Vol. III. Flutter and Vibration, Instruments, Miscellaneous, Parachutes, Plates and Panels, Propulsion. 130*s.* (post 3*s.* 3*d.*)
Vol. IV. Stability, Structures, Wind Tunnels, Wind Tunnel Technique. 130*s.* (post 3*s.* 3*d.*)

1946 Vol. I. Accidents, Aerodynamics, Aerofoils and Hydrofoils. 168*s.* (post 3*s.* 9*d.*)
Vol. II. Airscrews, Cabin Cooling, Chemical Hazards, Controls, Flames, Flutter, Helicopters, Instruments and Instrumentation, Interference, Jets, Miscellaneous, Parachutes. 168*s.* (post 3*s.* 3*d.*)
Vol. III. Performance, Propulsion, Seaplanes, Stability, Structures, Wind Tunnels. 168*s.* (post 3*s.* 6*d.*)

1947 Vol. I. Aerodynamics, Aerofoils, Aircraft. 168*s.* (post 3*s.* 9*d.*)
Vol. II. Airscrews and Rotors, Controls, Flutter, Materials, Miscellaneous, Parachutes, Propulsion, Seaplanes, Stability, Structures, Take-off and Landing. 168*s.* (post 3*s.* 9*d.*)

1948 Vol. I. Aerodynamics, Aerofoils, Aircraft, Airscrews, Controls, Flutter and Vibration, Helicopters, Instruments, Propulsion, Seaplane, Stability, Structures, Wind Tunnels. 130*s.* (post 3*s.* 3*d.*)
Vol. II. Aerodynamics, Aerofoils, Aircraft, Airscrews, Controls, Flutter and Vibration, Helicopters, Instruments, Propulsion, Seaplane, Stability, Structures, Wind Tunnels. 110*s.* (post 3*s.* 3*d.*)

Special Volumes

Vol. I. Aero and Hydrodynamics, Aerofoils, Controls, Flutter, Kites, Parachutes, Performance, Propulsion, Stability. 126*s.* (post 3*s.*)
Vol. II. Aero and Hydrodynamics, Aerofoils, Airscrews, Controls, Flutter, Materials, Miscellaneous, Parachutes, Propulsion, Stability, Structures. 147*s.* (post 3*s.*)
Vol. III. Aero and Hydrodynamics, Aerofoils, Airscrews, Controls, Flutter, Kites, Miscellaneous, Parachutes, Propulsion, Seaplanes, Stability, Structures, Test Equipment. 189*s.* (post 3*s.* 9*d.*)

Reviews of the Aeronautical Research Council

1939–48 3*s.* (post 6*d.*) 1949–54 5*s.* (post 5*d.*)

Index to all Reports and Memoranda published in the Annual Technical Reports

1909–1947 R. & M. 2600 (out of print)

Indexes to the Reports and Memoranda of the Aeronautical Research Council

Between Nos. 2351–2449	R. & M. No. 2450 2*s.* (post 3*d.*)
Between Nos. 2451–2549	R. & M. No. 2550 2*s.* 6*d.* (post 3*d.*)
Between Nos. 2551–2649	R. & M. No. 2650 2*s.* 6*d.* (post 3*d.*)
Between Nos. 2651–2749	R. & M. No. 2750 2*s.* 6*d.* (post 3*d.*)
Between Nos. 2751–2849	R. & M. No. 2850 2*s.* 6*d.* (post 3*d.*)
Between Nos. 2851–2949	R. & M. No. 2950 3*s.* (post 3*d.*)
Between Nos. 2951–3049	R. & M. No. 3050 3*s.* 6*d.* (post 3*d.*)
Between Nos. 3051–3149	R. & M. No. 3150 3*s.* 6*d.* (post 3*d.*)

HER MAJESTY'S STATIONERY OFFICE

from the addresses overleaf

Printed and published by
HER MAJESTY'S STATIONERY OFFICE

To be purchased from
York House, Kingsway, London W.C.2
423 Oxford Street, London W.1
13A Castle Street, Edinburgh 2
109 St. Mary Street, Cardiff
39 King Street, Manchester 2
50 Fairfax Street, Bristol 1
35 Smallbrook, Ringway, Birmingham 5
80 Chichester Street, Belfast 1
or through any bookseller

Printed in England

S.O. Code No. 23-3272